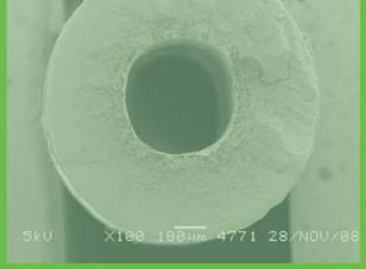

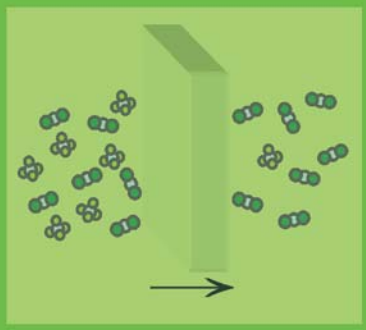

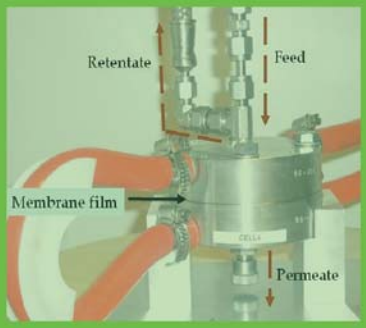

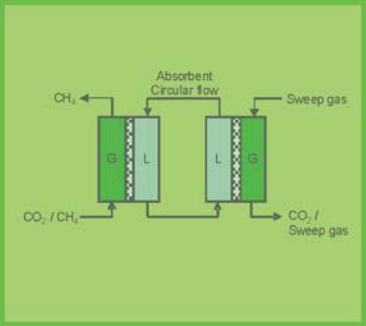

MEMBRANE TECHNOLOGIES FOR CO_2 CAPTURE

MEMBRANE TECHNOLOGIES FOR CO_2 CAPTURE

Graduation committee

Chairman	
Prof. Dr. G. van der Steenhoven	University of Twente
Promotor	
Prof. Dr.-Ing. M. Wessling	University of Twente
Assistant promotor	
Dr. Ir. D.C. Nijmeijer	University of Twente
Committee members	
Dr. Ir. D.W.F. Brilman	University of Twente
Prof. Dr. T.J. Dingemans	University of Delft
Prof. Dr. Ir. A. Nijmeijer	University of Twente
Prof. Dr. R.D. Noble	University of Colorado at Boulder, USA

Membrane technologies for CO_2 capture
K. Simons, PhD Thesis, University of Twente, The Netherlands
ISBN: 978-90-365-3020-0

Cover design by Katja Simons

Printed by Ipskamp Print Service, Enschede

MEMBRANE TECHNOLOGIES FOR CO_2 CAPTURE

DISSERTATION

to obtain
the degree of doctor at the University of Twente,
on the authority of the rector magnificus,
Prof.dr. H. Brinksma,
on account of the decision of the graduation committee,
to be publicly defended
on Thursday 17th of June 2010 at 13.15

by

Katja Simons
born on 18th of September 1980
in Oelde, Germany

This dissertation has been approved by
the promotor Prof. Dr.-Ing. M.Wessling
and the assistant promotor Dr. Ir. D.C. Nijmeijer

TABLE OF CONTENTS

CHAPTER 1

General introduction

This thesis investigates the potential of membrane technology for the effective removal of CO_2 from CH_4. The work focuses on two distinctively different membrane processes to accomplish the separation, i.e. the use of a gas-liquid membrane contactor for the selective absorption of CO_2 (described in Chapter 2 to 4) and the use of thin, dense gas separation membranes to establish the separation (described in Chapter 5 and 6).
This chapter describes the incentive for and the background of the research performed. Next to the motivation for the work, the investigated membrane technologies are discussed in more detail. Finally the scope and the structure of the thesis are presented.

CO_2 removal

The strong anthropogenic increase in the emission of CO_2 and the related environmental consequences force the developments in the direction of sustainability and Carbon Capture and Storage (CCS). Fossil fuels are with 86% the dominant energy source utilized in the world [1]. More than one-third of the CO_2 emissions come from the combustion of fossil fuels in power plants worldwide [2, 3] and also the emission of CO_2 associated with the use of CH_4 is more than significant. The combustion of gaseous fuels (e.g. natural gas) accounted for 1521 million metric tons of carbon in 2006, which equals 18.5% of the total emissions from fossil fuels [4]. In addition, also the emission of CO_2 associated with the exploration and production of natural gas is more than significant [1]. The number of easy accessible, low

CO_2 containing natural gas sources is only limited, urging the exploration of natural gas sources with high(er) concentrations of CO_2.

Next to its environmental impact, CO_2 reduces the heating value of the CH_4 gas streams in power plants [5]. Due to its acidic character, the presence of CO_2 can lead to corrosion in equipment and pipelines [6]. Pipeline specifications for natural gases give a maximum value of 2-5% for the CO_2 content while the CO_2 content for liquefied natural gas (LNG) even needs to be reduced to 50-100 ppm [7]. This makes the removal of CO_2 from natural gas of crucial importance.

After capturing, the removed CO_2 can be reused for different applications in the oil, food and chemical industry. Enhanced oil recovery [1] as well as algae biofixation, where CO_2 is used for microalgaes as carbon source [8], are important applications. Smaller fields of application, like CO_2 enrichment in greenhouses, where the increase in CO_2 concentration from 350 ppm to 500 ppm results in a production increase of 25% for certain bulk crops [9] are of additional interest. Although several possibilities for reuse of CO_2 exist, the total capacity of the different options for the reuse of CO_2 do not match with the current production and, to reduce the emission of CO_2 into the atmosphere, additional storage of CO_2 is currently inevitable. Possibilities to store CO_2 include ocean sequestrations, geological sequestrations and the sequestrations of CO_2 in saline aquifers [10]. In life cycle investigations, Khoo et al. [10] determined the effectiveness of the different CO_2 sequestration ways and the potential environmental impact. The results showed geological sequestration methods to be the safest methods with the least environmental burdens. Although CO_2 reuse and storage are, next to CO_2 capture, crucial aspects regarding the environmental impact of CO_2, it is not the focus of this thesis.

Separation technologies

The focus of this thesis is to investigate the potential of two distinctively different membrane processes for the energy-efficient and effective separation of CO_2 and CH_4. Traditional methods used to separate CO_2 from gas mixtures are pressure swing adsorption, cryogenic distillation and the most frequently used method amine absorption [10-12]. Also membrane processes are frequently used for gas separation. Examples are e.g. the separation of oxygen and nitrogen from air to produce nitrogen enriched air [13], but also for the separation of CO_2 from CH_4 [14-17]. The main limitation of currently existing membranes is the occurrence of severe plasticization of the membrane in the presence of (high) pressure CO_2. Due to excessive swelling of the polymer membrane upon exposure to CO_2, the performance (selectivity) decreases significantly, thus reducing the purity of the CO_2 and consequently reducing the possibilities for reuse of the gas.
Energy requirements on the other hand significantly benefit the use of membrane technology over other technologies: membrane technology uses 70-75 kWh per ton of recovered CO_2 compared to significantly higher values for pressure swing adsorption (160-180 kWh), cryogenic distillation (600-800 kWh) or amine absorption (330-340 kWh) [10], making membrane technology an attractive alternative.

Absorption

The selective physical or chemical absorption of CO_2 by a solvent is the most well-established method of CO_2 capture in power plants and from natural gas sources [10]. High product yields and purities can be obtained with this method. Aqueous alkanol amine solutions like mono ethanol amine (MEA) are commonly used absorption liquids. In this way, recovery rates of 95-98% are possible [10], but amine absorption suffers from several drawbacks like corrosiveness, instability in the presence of oxygen [18], high energy consumption, especially during desorption [19, 20], and high liquid losses due to evaporation of the solvent in the stripper [9, 21]. In addition, also the occurrence of flooding and entrainment of the

absorption liquid may occur and limits the process as the gas and the liquid streams cannot be controlled independently [22-25].

Membrane technology

Membrane technology is an attractive and competitive alternative to conventional absorption technology. It has a high energy efficiency, is easy to scale-up because of its modular design and it has a high area-to-volume ratio [19, 26-28]. A limitation can be found in the permeability-selectivity tradeoff relation: more permeable membrane materials are generally less selective and vice versa [29]. Since 1980s gas separation with membranes has emerged into a commercially viable method [30]. Nowadays, several hundreds of plants use membrane technology for the separation of gases. Most plants use cellulose-acetate membranes, which have CO_2/CH_4 selectivities of only 15 [31]. According to Baker [31], the competiveness of membranes for the separation of CO_2/CH_4 would strongly increase if stable membranes with a selectivity of 40 during operation would become available. Due to plasticization in the presence of CO_2, membranes often loose their performance at elevated pressure. Swelling stresses on the polymer network and an increase in free volume and segmental mobility upon exposure to CO_2 cause a rise in permeability for all components [32], and especially the permeability of the low permeating component, consequently resulting in a decrease in selectivity [33-35]. The development of polymeric membranes and membrane processes with improved plasticization resistance that maintain selectivity and permeability, even at higher CO_2 partial feed pressures is crucial and an important field of research.

Transport through dense membranes

According to Fick's law, gas diffusion through non-porous, dense polymer membranes can be described by [36]:

$$J = -D\frac{dc}{dx} \quad (1)$$

Where J is the gas flux through the membrane (cm^3 (STP)/cm^2·s), D is the diffusion coefficient (cm^2/s) and dc/dx is the driving force, or the concentration gradient over the membrane. Assuming steady-state conditions, Equation 1 can be integrated and results in the following Equation:

$$J_i = \frac{D_i\left(c_{i,f} - c_{i,p}\right)}{l} \quad (2)$$

Where D_i is the diffusion coefficient (cm^2/s) of component i, $c_{i,f}$ and $c_{i,p}$ are the concentrations (mol/cm^3) of component i on the feed and permeate side of the membrane, respectively and l equals the thickness (cm) of the membrane.

According to Henry's law the concentration of component i (c_i) is linearly related to its partial pressure (p_i):

$$c_i = S_i \cdot p_i \quad (3)$$

where S_i is the solubility coefficient of component i (cm^3 (STP)/cm^3·cmHg). As will be discussed in more detail in Chapter 6, the dependency of the solubility to the pressure is often more complex than described by Henry's law.

Combining Equations 2 and 3 and by taking into account that the product of solubility (S) and diffusivity (D) equals the permeability (P), this results in Equation 4:

$$J_i = \frac{P_i\left(p_{i,f} - p_{i,p}\right)}{l} \quad (4)$$

Where P_i is the permeability of component i ($cm^3(STP)\cdot cm/cm^2\cdot s\cdot cmHg$), $p_{i,f}$ and $p_{i,p}$ are the partial pressure of component i at the feed and at the permeate side, respectively and l equals the thickness (cm) of the membrane.

The equation $P=D\cdot S$ is generally known as the solution-diffusion model for transport of gases through dense polymeric membranes [37]. First the gas dissolves in the membrane material and then diffuses through the membrane.
The solubility is a thermodynamic factor, which reflects the number of molecules dissolved in the membrane material [38] and is determined by polymer-penetrant interactions, the inherent condensability of the gas, and the free volume in the polymer [39]. More specifically for the separation of CO_2 from CH_4, CO_2 is more condensable and more polar than CH_4 and a higher CO_2 solubility in the polymer membrane can be expected. The diffusivity is a kinetic parameter and is predominantly influenced by the size of the gas molecules under consideration. In general, the diffusion coefficient decreases with increasing kinetic diameter of the gas [36]. CO_2 has a smaller kinetic diameter (3.30 Å) than CH_4 (3.80 Å) [36]. Consequently, CO_2 has a higher diffusivity than CH_4. Figure 1 shows a schematic representation of CO_2 and CH_4.

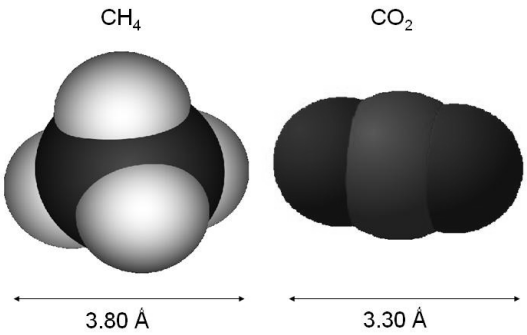

Figure 1: Schematic representation of CO_2 and CH_4.

Next to the permeability, the main factor to describe the performance of a membrane is its separation ability, called the selectivity α. The ideal

selectivity using pure gases is given by the ratio of the permeability coefficients (P_i), which is, when assuming solution-diffusion to occur, composed of a diffusivity selectivity term (D_{CO2}/D_{CH4}) and a solubility selectivity term (S_{CO2}/S_{CH4}):

$$\alpha_{ideal} = \frac{P_{CO_2}}{P_{CH_4}} = \frac{D_{CO_2}}{D_{CH_4}} \cdot \frac{S_{CO_2}}{S_{CH4}} \tag{5}$$

For gas mixtures the feed composition has to be taken into account as well and the membrane selectivity is expressed as:

$$\alpha = \frac{Y_{CO_2} / Y_{CH_4}}{X_{CO_2} / X_{CH_4}} \tag{6}$$

Where Y_i is the concentration of component i in the permeate stream and X_i is the concentration of component i in the feed.

Membrane gas absorption

In membrane gas absorption processes or more specifically in a membrane contactor (Figure 2) the advantages of membrane technology are combined with those of absorption technology.

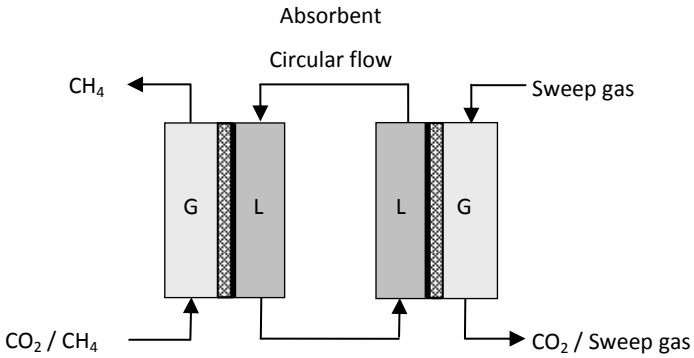

Figure 2: Schematic representation of a membrane contactor for the separation of CO_2 and CH_4.

In a membrane contactor the membrane acts as an interface between the feed gas and the absorption liquid. In the case of CO_2/CH_4 separation, CO_2 diffuses from the feed gas side through the membrane and is then absorbed in the selective absorption liquid. The loaded liquid circulates from the absorber to the desorber, which can be a traditional stripper or a second membrane contactor, in which desorption of CO_2 occurs. The selectivity of the process is not only determined by the absorption liquid, but also the membrane can play a significant role and contribute to the selectivity, depending on whether selective [13] or non-selective membranes are used. Gas-liquid membrane contactors offer a unique way to perform gas-liquid absorption processes in a controlled fashion and they have a high operational flexibility [40-42]. The advantages of gas-liquid membrane contacting processes make them a viable alternative for different applications, for example the separation of olefins and paraffins [41, 43], blood oxygenation [44] and the separation of CO_2 from light gases.

Scope of this thesis

This thesis investigates the potential of membrane technology for the effective removal of CO_2 from CH_4. The work focuses on two distinctively different membrane processes to accomplish the separation, i.e. the use of a gas-liquid membrane contactor for the selective absorption of CO_2 (described in Chapter 2 to 4) and the use of thin, dense gas separation membranes to establish the separation (described in Chapter 5 and 6). Chapter 2 to 4 predominantly focus on process technological and system design related aspects, whereas the focus of Chapter 5 and 6 is primarily on the development of new membrane materials for CO_2 separation.

In **Chapter 2** a membrane contactor for the separation of CO_2 from CH_4 is used and the influence of the type of membrane and of different process parameters on the overall process performance (permeance and selectivity) is investigated. Two types of commercially available hollow fiber membranes are used in this work: porous polypropylene (PP) hollow fiber membranes and asymmetric poly(phenylene oxide) (PPO) hollow fiber membranes with a dense, ultrathin skin at the outside of the membrane. The commonly used mono ethanol amine (MEA) is used as absorption liquid. The effect of the liquid flow rate, feed pressure and temperature of absorption and desorption for the two chosen membrane types on the overall process performance is investigated and the results allow identifying the operating window and potential of the process for the capture of CO_2 from CH_4.

In **Chapter 3** the potential of an aqueous sarcosine salt solution as competitive absorption liquid for CO_2 absorption in gas-liquid membrane contactor systems is investigated. Kinetic experiments in the pseudo-first-order regime are carried out using a gas-liquid stirred cell contactor to determine the reaction rate constant of CO_2 absorption in aqueous sarcosine salt solutions. Next to the influence of the sarcosine-salt concentration (0.5 to 3.8 M) and the temperature (298 to 308 K), the reaction rate constant for partially CO_2-loaded sarcosine salt solutions (0 to 0.5 mol CO_2/mol sarcosine salt solution) is determined.

In **Chapter 4** the performance of this amino acid salt solution (potassium salt of sarcosine) as absorption liquid in a gas-liquid membrane contactor is investigated and compared to the performance of the traditionally used amine solution mono ethanol amine. Process performance data for the real process consisting of an absorber and a desorber membrane module using feed mixtures are reported and compared to the corresponding data obtained when MEA is used as absorption liquid. The influence of the temperature difference between absorber and desorber and that of the liquid flow rate is evaluated.

In **Chapter 5** gas selective poly ionic liquid (poly(RTILs) membranes, which are polymerized room temperature ionic liquids (RTIL) are investigated. The RTIL is synthesized as a monomer and subsequently polymerized to obtain gas selective membranes. The ionic nature of the polymers may result in tight arrangements between the oppositely charged ionic domains in the poly(RTIL) eventually preventing the membrane from excessive swelling and deterioration of its performance at increased pressure and/or temperature. This intrinsic property of poly(RTIL)s is used as a tool to increase the resistance against plasticization and to restrict strong swelling of the polymer membrane to maintain its permeation properties in the presence of a strong plasticizing agent such as CO_2 at higher pressures. An imidazolium-based poly(RTIL) is used as base material and the length of the alkyl chain serves as a tool to strengthen or weaken the ionic interactions within the poly(RTIL). High pressure mixed CO_2/CH_4 gas separation measurements at different temperatures are performed to evaluate the potential of this concept.

In **Chapter 6** a specific group of polyetherimides, ODPA PEI's (3,3',4,4'-oxydiphthalic dianhydride polyetherimide), as membrane material with improved plasticization resistance for CO_2 removal is investigated. The effect of increasing number of para-arylene substitutions in the main chain on the gas solubility, swelling, permeability and selectivity is determined.

As swelling, transport and plasticization behavior in thin layers may significantly differ from that observed in bulk films, next to solubility tests on free standing bulk films, the swelling behavior of thin polymer layers exposed to high pressure CO_2 is investigated as well. The results are

compared to the corresponding values obtained for both the glassy polymers SPEEK and Matrimid, which is especially known for its low resistance to plasticization, and the rubbery material PEBAX.

Chapter 7 summarizes the main conclusions of the work and suggests directions for future research.

References

1. IPCC Special Report on Carbon Dioxide Capture and Storage, Cambridge University Press: Cambridge (England), (2005)

2. H.-Y. Zhang, R. Wang, D.T. Liang, J.H. Tay, Modeling and experimental study of CO_2 absorption in a hollow fiber membrane contactor, Journal of Membrane Science, 279 (2006) 301

3. IEA, CO_2 emissions from fuel combustion, 1971-2007, OECD/IEA, (2009)

4. T.A. Boden, G. Marland, and R.J. Andres., Global, Regional and National Fossil-Fuel CO_2 Emissions, Carbon Dioxide Information Analysis Center, Oak Ridge National Laborator, U.S. Department of Energy, Oak Ridge, Tenn., U.S.A. doi 10.3334/CDIAC/00001,

5. E.D. Bates, R.D. Mayton, I. Ntai, J.H. Davis, CO_2 Capture by a Task-Specific Ionic Liquid, J. Am. Chem. Soc., 124 (2002) 926-927

6. S. Ma'mun, V.Y. Dindore, H.F. Svendsen, Kinetics of the Reaction of Carbon Dioxide with Aqueous Solutions of 2-((2-Aminoethyl)amino)ethanol, Ind. Eng. Chem. Res., 46 (2007) 385-394

7. S. Ma'mun, V.Y. Dindore, H.F. Svendsen, Kinetics of the reaction of carbon dioxide with aqueous solutions of 2-((2-aminoethyl)amino)ethanol, Industrial and Engineering Chemistry Research, 46 (2007) 385

8. T.M. Mata, A.A. Martins, N.S. Caetano, Microalgae for biodiesel production and other applications: A review, Renewable and Sustainable Energy Reviews, 14 217

9. P.H.M. Feron, A.E. Jansen, Capture of carbon dioxide using membrane gas absorption and reuse in the horticultural industry, Energy Conversion and Management, 36 (1995) 411

10. H.H. Khoo, R.B.H. Tan, Life cycle investigation of CO_2 recovery and sequestration, Environmental Science and Technology, 40 (2006) 4016

11. S. Freni, S. Cavallaro, S. Donato, V. Chiodo, A. Vita, Experimental evaluation on the CO2 separation process supported by polymeric membranes, Materials Letters, 58 (2004) 1865

12. A.F. Ismail, N. Yaacob, Performance of treated and untreated asymmetric polysulfone hollow fiber membrane in series and cascade

module configurations for CO_2/CH_4 gas separation system, Journal of Membrane Science, 275 (2006) 151

13. Parker Filtration & Separation B.V., www.parker.com/pfs

14. Membrane Technology & Research (MTR), www.mtrinc.com,

15. MEDAL L.P. (Membrane Systems Du Pont Air Liquide), www.medal.airliquide.com

16. UBE America Inc., www.northamerica.ube.com

17. DOW, The Dow Chemical Company, www.dow.com/gastreating

18. J. Van Holst, S.R.A. Kersten, K.J.A. Hogendoorn, Physiochemical properties of several aqueous potassium amino acid salts, Journal of Chemical and Engineering Data, 53 (2008) 1286

19. S.-p. Yan, M.-X. Fang, W.-F. Zhang, S.-Y. Wang, Z.-K. Xu, Z.-Y. Luo, K.-F. Cen, Experimental study on the separation of CO_2 from flue gas using hollow fiber membrane contactors without wetting, Fuel Processing Technology, 88 (2007) 501

20. C. Alie, L. Backham, E. Croiset, P.L. Douglas, Simulation of CO_2 capture using MEA scrubbing: A flowsheet decomposition method, Energy Conversion and Management, 46 (2005) 475

21. J. Zhang, S. Zhang, K. Dong, Y. Zhang, Y. Shen, X. Lv, Supported Absorption of CO_2 by Tetrabutylphosphonium Amino Acid Ionic Liquids, Chemistry - A European Journal, 12 (2006) 4021-4026

22. J.-G. Lu, Y.-F. Zheng, M.-D. Cheng, L.-J. Wang, Effects of activators on mass-transfer enhancement in a hollow fiber contactor using activated alkanolamine solutions, Journal of Membrane Science, 289 (2007) 138

23. D. deMontigny, P. Tontiwachwuthikul, A. Chakma, Using polypropylene and polytetrafluoroethylene membranes in a membrane contactor for CO_2 absorption, Journal of Membrane Science, 277 (2006) 99

24. P.H.M. Feron, A.E. Jansen, CO_2 separation with polyolefin membrane contactors and dedicated absorption liquids: Performances and prospects, Separation and Purification Technology, 27 (2002) 231

25. S. Atchariyawut, R. Jiraratananon, R. Wang, Separation of CO_2 from CH_4 by using gas-liquid membrane contacting process, Journal of Membrane Science, 304 (2007) 163

26. J.L. Li, B.H. Chen, Review of CO_2 absorption using chemical solvents in hollow fiber membrane contactors, Separation and Purification Technology, 41 (2005) 109

27. B.D. Bhide, A. Voskericyan, S.A. Stern, Hybrid processes for the removal of acid gases from natural gas, Journal of Membrane Science, 140 (1998) 27

28. P.S. Kumar, J.A. Hogendoorn, P.H.M. Feron, G.F. Versteeg, New absorption liquids for the removal of CO_2 from dilute gas streams using membrane contactors, Chemical Engineering Science, 57 (2002) 1639

29. B.D. Freeman, Basis of permeability/selectivity tradeoff relations in polymeric gas separation membranes, Macromolecules, 32 (1999) 375

30. S. Sridhar, B. Smitha, T.M. Aminabhavi, Separation of carbon dioxide from natural gas mixtures through polymeric membranes - A review, Separation and Purification Reviews, 36 (2007) 113

31. R.W. Baker, Future Directions of Membrane Gas Separation Technology, Ind. Eng. Chem. Res., 41 (2002) 1393-1411

32. T. Visser, M. Wessling, When do sorption-induced relaxations in glassy polymers set in? Macromolecules, 40 (2007) 4992

33. A. Bos, I.G.M. Puent, M. Wessling, H. Strathmann, CO_2-induced plasticization phenomena in glassy polymers, Journal of Membrane Science, 155 (1999) 67

34. J.D. Wind, D.R. Paul, W.J. Koros, Natural gas permeation in polyimide membranes, Journal of Membrane Science, 228 (2004) 227

35. J.D. Wind, S.M. Sirard, D.R. Paul, P.F. Green, K.P. Johnston, W.J. Koros, Relaxation Dynamics of CO_2 Diffusion, Sorption, and Polymer Swelling for Plasticized Polyimide Membranes, Macromolecules, 36 (2003) 6442-6448

36. M.H.V. Mulder, Basic principles of membrane technology, Kluwer Academic Publishers, (1996)

37. J.G. Wijmans, R.W. Baker, The solution-diffusion model: A review, Journal of Membrane Science, 107 (1995) 1

38. R.W. Baker, Membrane Technology and Applications, John Wiley&Sons, Ltd., (2004)

39. C.-C. Hu, C.-S. Chang, R.-C. Ruaan, J.-Y. Lai, Effect of free volume and sorption on membrane gas transport, Journal of Membrane Science, 226 (2003) 51-61

40. A. Gabelman, S.T. Hwang, Hollow fiber membrane contactors, Journal of Membrane Science, 159 (1999) 61

41. K. Nymeijer, T. Visser, R. Assen, M. Wessling, Super selective membranes in gas-liquid membrane contactors for olefin/paraffin separation, Journal of Membrane Science, 232 (2004) 107

42. V.Y. Dindore, D.W.F. Brilman, P.H.M. Feron, G.F. Versteeg, CO_2 absorption at elevated pressures using a hollow fiber membrane contactor, Journal of Membrane Science, 235 (2004) 99

43. M. Teramoto, S. Shimizu, H. Matsuyama, N. Matsumiya, Ethylene/ethane separation and concentration by hollow fiber facilitated transport membrane module with permeation of silver nitrate solution, Separation and Purification Technology, 44 (2005) 19

44. S. Karoor, K.K. Sirkar, Gas absorption studies in microporous hollow fiber membrane modules, Ind. Eng. Chem. Res., 32 (1993) 674-684

CHAPTER 2

Gas-liquid membrane contactors for CO_2 removal

Abstract

In the present work we use a membrane contactor for the separation of CO_2 from CH_4 and we systematically investigate the influence of both the type of membrane and the different process parameters on the overall process performance (permeability and selectivity). This work is important because it reports real process performance data (permeances and selectivities) for the total process consisting of absorption and desorption under practical conditions using feed mixtures. Commercially available porous PP hollow fiber membranes and asymmetric PPO hollow fiber membranes have been applied and MEA was used as absorption liquid in the membrane contactor. The proposed approach allows us to identify the operating window and potential of the process. Although the performance of the PP membranes outperforms the performance of the PPO membranes in terms of productivity and selectivity, the PP fibers are extremely sensitive to only small variations in the feed pressure, resulting in severe performance loss. In addition to that, extremely high liquid losses are observed for the PP fibers especially at elevated temperatures. Factors that are significantly reduced when asymmetric PPO membranes with a dense, ultrathin top layer are used, which thus improves the performance

and significantly increases the operating window and potential of the membrane contactor process.

Introduction

CO_2 is one of the major contributors to the greenhouse effect. The power and industrial sectors combined account for about 60% of the global CO_2 emissions [1] and also natural gas can contain significant amounts of CO_2. High amounts of CO_2 in natural gas streams for electricity generation cause efficiency loss: The presence of CO_2 reduces the heating value of the gas in power plants and due to its acidic character, the presence of CO_2 leads to corrosion in equipment and pipelines [2]. This makes the removal of CO_2 from natural gas of crucial importance. The traditional method for CO_2 separation is amine scrubbing. Although high product yields and purities can be obtained, the disadvantage of this method is its high energy consumption, especially during desorption [3, 4], in combination with high liquid losses due to evaporation of the solvent in the stripper [5, 6]. In addition to that also the occurrence of flooding and entrainment of the absorption liquid limits the process and the liquid and gas streams cannot be controlled independently [7-10]. Membrane technology is a promising method to replace the conventional absorption technology. It has a high energy efficiency, is easy to scale-up because of its modular design and it has a high area-to-volume ratio [3, 11-13]. A limitation can be found in the permeability-selectivity tradeoff relation: more permeable membrane materials are generally speaking less selective and vice versa [14].
A membrane contactor (Figure 1) combines the advantages of membrane technology with those of an absorption liquid.

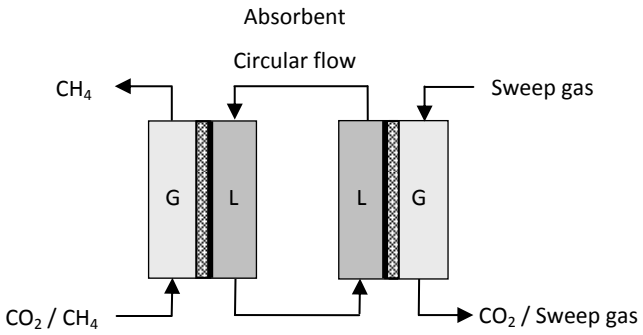

Figure 1: Schematic representation of a membrane contactor for the separation of CO_2 and CH_4.

In a membrane contactor the membrane acts as an interface between the feed gas and the absorption liquid. In the case of CO_2/CH_4 separation, CO_2 diffuses from the feed gas side through the membrane and is then absorbed in the selective absorption liquid. The loaded liquid circulates from the absorber to the desorber, which can be a traditional stripper or a second membrane contactor, in which desorption of CO_2 occurs. The selectivity of the process is not only determined by the absorption liquid, but also the membrane can play a significant role and contribute to the selectivity, depending on whether selective [13] or non-selective membranes are used. Gas-liquid membrane contactors offer a unique way to perform gas-liquid absorption processes in a controlled fashion and they have a high operational flexibility [15-17]. The advantages of gas-liquid membrane contacting processes make them a viable alternative for different applications, for example the separation of olefins and paraffins [16, 18], blood oxygenation [19] and the separation of CO_2 from light gases. Yeon et al. [20], who used a PVDF hollow fiber membrane contactor for absorption and a stripper column as desorber for the removal of CO_2 from nitrogen, showed that this configuration has a higher CO_2 removal efficiency than the conventional absorption column. The CO_2 absorption rate per unit volume of the membrane contactor was 2.7 times higher than that of the packed column, presumably caused by the increased gas-liquid contacting area, thus increasing the CO_2 mass transfer. Also long-term

stability tests with a CO_2 removal efficiency of 90-95% for 80 hours were successful.

Although alkanolamine solutions are traditionally used as absorption liquids for CO_2 removal because of their high CO_2 capacity and relatively high CO_2 absorption rates [21], a major disadvantage is their volatility, which results in high liquid losses due to evaporation of the solvent, especially in the desorption step which occurs at elevated temperatures. A method to limit the evaporation of the liquid is to not only use a membrane contactor as absorber, but to also use it as desorber. Lee et al. [22] used such a system with a membrane contactor for both absorption and desorption. They used hydrophobic porous membranes for absorber and desorber and an aqueous potassium carbonate solution as absorption liquid for CO_2 removal. With increasing flow rate the CO_2 permeation rate increased as well and fluxes as high as 0.001 mol/s at the highest flow rate and a concentration of 10 wt.% K_2CO_3 were obtained [22]. Kosaraju et al. used polypropylene hollow fiber membrane modules for absorption and desorption combined with an aqueous solution of poly amido amines dendrimers of generation 0 and a 55-day experiment demonstrated a stable performance without pore wetting by the dendrimer solution [23].

Most often non-selective, porous membranes are used as interface between gas feed and absorption liquid in the absorber and desorber. In this case, the membrane does not impart any selectivity to the separation [7, 13, 15], but the trans-membrane pressure has to be set very carefully. Too high feed pressures lead to the formation of gas bubbles in the absorption liquid thus introducing no selective flow of the feed gas into the absorption liquid, whereas at too low feed pressures wetting of the porous membrane by the absorption liquid occurs. Wetting of the porous membrane is a serious problem as it significantly increases the resistance to mass transfer through the introduction of a stagnant liquid layer in the pores of the membrane [13, 24]. A method proposed to overcome this limitation is the use of hydrophobic porous membranes when hydrophilic absorption liquids are used, but especially the long term effect can be limited. Dindore et al. [17] investigated CO_2 absorption in a membrane contactor using hydrophobic, porous polypropylene hollow fiber

membranes and an aqueous absorption liquid. If the feed pressure was too low, wetting of the pores by the absorption liquid occurred, which increased the mass transfer resistance. When the gas-side pressure was too high, gas bubble formation in the liquid most likely occurred and the feed gas mixture was pushed directly into the absorption liquid without any selective absorption to occur, thus decreasing the selectivity of the process tremendously [17].

To prevent wetting, instead of using hydrophobic, porous membranes, the use of composite membranes consisting of a porous support and a dense (selective) top layer, is considered [25, 26]. Li et al. [26] concluded that when applying a dense layer on top of the porous support, the wetting problem could be eliminated and no bubble formation in the liquid phase was observed. Of course this extra layer induces a significant additional resistance to mass transfer. This is in contrast to the use of a non-wetted porous membrane which would not have an influence on the absolute mass transfer coefficient [27]. Kosaraju et al. [23] tested asymmetric poly(4-methyl-1-pentene) (PMP) hollow fiber membranes with an ultrathin dense skin layer for absorption and desorption, and MEA as absorption liquid for the separation of humidified CO_2/N_2 mixtures. They investigated the effect of the liquid velocity on the overall mass transfer coefficient and the CO_2 concentration at the absorber outlet over time. A long-term test showed a decreased CO_2 absorption performance after 55 days [23]. Additional analysis, e.g. determination of the CO_2 permeance through the system, process selectivity and the influence of other parameters such as temperature and pressure would be interesting to complete the characterization and to allow evaluation of the process for the capture of CO_2. Shelekhin et al. [28] used a mathematical approach to investigate membrane gas absorption processes. Although the model failed to predict quantitatively the experimental data, it identified the limits imposed to the system. At low absorbent flow rates, the process selectivity is determined by the selectivity of the liquid, whereas at high absorbent flow rates the system will operate as a simple membrane module and the selectivity is determined by the selectivity of the membrane [28]. In addition to the model calculations, they did experiments with polyvinyltrimethylsilane

(PVTMS) asymmetric membranes as absorber and desorber for the separation of CO_2/CH_4, and found that for very low liquid flow rates CO_2/CH_4 selectivities up to 3500 could be obtained with MEA as absorption liquid [28].

Next to the type of membrane and absorption liquid, also the process parameters such as temperature of absorption and desorption, liquid flow rate, and feed pressure, play an important role and contribute to the overall process performance. Both absorption, desorption and the chemical reaction between the gaseous component to be removed and the absorption liquid are influenced by the temperature. With increasing temperature, the CO_2 physical loading or absorption capacity of the absorption liquid decreases [29, 30], whereas for most absorption liquids, the equilibrium reaction between CO_2 and e.g. the amine solution shifts to the side of the reactants at higher temperature. Absorption is preferably conducted at lower temperatures, whereas higher temperatures are preferred for desorption. Limited literature is found concerning the effect of absorber and desorber temperature on the membrane contactor process performance. Daneshvar et al. [29] showed decreasing CO_2 loading capacity with increasing temperature for aqueous amine solutions tested for a temperature range from 30 to 70°C and CO_2 partial pressure below 100kPa. The flow rate of the absorption liquid is another important variable, as it influences the resistance to mass transfer in the liquid phase boundary layer and determines the time available for absorption and desorption. Yan et al. [3], who worked on the removal of CO_2 from flue gas mixtures using a membrane absorber and a traditional desorber column, studied the influence of the liquid flow rate on the CO_2 mass transfer rate. They showed that the CO_2 mass transfer rate increased with increasing liquid flow rate, which is caused by a decrease of the boundary layer thickness of the liquid phase, thus decreasing the resistance of the liquid phase. Zhang et al. [31] focused on the CO_2 removal from CO_2/N_2 mixtures with an absorber membrane contactor and concluded that in the case of only physical absorption, the resistance to mass transfer of the liquid phase boundary layer was the dominant factor, determining the CO_2 flux. Increase of liquid flow rate decreased this resistance and consequently

resulted in an improved process performance. In the case of chemical absorption (absorption with chemical reaction) of CO_2 in diethanolamine (DEA), the liquid flow rate had only little effect on the performance, and mass transfer at the feed gas side was the limiting factor.

In this work we use a membrane contactor for the separation of CO_2 from CH_4 and we systematically investigate the influence of both the type of membrane and the different process parameters on the overall process performance (permeability and selectivity). Two types of commercially available hollow fiber membranes which differ significantly with respect to their structure are used: hydrophobic, porous polypropylene (PP) hollow fiber membranes and asymmetric poly(phenylene oxide) (PPO) hollow fiber membranes with a dense, ultrathin skin at the outside of the membrane. The PPO membranes are selected because of their extremely high gas permeances despite the dense skin layer (600 GPU for CO_2). They have an intrinsic CO_2/CH_4 selectivity of 22. Monoethanolamine (MEA) is used as the absorption liquid. It is the most often industrially used solvent for the chemical absorption of CO_2. The amine groups present in the solvent selectively and reversibly react with the CO_2 from the feed, a mechanism that has been studied frequently [32-34]. We investigate the effect of the liquid flow rate, feed pressure and temperature of absorption and desorption for the two chosen membrane types. Although our mini plant system is not optimized and optimization would result in much better absolute performance data, this approach allows us to identify the operating window and potential of the process for the capture of CO_2 from CH_4.

This work is unique in a sense that it reports real process performance data (permeances and selectivities) for the total process consisting of an absorption and a desorption step under practical conditions using feed mixtures instead of a single components (e.g. only CO_2). In literature, very frequently only mass transfer coefficients for single gas CO_2 absorption are reported, which provide only limited information about the performance of the process in the real application. In addition we systematically

investigate the influence of both type of membrane and process parameters on the overall process performance.

Experimental Part

Materials

Nitrogen and the gas mixture (CO_2/CH_4 20/80%) were obtained from Praxair, Belgium. Monoethanolamine (purity > 99%) was obtained from Merck, The Netherlands. All chemicals were used without further purification.

Membrane and module preparation

Porous, microfiltration Accurel® S6/2 polypropylene (PP) hollow fibers were purchased from Membrana GmbH (Germany). These fibers had an outer diameter of 2.7 mm, an inner diameter of 1.8 mm and according to the supplier an average pore size of 0.27 µm.
Asymmetric poly phenylene oxide (PPO) hollow fibers were kindly provided by Parker Filtration & Separation B.V. (Etten-Leur, The Netherlands). These fibers had an outer diameter of 0.54 mm and an inner diameter of 0.36 mm. The thickness of the dense, ultrathin skin at the outer side of these fibers was approximately 40-70 nm.

Multiple fiber modules, which contained PP or PPO hollow fibers, were prepared using PVC tubing. The fibers were glued into PVC tubing using poly urethane glue. The inner diameter of the modules was 2.7 cm and the outer diameter was 3.2 cm. Figure 2 shows a schematic picture of the multiple fiber modules.

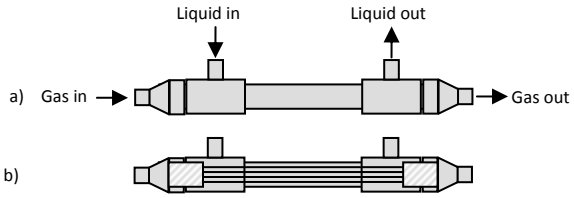

Figure 2: Schematic representation of the modules: a) outside view, b) inside view.

The gas flows through the inner side of the fibers and the liquid circulates at the shell side of the fibers.

Membrane modules with 10 uncoated PP fibers and an effective length of 23.5 cm each were prepared, which resulted in a membrane area of 200.5 cm2 per module. The modules with asymmetric PPO fibers contained 50 fibers with a length of 17 cm each, and the total membrane area per module was 138.2 cm2.

Prior to use the asymmetric, PPO hollow fiber membrane modules were characterized with single gas N_2 and CO_2 permeability measurements to determine the CO_2 over N_2 selectivity. The modules were considered to be defect free when the CO_2/N_2 selectivity was 20.

Membrane contactor experiments

To evaluate the performance of the different membrane types in a membrane contactor, membrane contactor experiments under different conditions were performed. The configuration of the setup used to evaluate the performance of the multiple fiber membrane modules is presented in Figure 3, where both absorber and desorber use a membrane module.

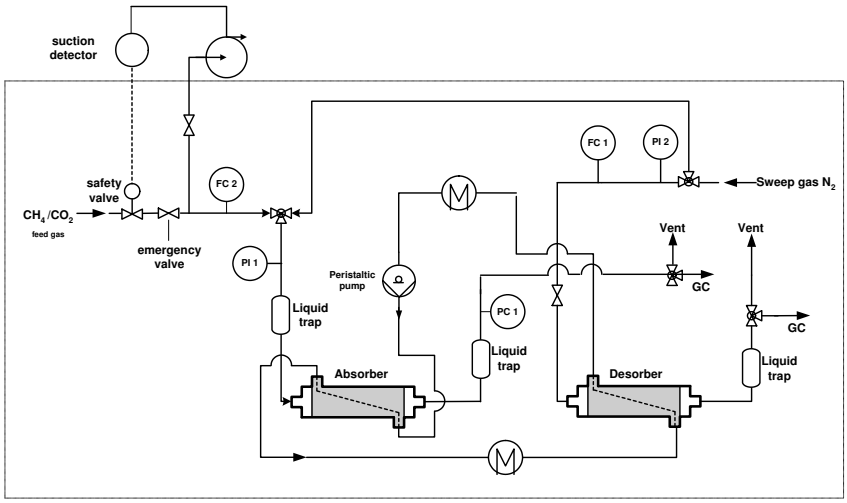

Figure 3: Schematic representation of the experimental membrane contactor setup used for CO_2/CH_4 separation.

The feed gas mixture (CO_2/CH_4 20/80 vol.%) was fed with a flow rate of 10 ml/min through the lumen side of the absorber membranes. The feed pressure was controlled by a back-pressure controller in the retentate flow and this pressure was varied between 1.2 and 3.5 bar. The absorption liquid was circulated at the shell side of the membranes using a Masterflex peristaltic pump. Monoethanolamine (MEA, 10 wt.% aqueous solution) was used as absorption liquid and the flow rate was varied between 19 and 315 ml/min.

The gas-loaded liquid was circulated to the desorber (second membrane contactor). In the desorber, nitrogen, with a flow rate of 5 ml/min, was used as a sweep gas to provide a driving force for desorption of the absorbed gas from the circulation liquid.

The temperature of the absorber was varied from 29°C to 39°C, whereas the temperature of desorption was changed from 29°C to 64°C. This resulted in an effective temperature difference between absorption and desorption from 0 to 35°C. The composition of the gas mixture and the gas flow rate in the retentate and permeate were analyzed using a gas chromatograph (Shimadzu GC-14B).

The gas permeance P (in GPU = 1·10-6 cm_3(STP)/cm_2·s·cmHg) is calculated as the volume flow rate of the permeate stream V multiplied by the volume fraction of the gas in the permeate stream γ, divided by the partial pressure difference over the membrane (Δp) and the membrane area A of one membrane module.

$$P = \frac{\gamma \cdot \mathrm{V}}{A \cdot \Delta p}$$

Calculation of the CO_2 permeance is based on the membrane area of one membrane module only, because either absorption or desorption limits the process and determines the final CO_2 flux of the process: under steady state conditions the gas flow that enters the liquid through the absorber membranes, can only leave the liquid through the desorber membranes. Because absorber and desorber have the same membrane area, permeance values based on the total membrane area can be easily calculated as half the permeances shown.

The selectivity α (CO_2/CH_4) is calculated as:

$$\alpha = \frac{\mathrm{Y}_{\mathrm{CO}_2} / \mathrm{Y}_{\mathrm{CH}_4}}{\mathrm{X}_{\mathrm{CO}_2} / \mathrm{X}_{\mathrm{CH}_4}}$$

Where Y_i is the concentration of component i in the permeate stream that leaves the desorber and X_i is the concentration of component i in the feed.

Results

An important process parameter that influences the performance of the process is the liquid flow rate. Figure 4 shows the effect of the liquid flow rate on a) the CO_2 permeance and b) the CO_2/CH_4 selectivity for the two types of hollow fiber membranes investigated: the hydrophobic, porous polypropylene (PP) hollow fiber membranes and the asymmetric poly(phenylene oxide) (PPO) hollow fiber membranes with a dense, ultrathin skin at the outside of the membrane.

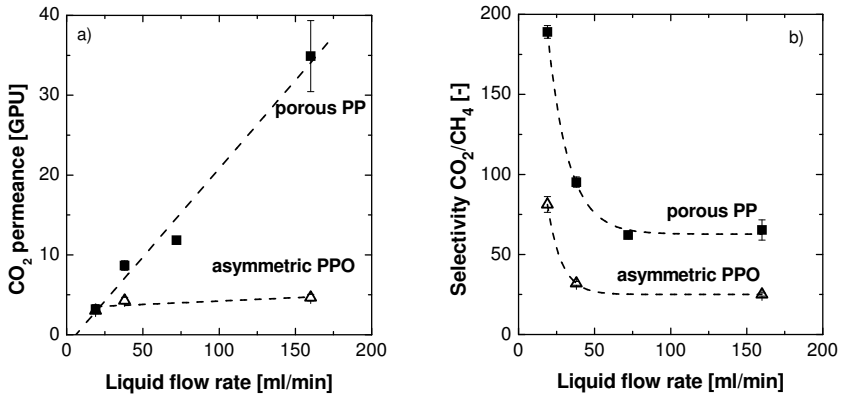

Figure 4: CO_2 permeance (a) and CO_2/CH_4 selectivity (b) as a function of the absorbent liquid flow rate for the two different membranes investigated (Δ T = 35°C; Tabs = 29°C; Δp = 0.2 bar).

In a membrane contactor, three consecutive mass transfer resistances play a role: the resistance of the gas feed boundary layer, the resistance of the membrane and the resistance of the liquid phase boundary layer. Depending on the relative importance of each of these resistances, decrease of the mass transfer resistance of a specific phase may immediately induce an increase in process perfomance. The easiest way to decrease the mass transfer resistance of the liquid phase boundary layer is to increase the liquid flow rate. For the porous PP hollow fiber

membranes, the CO_2 permeance significantly increases with increasing liquid flow rate, whereas for the asymmetric PPO membranes, the liquid flow rate hardly influences the CO_2 permeance. Apparently the resistance of the liquid boundary layer dominates the mass transfer process when porous PP membranes are used, whereas in the case of the asymmetric PPO membranes, mass transfer is governed by the resistance of the membrane with its dense, although ultrathin, top layer. The lower resistance to mass transfer of the liquid boundary layer of course contributes in both absorber and desorber. The decrease in mass transfer resistance leads to a higher absorption and desorption rate and consequently also to a higher degree of saturation in the absorber of the CO_2 loaded solution and higher degree of desorption in the desorber, which increases the driving force for desorption and absorption and thus increases the permeance. As a consequence, the CO_2 absorption capacity of the absorption liquid is more effectively used.

The CO_2/CH_4 selectivity of the process decreases with increasing liquid flow rate. By increasing the liquid flow rate, the supply of absorption liquid (or absorption capacity) is increased, not only for the chemical absorption of CO_2 but also for the physical absorption of both CO_2 and CH_4. Because the selectivity decreases with increasing liquid flow rate, the obtained increase in CH_4 productivity is relatively larger than the increase in CO_2 productivity for both membranes. Apparently especially the physical absorption/desorption is influenced by the hydrodynamic conditions at the liquid side and more sensitive towards the limitation in supply of absorption liquid at low liquid flow rates than the process of chemical absorption of CO_2. So although in an absolute sense the CO_2 capacity of the system increases, its relative increase is lower than the relative increase in CH_4 productivity because of the smaller effect of the liquid flow rate on the chemical absorption compared to the physical absorption. Consequently the selectivity will decrease with increasing liquid flow rate. The same effect was observed by Nymeijer et al. for the separation of ethylene and ethane in a membrane contactor [16].

The selectivity of the system with the asymmetric PPO membranes drops to almost the selectivity of the membrane, as expected, because the membrane is the dominant resistance in this case. For the porous PP membranes, the resistance of the liquid phase boundary layer still dominates the process, and the selectivity of the membrane has not been reached yet, although it is expected that further increase of the liquid flow rate would finally lead to a process selectivity equal to the membrane selectivity [28].

The temperature of the absorber and desorber has a tremendous effect on not only the physical absorption of gases in the liquid, but also influences the reaction kinetics of the system. The effect of the temperature on the CO_2 removal efficiency for the different membrane types has been investigated in two ways. In the first series of experiments, the absorber temperature was set at a constant value and the desorber temperature, was varied. In the second series, the temperature difference between absorber and desorber was kept constant and the absorber and desorber temperature were varied simultaneously. Figure 5 shows the result of the first series of experiments were the temperature of the absorber was kept constant at 29ºC and the temperature difference between the absorption and desorption step was varied.

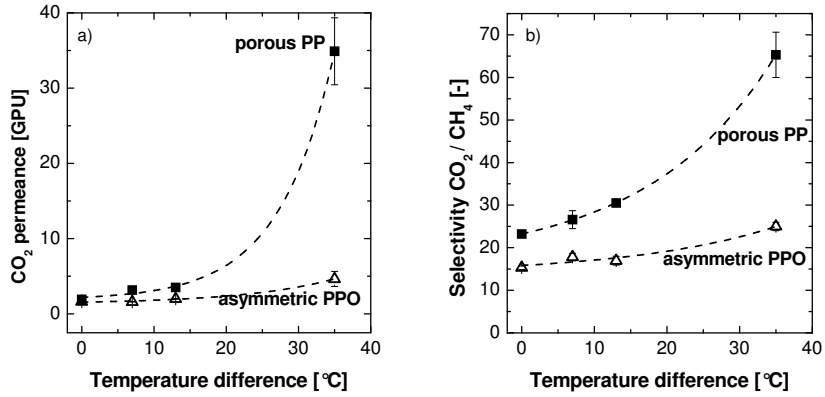

Figure 5: CO_2 permeance (a) and CO_2/CH_4 selectivity (b) as a function of the temperature difference between absorber and desorber. The temperature of the absorber was kept at a constant value of 29°C (liquid flow rate = 160 ml/min; Δp = 0.2 bar).

The CO_2 permeance increases with increasing temperature difference between absorber and desorber. Although the temperature to some extend also influences the membrane permeation characteristics, it mainly influences the physical absorption and desorption processes of CO_2 and CH_4 in the absorption liquid and the chemical absorption, thus the location of the equilibrium of the reversible chemical reaction between CO_2 and the amine solution. Because in the case of the porous membranes, the performance is dominated by these processes occurring in the liquid phase boundary layer, the increase in CO_2 removal with increasing temperature is more pronounced when porous hollow fiber membranes are used. Especially at higher temperature differences between absorber and desorber a significant improvement can be obtained. Because the temperature of the absorber is kept constant and only the temperature of the desorber is increased, the results show that desorption limits the process when porous PP fibers are used.

For the asymmetric PPO fibers, both the membrane and the liquid boundary layer determine the mass transfer process and the positive effect of the temperature, although present, is less significant.

Although the temperature affects both the physical (CO_2 and CH_4) and chemical (CO_2) absorption, the CO_2/CH_4 selectivity increases with increasing desorber temperature, this increase is especially visible when porous PP membranes are used, as expected. Because the absorber temperature is kept constant, an increase in temperature difference stems from an increase in desorber temperature. Increased desorber temperatures decrease the physical absorption capacity of the liquid and as such increases the desorption of both CO_2 and CH_4. In addition to that the increase in desorption temperature shifts the equilibrium to the free CO_2 side thus further increasing the CO_2 productivity. Although the increase in desorber temperature induces an increase in both CO_2 and CH_4 productivity, the relative increase in CO_2 productivity is higher due to the occurrence of the chemical reaction, thus resulting in a strong increase in selectivity with increasing operating temperature of the desorber.

Figure 6 shows the experiments for the porous PP and the asymmetric PPO fibers where the temperature difference between absorber and desorber is kept constant and the temperature of the absorber and desorber are increased simultaneously.

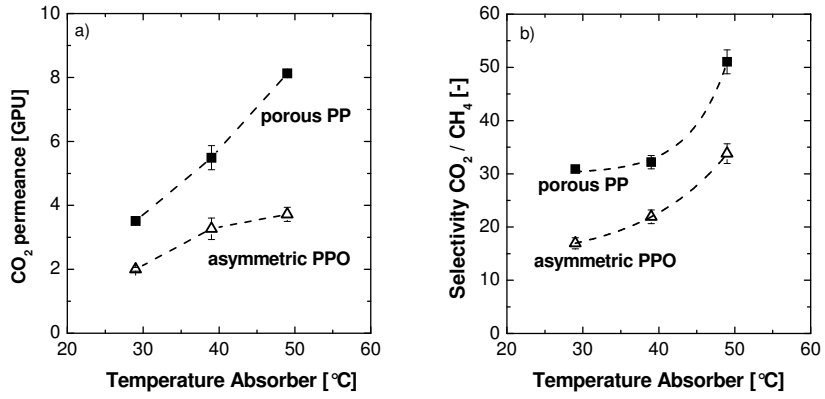

Figure 6: CO_2 permeance (a) and CO_2/CH_4 selectivity (b) as a function of the absorber temperature. The difference in temperature between absorber and desorber is kept constant at Δ T = 13°C (liquid flow rate = 160 ml/min; Δp = 0.2 bar).

Figure 6 confirms that especially the desorption step limits the process. Absorption preferably takes place at lower temperatures, because of the higher physical absorption capacity of the liquid and the location of the equilibrium, which is, at lower temperatures strongly forced to the CO_2-amine reaction product side. Desorption is preferably performed at higher temperatures as it shifts the equilibrium to the free CO_2 side (chemical desorption) and decreases the physical absorption capacity, thus increasing the release of CO_2 from the liquid. Simultaneous increase of both absorber and desorber temperature thus favors desorption, but limits absorption. Nevertheless the performance in terms of CO_2 permeance and CO_2/CH_4 selectivity still increases with increasing temperature, indicating the dominant effect of desorption in this respect. Especially the desorber temperature is an effective process parameter to increase simultaneously the CO_2 productivity and the CO_2/CH_4 selectivity.

So far the performance in terms of both productivity and selectivity of the porous PP membranes showed to be superior over the asymmetric PPO membranes with the dense, ultrathin top layer. A drawback of the use of these porous membranes is their sensitivity towards the feed pressure. To visualize this, Figure shows the CO_2 permeance (a) and the CO_2/CH_4 separation factor (b) as a function of the total feed pressure for the porous PP membranes and for the asymmetric PPO membranes.

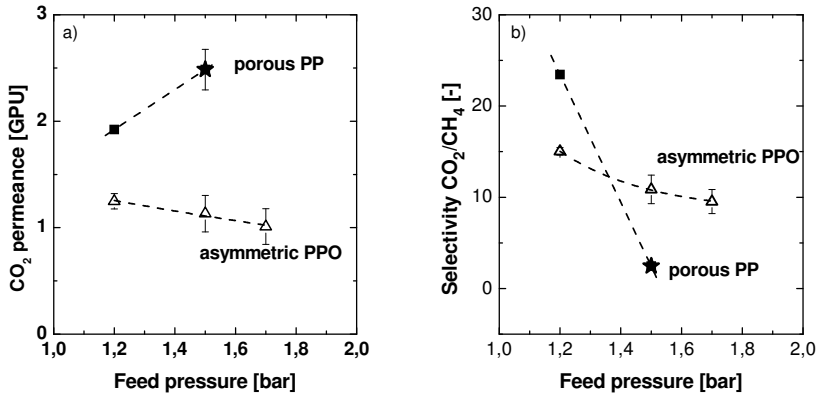

Figure 7: CO_2 permeance (a) and CO_2/CH_4 selectivity (b) as a function of the feed pressure for both the porous PP membranes and the asymmetric PPO membranes (Tabs = Tdes = 29°C; liquid flow rate = 160 ml/min). The star for the PP fibers at a feed pressure of 1.6 bar represents the occurrence of visible gas bubble formation in the absorption liquid.

Although the CO_2 productivity of the porous PP membranes strongly increases with increasing feed pressure, it immediately also results in a tremendous decrease in selectivity, already at very low feed pressures. The reason for this strong increase in productivity and decrease of the selectivity is the formation of feed gas bubbles in the liquid flow instead of selective absorption of CO_2 in the absorption liquid, which is indicated with the star in Figure 7, to account for the occurrence of this additional phenomenon. Due to the only slightly higher feed pressures, the gas can freely flow into the liquid and selective absorption of CO_2 over CH_4 hardly occurs anymore. This shows the strong limitation in the operating

flexibility of the process when porous membranes are used. Small fluctuations in feed pressure immediately result in non-selective absorption and a severe drop in selectivity, already at very low feed pressures. Here the PPO membranes show their superior performance: The sensitivity of the system towards an increase in feed pressure is tremendously reduced when using the asymmetric PPO membranes and only a small decrease in productivity and selectivity is observed with increasing feed pressure. In addition to this, although not quantitatively analyzed but only qualitatively observed, the system with the porous membranes suffers from significant liquid losses due to unlimited evaporation of the solvent through the porous membrane, especially at increased desorption temperatures. In contrast, the asymmetric PPO membrane with its dense, ultrathin top layer, imposes an additional barrier and restricts evaporation of the liquid, thus improving the process. The asymmetric PPO membranes with the dense top layer are more resistant to pressure fluctuations and limits the loss of absorption liquid, which thus significantly increases the performance and operating window of the process.

Conclusions

In this work both commercially available porous PP hollow fiber membranes and asymmetric PPO hollow fiber membranes have been used in a membrane contactor for the separation of CO_2 and CH_4 and the influence of the different process parameters on productivity and selectivity has been evaluated. The proposed approach allows us to identify the operating window and potential of the process. In the case of the porous PP fibers, the main resistance against mass transfer is located in the liquid boundary layer, whereas in the case of the asymmetric PPO membranes the resistance of the membranes is the dominant factor and determines the performance. For the PP membranes, an increase in liquid flow rate thus results in a direct increase in CO2 productivity. Desorption is the limiting step in the process and ways to overcome this by e.g. increasing the temperature of desorption immediately result in improved performance data. Although the performance of the PP membranes outperforms the performance of the PPO membranes in terms of productivity and selectivity, the PP fibers are extremely sensitive to only small variations in the feed pressure, resulting in severe performance loss. In addition to that, extremely high liquid losses are observed for the PP fibers especially at elevated temperatures. In contrast, the asymmetric PPO membranes with the dense, ultrathin top layer restrict evaporation of the liquid. Also in terms of the sensitivity of the system towards variations in feed pressure, the PPO membranes show their superior character, which thus improves the performance and significantly increases the operating window and potential of the membrane contactor process.

References

1. C.-S. Tan, J.-E. Chen, Absorption of carbon dioxide with piperazine and its mixtures in a rotating packed bed, Separation and Purification Technology, 49 (2006) 174

2. S. Ma'mun, V.Y. Dindore, H.F. Svendsen, Kinetics of the Reaction of Carbon Dioxide with Aqueous Solutions of 2-((2-Aminoethyl)amino)ethanol, Ind. Eng. Chem. Res., 46 (2007) 385-394

3. S.-P. Yan, M.-X. Fang, W.-F. Zhang, S.-Y. Wang, Z.-K. Xu, Z.-Y. Luo, K.-F. Cen, Experimental study on the separation of CO_2 from flue gas using hollow fiber membrane contactors without wetting, Fuel Processing Technology, 88 (2007) 501

4. C. Alie, L. Backham, E. Croiset, P.L. Douglas, Simulation of CO_2 capture using MEA scrubbing: A flowsheet decomposition method, Energy Conversion and Management, 46 (2005) 475

5. J. Zhang, S. Zhang, K. Dong, Y. Zhang, Y. Shen, X. Lv, Supported Absorption of CO_2 by Tetrabutylphosphonium Amino Acid Ionic Liquids, Chemistry - A European Journal, 12 (2006) 4021-4026

6. P.H.M. Feron, A.E. Jansen, Capture of carbon dioxide using membrane gas absorption and reuse in the horticultural industry, Energy Conversion and Management, 36 (1995) 411

7. J.-G. Lu, Y.-F. Zheng, M.-D. Cheng, L.-J. Wang, Effects of activators on mass-transfer enhancement in a hollow fiber contactor using activated alkanolamine solutions, Journal of Membrane Science, 289 (2007) 138

8. D. deMontigny, P. Tontiwachwuthikul, A. Chakma, Using polypropylene and polytetrafluoroethylene membranes in a membrane contactor for CO2 absorption, Journal of Membrane Science, 277 (2006) 99

9. P.H.M. Feron, A.E. Jansen, CO_2 separation with polyolefin membrane contactors and dedicated absorption liquids: Performances and prospects, Separation and Purification Technology, 27 (2002) 231

10. S. Atchariyawut, R. Jiraratananon, R. Wang, Separation of CO_2 from CH4 by using gas-liquid membrane contacting process, Journal of Membrane Science, 304 (2007) 163

11. J.L. Li, B.H. Chen, Review of CO_2 absorption using chemical solvents in hollow fiber membrane contactors, Separation and Purification Technology, 41 (2005) 109

12. B.D. Bhide, A. Voskericyan, S.A. Stern, Hybrid processes for the removal of acid gases from natural gas, Journal of Membrane Science, 140 (1998) 27

13. P.S. Kumar, J.A. Hogendoorn, P.H.M. Feron, G.F. Versteeg, New absorption liquids for the removal of CO_2 from dilute gas streams using membrane contactors, Chemical Engineering Science, 57 (2002) 1639

14. B.D. Freeman, Basis of permeability/selectivity tradeoff relations in polymeric gas separation membranes, Macromolecules, 32 (1999) 375

15. A. Gabelman, S.T. Hwang, Hollow fiber membrane contactors, Journal of Membrane Science, 159 (1999) 61

16. K. Nymeijer, T. Visser, R. Assen, M. Wessling, Super selective membranes in gas-liquid membrane contactors for olefin/paraffin separation, Journal of Membrane Science, 232 (2004) 107

17. V.Y. Dindore, D.W.F. Brilman, P.H.M. Feron, G.F. Versteeg, CO_2 absorption at elevated pressures using a hollow fiber membrane contactor, Journal of Membrane Science, 235 (2004) 99

18. M. Teramoto, S. Shimizu, H. Matsuyama, N. Matsumiya, Ethylene/ethane separation and concentration by hollow fiber facilitated transport membrane module with permeation of silver nitrate solution, Separation and Purification Technology, 44 (2005) 19

19. S. Karoor, K.K. Sirkar, Gas absorption studies in microporous hollow fiber membrane modules, Ind. Eng. Chem. Res., 32 (1993) 674-684

20. S.-H. Yeon, K.-S. Lee, B. Sea, Y.-I. Park, K.-H. Lee, Application of pilot-scale membrane contactor hybrid system for removal of carbon dioxide from flue gas, Journal of Membrane Science, 257 (2005) 156

21. S. Ma'mun, R. Nilsen, H.F. Svendsen, O. Juliussen, Solubility of carbon dioxide in 30 mass % monoethanolamine and 50 mass % methyldiethanolamine solutions, Journal of Chemical and Engineering Data, 50 (2005) 630

22. Y. Lee, R.D. Noble, B.-Y. Yeom, Y.-I. Park, K.-H. Lee, Analysis of CO_2 removal by hollow fiber membrane contactors, Journal of Membrane Science, 194 (2001) 57

23. P. Kosaraju, A.S. Kovvali, A. Korikov, K.K. Sirkar, Hollow Fiber Membrane Contactor Based CO_2 Absorption-Stripping Using Novel Solvents and Membranes, Ind. Eng. Chem. Res., 44 (2005) 1250-1258

24. H. Kreulen, C.A. Smolders, G.F. Versteeg, W.P.M. Van Swaaij, Microporous hollow fibre membrane modules as gas-liquid contractors. Part 1. Physical mass transfer processes. A specific application: Mass transfer in highly viscous liquids, Journal of Membrane Science, 78 (1993) 197

25. D.C. Nymeijer, B. Folkers, I. Breebaart, M.H.V. Mulder, M. Wessling, Selection of Top Layer Materials for Gas-Liquid Membrane Contactors, Journal of Applied Polymer Science, 92 (2004) 323

26. K. Li, W.K. Teo, An Ultrathin Skinned Hollow Fibre Module for Gas Absorption at Elevated Pressures, Chemical Engineering Research and Design, 74 (1996) 856

27. H. Kreulen, C.A. Smolders, G.F. Versteeg, W.P.M. Van Swaaij, Determination of mass transfer rates in wetted and non-wetted microporous membranes, Chemical Engineering Science, 48 (1993) 2093

28. A.B. Shelekhim, I.N. Beckman, Gas separation processes in membrane absorber, Journal of Membrane Science, 73 (1992) 73

29. N. Daneshvar, M.T. Zaafarani Moattar, M. Abedinzadegan Abdi, S. Aber, Carbon dioxide equilibrium absorption in the multi-component systems of CO_2 + TIPA + MEA + H_2O, CO_2 + TIPA + Pz + H_2O and CO_2 + TIPA + H_2O at low CO_2 partial pressures: experimental solubility data, corrosion study and modeling with artificial neural network, Separation and Purification Technology, 37 (2004) 135

30. O.F. Dawodu, A. Meisen, Solubility of carbon dioxide in aqueous mixtures of alkanolamines, Journal of Chemical and Engineering Data, 39 (1994) 548

31. H.-Y. Zhang, R. Wang, D.T. Liang, J.H. Tay, Modeling and experimental study of CO_2 absorption in a hollow fiber membrane contactor, Journal of Membrane Science, 279 (2006) 301

32. P.M.M. Blauwhoff, G.F. Versteeg, W.P.M. Van Swaaij, A study on the reaction between CO_2 and alkanolamines in aqueous solutions, Chemical Engineering Science, 38 (1983) 1411

33. G.F. Versteeg, L.A.J. Van Dijck, W.P.M. Van Swaaij, On the kinetics between CO_2 and alkanolamines both in aqueous and non-aqueous solutions. An overview, Chemical Engineering Communications, 144 (1996) 133

34. R.J. Littel, G.F. Versteeg, W.P.M. Van Swaaij, Kinetics of CO_2 with primary and secondary amines in aqueous solutions-II. Influence of temperature on zwitterion formation and deprotonation rates, Chemical Engineering Science, 47 (1992) 2037

CHAPTER 3

Kinetics of CO_2 absorption in aqueous sarcosine salt solutions – Influence of concentration, temperature and CO_2 loading

Abstract

Amino acid salt solutions are a promising alternative to alkanolamines (e.g. MEA) as absorption liquid for CO_2 removal due to their ionic nature, low evaporative losses and higher oxidative and thermal stability. Screening of literature indicates that within the class of amino acid salts, sarcosine is a promising candidiate because of its relatively high CO_2 loading capacity and reactivity.

In this work CO_2 absorption experiments in the so-called pseudo-first-order regime were carried out to determine the reaction rate expression and reaction rate constant of CO_2 absorption in aqueous sarcosine salt solutions. Next to the influence of the sarcosine concentration (0.5 to 3.8 M) and temperature (298 to 308 K) on the rate of reaction, the reaction rate constants for partially loaded sarcosinate solutions were investigated.

Compared to MEA, very high reaction rate constants for the carbamate formation were obtained for aqueous sarcosine salt solutions. The reaction order in CO_2 was found to be one (in accordance with literature) and for potassium sarcosinate an (apparent) reaction order of 1.66 was found. The activation energy was found to be approximately 26 kJ/mol. The apparent

rate of the reaction strongly decreases with increasing partial loading of the solution with CO_2 and was found to be directly related to the decrease in free amine concentration in the solution. This observation is especially relevant for cyclic absorption processes such as gas-liquid membrane contactors, were incomplete solvent regeneration is likely to occur.

Introduction

Amino acid salt solutions have been recognized as an alternative to the traditional aqueous amine solutions for CO_2 removal [1, 2]. The conventional (alkanol-)amine based absorption liquids, like mono ethanol amine (MEA), have the advantages of high product yields and purities, but suffer from drawbacks like corrosiveness, unstability in the presence of oxygen [3] and high liquid losses due to evaporation. In contrast to MEA, amino acids exhibit a high oxidative stability [1, 3, 4], have a better resistance to degradation [2] and can be made non-volatile by adding a salt functionality as counter ion, which significantly reduces the liquid losses [2, 3, 5]. Furthermore, amino acids have similar reactivity and CO_2 absorption capacity as related classes of alkanolamines [6].

One potential drawback of amino acid salt solutions is the possibility that the salts can precipitate during CO_2 absorption. Majchrowicz et al. [7] showed the relationship between precipitation behavior, CO_2 partial presssure and salt concentrations. For the use of an amino acid salt solution as absorption liquid in gas-liquid contacting processes and more specifically in gas-liquid membrane contactors, amino acid salt solutions that do not precipitate at working conditions are preferred.

A promising amino acid which shows a relatively large window of operation without precipitation [7] and has an expected high CO_2 loading capacity due to its secondary amine group, is the potassium salt of sarcosine. The structure of sarcosine and its potassium salt form are shown in Figure 1.

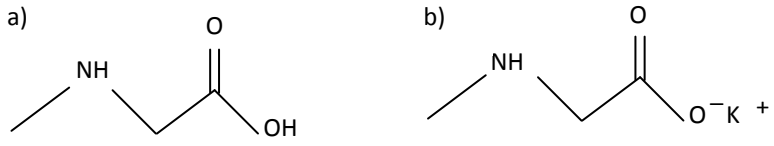

Figure 1: Chemical structure of a) sarcosine and b) the potassium salt of sarcosine.

For CO_2 removal, a fast reaction between CO_2 and the absorption liquid is required to minimize absorber equipment size and hence investment

costs. To enable the evaluation of a new solvent in a cyclic absorption-desorption process (e.g. gas-liquid (membrane) contacting processes), knowledge on the absorption capacity and reaction kinetics of the specific gas-liquid combination is required.

For the absorption kinetics, important variables are the process temperature and the concentration of the solvent in the aqueous solution. Generally, the reaction rate strongly depends on the temperature [8-11] and the concentration of the amine-containing solvent. In addition to concentration and temperature, also the degree of CO_2 loading of the solution is of interest. As absorption liquids are often used in continuous CO_2 absorption-desorption cycles, the effect of the CO_2 loading of the solvent on the absorption kinetics is highly relevant. Often, desorption is not complete, and hence partially CO_2 loaded solutions reach the absorber. Feron et al. [5] showed for a membrane absorber that a significant reduction in the CO_2 mass flux was obtained at higher CO_2 loading of the circulating liquid. Evaluation of the absorption rate and reaction rate constant as a function of the CO_2 loading provides useful input for the design of absorber systems.

In this work, the properties of an aqueous sarcosine salt solution as new absorption liquid for CO_2 absorption in gas-liquid contacting processes are quantified [12]. Kinetic experiments in the pseudo-first-order regime are carried out using a gas-liquid stirred cell contactor to determine the reaction rate constant of CO_2 absorption in aqueous sarcosine salt solutions. Next to the influence of the sarcosine-salt concentration (0.5 to 3.8 M) and the temperature (298 to 308 K), the reaction rate constant for partially CO_2-loaded sarcosine salt solutions (0 to 0.5 mol CO_2/mol sarcosine salt solution) is determined.

Theory

Absorption of carbon dioxide in a primary or secondary amino acid salt (RR'NH) solution occurs according to the following reactions:

$$CO_2 + 2\ RR'NH \rightleftharpoons RR'NCOO^- + RR'NHH^+ \quad (1)$$

$$CO_2 + OH^- \rightleftharpoons HCO_3^- \quad (2)$$

$$CO_2 + H_2O \rightleftharpoons H_2CO_3 \quad (3)$$

The first reaction (carbamate formation) between carbon dioxide and the amino acid salt is the most relevant for primary and (most) secondary amines, except for solvents with strong sterical hindrance that form bicarbonate rather than carbamates. For amino acid salt solutions, Kumar et al. showed that the third reaction has a negligible contribution, but the second reaction (bicarbonate formation) has to be taken into account [6].

Reaction 1 can be described using the zwitterion mechanism [6, 13-15], where the reaction between an amino acid salt and CO_2 is described to proceed as follows:

$$CO_2 + RR'NH \underset{k_{-1}}{\overset{k_2}{\rightleftharpoons}} RR'N^+HCOO^- \quad (4)$$

Where RR'NH is the amino acid (AmA) that reacts with carbon dioxide to become a zwitterion, $RR'N^+HCOO^-$ (Zwit). The equilibrium of the reaction is predominantly to the right hand side. Then the zwitterion is deprotonated by a base B (e.g. another amino acid salt) according to:

$$RR'N^+HCOO^- + B \overset{k_b}{\rightleftharpoons} RR'NCOO^- + BH^+ \quad (5)$$

The deprotonation reaction is assumed to be essentially irreversible (equilibrium predominantly to the right hand side of the reaction). The kinetics of these reactions can be described by Equation 6 for the reaction of the amino acid (AmA) with CO_2 and subsequently by Equation 7 for the deprotonation of the zwitterion (Zwit):

$$-R_{CO2} = k_2[AmA]\cdot[CO_2] - k_{-1}[zwit] \quad (6)$$

$$-\frac{d[zwit]}{dt} = k_2[AmA]\cdot[CO_2] - \sum_b k_b[B]\cdot[zwit] - k_{-1}[zwit] \quad (7)$$

Where $\sum k_b \cdot [B]$ indicates the contribution of the bases (amine, H_2O, OH^-), which are present in the solution for the deprotonation step.
Taking into account the assumption of quasi-steady state condition for the zwitterion concentration, the overall forward reaction rate is given by:

$$R_{CO2} = \frac{k_2[AmA]\cdot[CO_2]}{1 + \frac{k_{-1}}{\sum k_b[B]}} \quad (8)$$

Kinetics

Pseudo-first-order regime

In the case of CO_2 absorption in an aqueous sarcosine salt solution, both physical gas absorption and a chemical reaction occur simultaneously. Certain conditions need to be fulfilled to accurately determine the reaction rate constant, which are conveniently summarized in the Hatta-number (Ha). It correlates the maximum reaction rate of the absorbed gas phase component (here: CO_2) in the liquid phase boundary layer at the gas-liquid interface to the maximum rate of diffusion (transport) through that mass transfer zone.

When the Hatta number is larger than 3 (Ha>3), the absorption flux is dominated by the chemical reaction under the assumption that sufficient liquid phase reactant (here: sarcosine) is available within the boundary layer. In that specific case, the enhancement factor (E), which represents the ratio of the absorption flux in the presence of chemical reaction to the absorption flux in the same liquid without chemical reaction, equals the Hatta-number.

The absorption of the gas into the liquid can however be limited by the diffusion (transport) of the liquid phase reactant to the reaction zone at the gas-liquid interface. In that case the maximum enhancement factor (E_∞) is reached when the diffusion of the reactants to the reaction zone is rate determining. Hence, in order for the chemical reaction to be rate determining in the absorption process, the Hatta number needs to be considerably smaller than the infinite enhancement factor. When these conditions are fulfilled i.e. $3<Ha$ and $E_\infty/Ha>5$, the actual enhancement factor E equals the Hatta number and gas absorption occurs in the pseudo-first-order regime [16].

For each experiment the Hatta number and infinite enhancement factor needs to be calculated. The Hatta number can be calculated with Equation 9 [13]:

$$Ha = \frac{\sqrt{k_{ov} D_{CO_2-solution}}}{k_L} \quad (9)$$

Where k_{ov} is the overall reaction rate constant of the carbamate formation and the bicarbonate formation (Equation 1 and 2), $D_{CO_2-solution}$ is the diffusion coefficient of CO_2 in the solution and k_L equals the liquid-side physical mass transfer coefficient, which can be estimated from experimental data for CO_2 absorption in water and/or N_2O absorption in the amino acid salt solution, taking into account temperature and viscosity corrections.

The infinite enhancement factor, E_∞, is estimated by Equation 10 [13] (derived for irreversible reactions, as the equilibrium of the reaction is predominantly to the right hand side, and using the penetration theory to describe mass transfer):

$$E_\infty = \sqrt{\frac{D_{CO_2-solution}}{D_{AmA-solution}}} + \frac{[AmA]\cdot 10^3}{\nu_{AmA}\frac{p_{CO_2}}{H_{CO_2}}} \sqrt{\frac{D_{AmA-solution}}{D_{CO_2-solution}}} \quad (10)$$

Where $D_{AmA-solution}$ is the diffusion coefficient of sarcosine in an aqueous sarcosine salt solution (values available in literature [17]), $D_{CO_2-solution}$ equals the diffusivity of CO_2 in the solution, P_{CO2} is the partial pressure of CO_2, H_{CO2} is the Henry coefficient and ν_{AmA} is the stoichiometric coefficient for the amino acid salt, which has according to reaction 1 in analogy with alkanolamines a value of 2 [18, 19].

Reaction rate constant

In the pseudo-first-order regime, the overall reaction rate constant k_{ov}, can be determined by measuring the CO_2 absorption rate in a stirred cell contactor with known gas-liquid interfacial area (Equation 11) [20]. In this regime, the CO_2 flux is independent of the liquid side physical mass transport coefficient k_L, viz. independent of the liquid phase stirring speed.

$$J_{CO_2} A = (\sqrt{k_{ov} D_{CO_2-solution}}) \cdot m_{CO_2-solution} \cdot \left(\frac{P_{CO_2}}{RT} \right) \cdot A \qquad (11)$$

$D_{CO_2-solution}$ is the diffusivity of CO_2 in the solution, P_{CO_2} is the partial pressure of CO_2 in the stirred cell and A is the geometric gas-liquid contacting area. The parameter $m_{CO_2-solution}$ (also called m-value) is a dimensionless distribution coefficient of CO_2 between the gas and the liquid phase. It describes the physical solubility of CO_2 in the solution and equals (R·T) divided by the Henry coefficient (H_{CO2}). The parameter m is defined by $m = C_{l,i} / C_{g,i}$, in which $C_{g,i}$ equals the CO_2 concentration in the gas phase and $C_{l,i}$ the corresponding physical solubility in the liquid phase.
When the CO_2 partial pressure in the reactor vessel is kept constant by continuously feeding the gas from the storage vessel to the reaction vessel, the CO_2 absorption rate into the liquid phase can be calculated from the pressure decay in the storage tank with the following Equation:

$$J_{CO_2} A = \frac{dP_{storage}}{dt} \frac{V_{storage}}{R, T_{storage}} \qquad (12)$$

Where $V_{storage}$ is the volume and $T_{storage}$ is the temperature of the gas storage vessel. In this case the decrease in feed pressure in the gas storage vessel in time ($dP_{storage}/dt$) is directly related to the CO_2 absorption flux (J_{CO2}).

From Equations (11) and (12) the k_{ov}-values can be determined from the monitored pressure-time curves of the feed gas reservoir. The overall rate constant, k_{ov}, predominantly comprises the contribution of the chemical reactions in Equation 1 and 2.

$$k_{ov} = k_{OH^-} \cdot [OH^-] + k_{app} \qquad (13)$$

Where k_{OH^-} is the zwitterion mechanism deprotonation rate constant for OH^-, which was obtained from Pohorecki et al. [21], k_{app} the apparent rate constant for the chemical reaction (4) and $[OH^-]$ the concentration of OH^-, which is determined by pH measurements.
From the k_{app}-values the reaction rate expression can be further evaluated assuming power-law kinetics with respect to the concentration of the amino acid salt reactant to hold:

$$k_{app} = k_2 \cdot [AmA]^n \tag{14}$$

Physical solubility of CO_2

Due to the chemical reaction of CO_2 and the amino acid, it is not possible to directly determine the physical solubility of CO_2 in the amino acid salt solution ($m_{CO2\text{-}solution}$). Based on the similarities concerning configuration, molecular volume and electronic structure between CO_2 and the non-reactive N_2O, N_2O is used to estimate the physical solubility of CO_2 in the absorption liquid. The physical solubility of N_2O ($m_{N2O\text{-}solution}$) is determined experimentally and using the analogy between both gases, the physical solubility of CO_2 can be estimated according to [8, 22]:

$$m_{CO_2-solution} = \frac{m_{CO_2-H_2O}}{m_{N_2O-H_2O}} \cdot m_{N_2O-solution} \tag{15}$$

This N_2O-CO_2 analogy is frequently used for this purpose. The relative solubility in water is given by [8]:

$$\frac{m_{CO_2-H_2O}}{m_{N_2O-H_2O}} = 3.04 \exp\left(-\frac{240}{T}\right) \tag{16}$$

Where $m_{CO2\text{-}H2O}$ and $m_{N2O\text{-}H2O}$ are the physical solubility of CO_2 and N_2O in water.

The physical solubility of N_2O in the amino acid salt solution can also be estimated from the methodology developed by Schumpe et al. [23], which is based on the salting-out effect and relates the physical distribution coefficient of N_2O in the absorption solution to its corresponding value in water:

$$\log\left(\frac{m_{N_2O-H_2O}}{m_{N_2O-solution}}\right) = \sum (h_i + h_g) c_{i,solution} \qquad (17)$$

Where h_i is the ion-specific parameter, h_g is the gas specific parameter and c is the concentration of ions in the solution. The N_2O solubility in water depends on the temperature according to the following relation [24]:

$$m_{N_2O-H_2O} = 1.17\,x10^{-7} \cdot RT \cdot \exp\left(\frac{2284}{T}\right) \qquad (18)$$

Also the gas specific parameter h_g is temperature dependent and Weisenberger et al. [25] suggested the following relation:

$$h_g = h_{g,o} + h_T\,(T - 298.15) \qquad (19)$$

Where h_i is the ion specific parameter, $h_{g,0}$ is the gas specific parameter at 298K and h_T is the temperature correction parameter. The values for the Schumpe parameters h_i, $h_{g,0}$ and h_T are given in Table 1.

Table 1: Schumpe model parameters h_i, $h_{g,0}$ and h_T [24, 25]

h^+ (K^+) (L/mol)		0.0922
h^- (sarcosine) (L/mol)	0.068[a]	0.056[b]
$h_{g,0}$ (N_2O) (L/mol)		-0.0085
$10^3 \cdot h_T$ (L/mol K)		-0.479

[a] data from van Holst et al. [24]

[b] this work

Diffusivity of CO_2

The diffusivity of CO_2 in the aqueous sarcosine salt solution ($D_{CO2\text{-}solution}$) can be estimated with the modified Stokes-Einstein relation [16, 26]:

$$\mu_{solution}^{0.6} D_{CO_2-solution} = \mu_{H_2O}^{0.6} D_{CO_2-H_2O} \qquad (20)$$

Where $D_{CO_2-H_2O}$ is the diffusivity of CO_2 in water and $\mu_{solution}$ and μ_{H_2O} are the viscosities of the solution and water, respectively. The values for the CO_2 diffusivities in water and the viscosities of the solution for the system under investigation can be taken from literature [3, 20].

Experimental part

Materials

Carbon dioxide (5.0) was obtained from Praxair, Belgium. Sarcosine was obtained from Fluka, Germany. Potassium hydroxide and the hydrochloric acid solution were purchased from Merck, The Netherlands. Monoethanolamine (MEA) was purchased from Merck, Germany. All chemicals were used without further purification.

Solution preparation

The solid sarcosine was mixed with an equimolar amount of solid potassium hydroxide. The actual purity of the KOH was determined by acid titration. The reaction is exothermic and gives water as side product. The actual concentration of the aqueous sarcosine salt solution was determined by titration with a standard 1 mol/L HCl solution.

The addition of potassium hydroxide is necessary to transform sarcosine (see Figure 1a) into its salt form (see Figure 1b) and to support the amino acid reaction with CO_2. If no KOH would be added, the amino acid would remain in zwitterionic form when it is dissolved in water. The amine group would be protonated and CO_2 would not be able to form a carbamate with the amino acid.

Physical solubility of N_2O

The physical solubility of N_2O was determined experimentally in a thermostated glass vessel. A certain amount of solution was put in this vessel and evacuated under continuous stirring to remove inert gasses from the system. Afterwards the reactor vessel was closed and the stirrer was switched off. When the temperature was constant at the set-point and the vapor-liquid equilibrium was reached (p_{vap}), N_2O gas was fed to the vessel until a certain pressure was reached. The vessel was closed, the stirrer was switched on and the pressure decrease in the vessel in time was

measured using a pressure transducer. When equilibrium was reached, the measurement was stopped and the physical solubility was determined the using following Equation, which is based on Henry's law:

$$m_{N_2O-solution} = \frac{p_{\text{int}} - p_{eq}}{P_{eq} - p_{vap}} \cdot \frac{V_g}{V_l} \qquad (21)$$

Where p_{int} is the initial pressure at the start of the experiment just after gas inlet, p_{eq} is the equilibrium pressure and p_{vap} the vapor pressure of the solution. V_g is the volume of the gas phase and V_l is the volume of the liquid phase.

Liquid phase mass transfer coefficient

To calculate the Hatta number for the verification of the assumption of the pseudo-first-order regime, the mass transfer coefficient of the liquid phase boundary layer (k_L) has to be determined. This value can be extracted from the the batchwise absorption of CO_2 in water and/or N_2O in the amine solution. A double-walled reactor vessel was filled with a volume of water and the temperature regulated with a heating bath. After degassing of the vessel, and when the vapor-liquid equilibrium was reached (p_{vap}), the stirrer was stopped and the reactor was pressurized with CO_2 to approximately atmospheric pressure. This initial pressure (p_{int}) was measured, the stirrer was started and the pressure decrease in the vessel in time was measured. The liquid-side mass transfer coefficient can be derived from a molar balance over the gas phase:

$$\frac{dN_{CO_2}}{dt} = \frac{dp_{CO_2}}{dt}\frac{V_g}{RT_g} = -k_l A\left(\frac{p_{CO_2}}{H_{CO_2}} - c_{CO_2-liquid}\right) \qquad (22)$$

in which p_{CO2} is the partial pressure of CO_2 in the gas phase of the reactor vessel and $c_{CO2\text{-}liquid}$ is the concentration of CO_2 in the liquid phase. The

amount of CO_2 absorbed by the liquid can be determined from the overall CO_2 balance over the reactor vessel:

$$c_{CO_2-liquid} = \frac{V_g}{RT_g V_l}\left(p_{\text{int}-CO_2} - p_{CO_2}\right) \tag{23}$$

Integrating p_{CO2} over dp_{CO2} gives Equation 24 [27]

$$\ln\left[\frac{\left(\frac{RT_g}{H_{CO_2}}V_l + V_g\right)\frac{p_{CO_2}}{p_{\text{int}-CO_2}} - V_g}{\frac{RT_g}{H_{CO_2}}V_l}\right] = -k_l A\left(\frac{RT_g}{V_g H_{CO_2}} + \frac{1}{V_l}\right)t \tag{24}$$

The values for the partial pressure of CO_2 (p_{CO2}) and the initial partial pressure of CO_2 ($p_{int\text{-}CO2}$) are corrected for the vapor pressure of the liquid:

$$p_{CO_2} = p_{tot} - p_{vap} \tag{25}$$

Kinetic measurements

To determine the reaction rate constants the experiment was performed in the reactor vessel described by Haubrock et al [20] and presented in Figure 2.

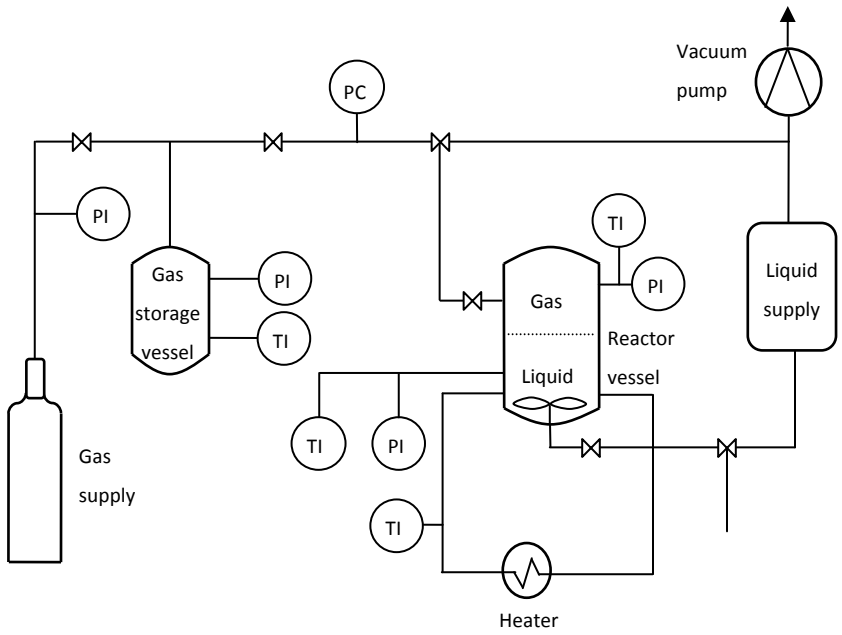

Figure 2: Schematic flow sheet of the setup used to determine reaction kinetics.

The glass reactor vessel has a total volume of 1070 ml, of which ±600 ml was filled with the absorption liquid. The liquid phase in the reactor was stirred by a flat-blade stirrer at a rotational speed of around 60 rpm. The temperature in the reactor vessel was regulated by a heating bath. The gas and the liquid phase had a contact surface area of 71.5 cm^2. The reactor vessel was fed with carbon dioxide from a reservoir, which has a volume of 100 ml. At the beginning of an experiment the pressure in the reservoir was 5 bar. The decrease in pressure in the reservoir in time was measured with a digital pressure transducer. During the experiments the CO_2 partial pressure in the reactor vessel was kept between 4 and 13 mbar.

Before the experiment started, fresh absorption liquid was added and the liquid in the reactor vessel was evacuated under continuous stirring for 30

minutes to remove (dissolved) inert gasses from the liquid and gas phase. Afterwards the reactor vessel was closed and the stirrer was switched off. When the pressure in the reactor was constant and the equilibrium vapor pressure was reached, the experiment was started. The valve from the gas reservoir to the reactor vessel was opened and the stirrer was switched on. The actual absorption experiment were the pressure decrease in the gas reservoir in time was monitored was performed for at least 15 minutes.

Experimental variables

Three different sets of kinetic experiments were performed with sarcosine salt solutions:

1. The influence of the concentration of the sarcosine salt solution as absorption liquid on the kinetics of the reaction was determined from absorption experiments at various concentrations of the aqueous sarcosine salt solution in the range of 0.5 to 3.8 mol/L at 298 K;
2. The influence of the temperature on the reaction rate constant was determined for a range of 298 to 308 K for an aqueous sarcosine salt solution of 1.5 M;
3. The effect of the degree of CO_2 loading (α) of the sarcosine salt solution on the reaction kinetics was investigated. For these experiments a 1.45 M sarcosine salt solution was pre-loaded with a certain amount of CO_2, and the reaction rate constant for the absorption of CO_2 in this partially loaded solution at a temperature of 298 K was determined. The exact CO_2 loading of the solution was determined by titration, as explained by Blauwhoff [28].

Next to the experiments with sarcosine salt solutions, for validation of the measurement technique CO_2 absorption experiments in MEA in the pseudo-first-order regime were performed as a function of concentration (1.5 – 2M) and compared to literature data.

Results

Physical solubility of CO_2

For the determination of the reaction rate constant, the values of the physical solubility of CO_2 are required. These can be calculated from the experimentally determined physical solubility data of N_2O or from the correlations proposed by Schumpe [23] as described in the previous part. Figure 3 shows both the experimentally determined and the calculated N_2O solubility coefficients (m-values) as a function of a) the solution concentration b) the temperature.

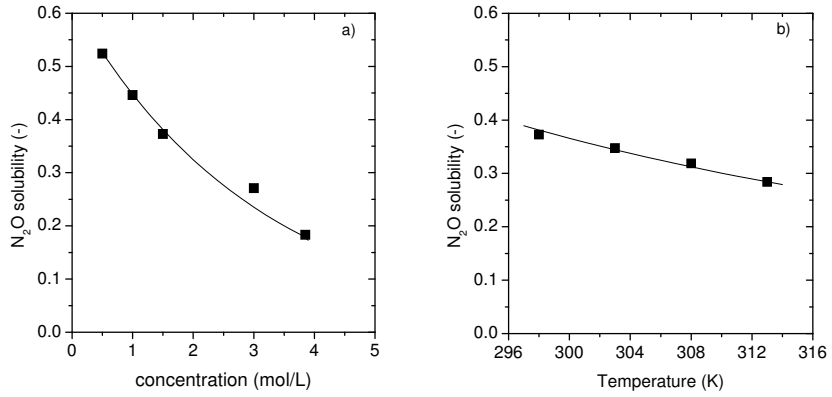

Figure 3: Experimentally determined physical N_2O solubility coefficients (m-value) (■) and the calculated physical N_2O solubility coefficients according to the correlations of Schumpe and Weisenberg [23, 25] (line) as a function of a) concentration (T = 298 K) and b) temperature ([AmA] = 1.5 M).

The experimental values are in good agreement with the solubility values determined using the correlations proposed by Schumpe, as shown in Figure 3. The physical solubility strongly decreases with increasing sarcosine concentration in the absorption liquid, as expected due to the salting-out effect.

Using the CO_2/N_2O analogy, the physical solubility of CO_2 in the solution can be calculated. At a concentration of 0.5 M, the calculated physical CO_2

solubility has a value of over 0.7, which is in good agreement with literature [3]. With increasing the concentration to 3.8 M a physical CO_2 solubility of below 0.3 is obtained, which shows the strong influence of the concentration on the physical solubility.

The physical N_2O solubility values for the temperature decrease linearly with increasing temperature for the range from 298 K to 313 K and follow the Equation: m = -0.0059·T [in K] + 2.1394.

The trends observed in Figure 3 are in agreement with literature. Lee et al. [29] determined the physical N_2O solubility in aqueous sodium glycinate solutions as a function of the sodium glycinate mass fraction and temperature. They found the same trend and the physical N_2O solubility decreased with increasing mass fraction and temperature. For a 1 M sodium glycinate solution they observed a decrease of 15 % when the temperature was increased from 303 to 313 K. For a 1.5 M sarcosine salt solution, we observed a decrease of 18 %. For a 2 M MEA solution Mandal et al. [30] found a decrease in physical solubility of N_2O of 13 % when the temperature was increased from 303 to 313 K.

For the solutions (1.5 M) that were partially loaded with CO_2, the experimental N_2O solubility was determined in the same way and the CO_2 solubility was again calculated using the analogy between CO_2 and N_2O. For the partially loaded solutions, with a certain degree of CO_2 loading (α = 0 – 0.5 mol CO_2/mol sarcosine), the experimentally determined N_2O solubility could be described by $m_{N2O} = 0.0558 \cdot \alpha + 0.3968$, and hence only a very slight dependency of the N_2O solubility on the degree of CO_2 loading of the solution was observed. This observation is in agreement with the work of Kumar et al. [31], who considered that the physical N_2O solubility of a partially loaded potassium taurate solution is identical to that of the unloaded solution.

Reaction rate constant

To determine the influence of the sarcosine concentration, the temperature and the partial CO_2 loading of the solution on the rate of CO_2 absorption, the reaction rate constant (k_2) was determined under different experimental conditions. From preliminary absorption tests at 303 K with different CO_2 partial pressures (ranging of 5 to 9 mbar) it was found that the absorption flux was proportional to the CO_2 partial pressure, confirming the first order dependency on CO_2, which is in accordance with literature [6].

Effect of solution concentration

To verify the assumption of the pseudo-first-order regime, Table 2 shows the data for Ha and E_∞/Ha for the absorption experiments with different sarcosine salt solution concentrations. For completeness, but not further discussed, also values of the partial CO_2 pressure, $m \cdot D^{0.5}$, the flux and the overall reaction rate constant as a function of the amine concentration are presented.

Table 2: Flux, partial pressure of CO_2, $m \cdot D^{0.5}$, Ha, E_∞/Ha and overall and apparent reaction rate constant data for the absorption of CO_2 in aqueous sarcosine salt solutions in the pseudo-first-order regime as a function of the concentration at 298 K.

c	Flux	p_{CO2}	$m \cdot D^{0.5}$	Ha	E_∞/Ha	k_{ov}	k_{app}
(mol/L)	($\cdot 10^{-3}$ mol/m^2·s)	(mbar)	($\cdot 10^{-5}$ m/s$^{0.5}$)	(-)	(-)	(1/s)	(1/s)
0.5	0.7	6.2	3.1	160	6.5	7440	7180
1.0	1.6	10.5	2.5	264	5.6	22200	21600
1.5	1.5	8.6	2.0	359	9.6	44800	43200
3.0	1.7	8.1	1.2	593	19.5	177000	152000
3.8	2.1	12.8	0.8	709	20.8	294000	191000

The Ha and E_∞/Ha values in Table 2 show that the assumption for the pseudo-first-order regime ($3<$Ha and E_∞/Ha>5) is fulfilled for all conditions.

It shows that the overall reaction rate constant strongly increases with increasing amine concentration. Comparison of the overall reaction rate constant (k_{ov}) with the apparent reaction rate constant (k_{app}) shows that a stronger deviation between these two can be observed at higher concentration. This observation can be explained by the strong increase in the pH of the solution with increasing sarcosine concentration; reaction (2) is increasingly contributing to the overall absorption flux. For comparison, Figure 4 graphically represents the concentration dependence of the apparent reaction rate constant for the absorption of CO_2 in sarcosine salt solutions (■). Here we assumed an order of n=1 for sarcosine for the reaction rate of CO_2 in sarcosine salt solutions. This corresponds to the value for the reaction between CO_2 and MEA. Consequently the reaction rate constant k_2 can be plotted as $k_{app}/c_{amine.}$ Next to the reaction rate constant of the CO_2 absorption in aqueous sarcosine salt solutions, we also measured the corresponding values for the absorption of CO_2 in MEA (●). These values are also shown in Figure 4. For reference we also added data found in literature (○ and –) [8, 22].

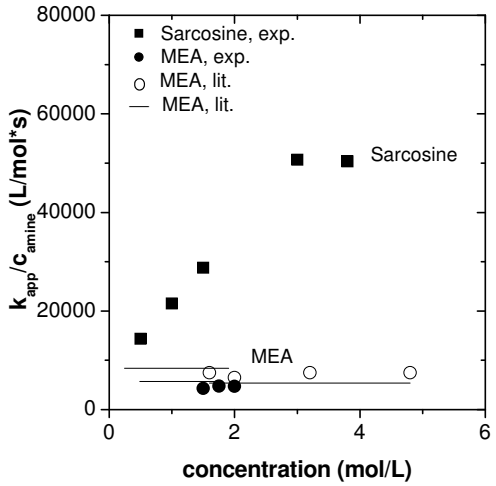

Figure 4: Reaction rate constant (k_{app}/c_{amine}) as a function of the amine concentration at 298 K under the assumption that the reaction rate order (n) for sarcosine salt equals the one for MEA and has a value of one. (■) Results for sarcosine salt solution; (●) Results for MEA (this work); (○) and (–) Data for MEA taken from literature [8, 22].

Compared to MEA, a primary alkanolamine, very high values for the reaction rate constants for the absorption of CO_2 in aqueous sarcosine salt solutions were obtained, as shown in Figure 4. In a review, Blauwhoff et al. [22] showed that reaction rate constants in MEA as reported in literature are in the range from 5720 to 8400 L/mol·s. Versteeg et al. [8] found reaction rate constants of 5400 to 7500 L/mol·s at 298 K for MEA in a concentration range from 0 to 4.8 M. For the absorption of CO_2 in the secondary alkanolamine DEA, Versteeg et al. [32] found a reaction rate constant of 3240 L/mol·s for DEA concentrations ranging from 0 to 4.358 mol/L and 298 K, which is somewhat lower than the values obtained for the primary alkanolamine MEA.

Interestingly, Figure 4 shows that with increasing sarcosine concentration, the reaction rate constant increases. In comparison to MEA, which has an order of one for the reaction with CO_2, the reaction rate for sarcosine seems to be more than proportional to the potassium sarcosinate

concentration. To evaluate the apparent reaction order in sarcosine, the apparent reaction rate constant as a function of the sarcosine salt concentration is plotted in Figure 5. In general, the slope of the natural logarithm of k_{app} as a function of concentration, equals the order of the reaction [6].

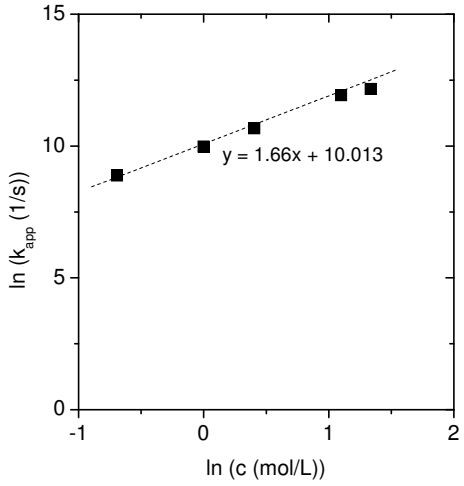

Figure 5: Natural logarithm of the apparent reaction rate constant (k_{app}) as a function of the amine concentration at 298 K. The slope of the line represents the order of the reaction in sarcosine.

Figure 5 shows that the reaction order of CO_2 in aqueous sarcosine salt solution appears to be constant at a value of 1.66 over the concentration range investigated (as opposed to a value of one for MEA).

Effect of temperature

The effect of the temperature on the reaction rate constant was determined for a temperature range from 298 to 308 K. The flux data, the values of the partial CO_2 pressure, $m \cdot D^{0.5}$, the flux and the calculated rate

constants as a function of the amine concentration are presented in Table 3.

Table 3: Flux, partial pressure of CO_2, $m \cdot D^{0.5}$, Ha, E_∞/Ha and overall and apparent reaction rate constant data for the absorption of CO_2 in 1.5M aqueous sarcosine salt solutions in the pseudo-first-order regime as a function of the temperature.

Temperature (K)	Flux ($\cdot 10^{-3}$ mol/m^2·s)	p_{CO2} (mbar)	$m \cdot D^{0.5}$ ($\cdot 10^{-5}$ m/s$^{0.5}$)	Ha (-)	E_∞/Ha (-)	k_{ov} (1/s)	k_{app} (1/s)
298	1.5	8.7	2.00	359	9.6	44800	43200
303	1.6	8.5	1.97	418	9.3	55900	53600
308	1.1	5.9	1.95	476	12.8	63800	61000

As shown in Table 3, the condition of pseudo-first-order regime (3<Ha and E_∞/Ha>5) is met in all experiments in the investigated temperature range. Figure 6 shows the influence of the temperature on the reaction rate constant taking into account the value of 1.66 for the order of sarcosine in the reaction rate expression.

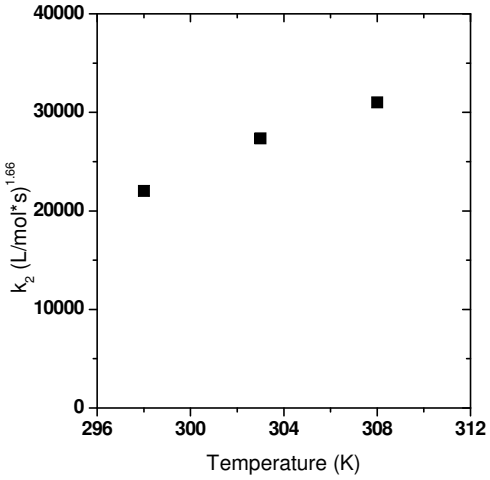

Figure 6: Reaction rate constant (k_2) as a function of the temperature for the absorption of CO_2 in a 1.5M aqueous sarcosine salt solution.

Figure 6 shows that with increasing temperature the reaction rate constant increases, and at higher temperatures the reaction is faster.

To determine the activation energy of the reaction, Figure 7 shows the Arrhenius plot of the reaction of CO_2 and the aqueous sarcosine salt solution.

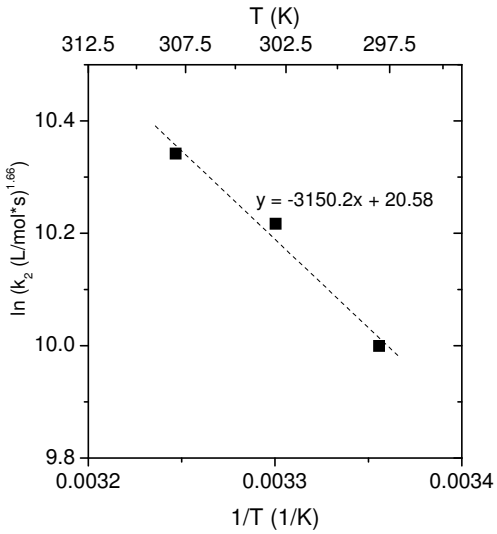

Figure 7: Arrhenius plot for the reaction between CO_2 and a 1.5 M aqueous sarcosine salt solution.

Figure 7 shows the natural logarithm of the reaction rate constant as a function of the reciprocal value of the temperature. The activation energy can be determined from the slope of this plot and has a value of approximately 26 kJ/mol for the temperature range investigated (298 till 308 K). This value is in reasonable good agreement with the values found in literature. For comparison, Blauwhoff et al. [22] summarized values found for the activation energy of the reaction of CO_2 and DEA and found values of approximately 42 kJ/mol for the same reaction. Based on all kinetic data present in literature, combined with the kinetic data reported by Versteeg et al. [32], Littel et al. [11] obtained an activation energy of 19 kJ/mol for the absorption of CO_2 in the secondary alkanolamine

diethanolamine (DEA). For the reaction between CO_2 and aqueous MEA, Versteeg et al. [8] used a value of 45 kJ/mol.

Effect of partial CO_2 loading

For cyclic absorption processes such as gas-liquid contacting systems or more specifically membrane contactors for CO_2 absorption, were incomplete solvent regeneration is likely to occur, the influence of the CO_2 loading of the absorption liquid on the reaction rate is of importance. Table 4 shows flux data, parameter values and calculated rate constants as a function of the CO_2 loading of the solution. Because changes in the viscosity were not observed, it was assumed that also the diffusivity remained constant and independent of the CO_2 loading.

Table 4: Flux, partial pressure of CO_2, $m \cdot D^{0.5}$, Ha, E_∞/Ha and overall and apparent reaction rate constant data for the absorption of CO_2 in a partially CO_2 loaded 1.45M aqueous sarcosine salt solution in the pseudo-first-order regime as a function of the CO_2 loading (298 K).

CO_2 loading (mol/mol)	Flux ($\cdot 10^{-4}$ mol/m^2·s)	p_{CO2} (mbar)	$m \cdot D^{0.5}$ ($\cdot 10^{-5}$ m/s$^{0.5}$)	Ha (-)	E_∞/Ha (-)	k_{ov} (1/s)	k_{app} (1/s)
0.00	9.9	5.7	2.13	343	13.8	41100	39600
0.03	7.2	4.3	2.14	334	19.0	38900	37900
0.07	6.7	4.4	2.15	294	20.5	30100	29600
0.08	9.5	6.3	2.15	294	14.4	30200	29800
0.11	9.4	6.3	2.16	290	14.6	29300	29000
0.11	6.7	4.8	2.16	272	20.5	25700	25500
0.17	8.0	6.3	2.18	244	17.1	20800	20700
0.19	6.9	6.1	2.18	216	19.8	16300	16200
0.22	8.5	7.7	2.19	212	16.2	15600	15600
0.26	4.9	5.0	2.21	190	27.7	12500	12500
0.31	5.3	6.0	2.22	167	25.7	9780	9670
0.33	4.7	5.6	2.22	157	29.3	8540	8540
0.35	4.9	7.6	2.23	121	28.1	5100	5090
0.36	3.6	5.6	2.23	120	38.4	5060	5050
0.39	3.1	5.4	2.24	107	44.8	3980	3970
0.43	2.3	5.3	2.26	80.5	59.7	2260	2260
0.46	1.4	6.1	2.26	43.2	96.0	651	650

Table 4 demonstrates that in all experiments performed the assumption of the pseudo-first-order is fulfilled (3<Ha and E_∞/Ha>5).

Figure 8 shows the influence of the partial loading of the absorption liquid with CO_2 on the apparent reaction rate constant and on the amine concentration normalized reaction rate constant k_2 for the reaction between CO_2 and the aqueous sarcosine salt solution. For comparison the value obtained for MEA for a non-loaded solution is also shown.

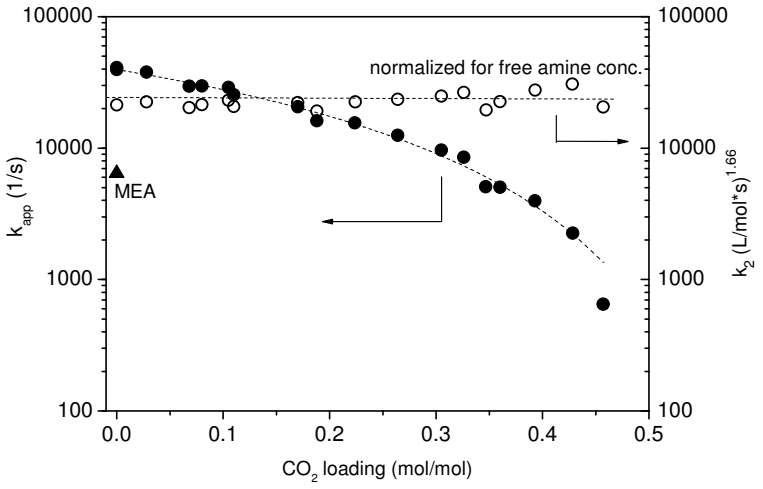

Figure 8: Apparent reaction rate constant for sarcosine k_{app} (●) and the amine concentration normalized reaction rate constant k_2 (○) as a function of the degree of CO_2 loading of a 1.45M aqueous sarcosine salt solution at 298 K (MEA value is given as a reference).

A strong decrease in the apparent reaction rate constant (●) is visible with increasing CO_2 loading of the absorption liquid. Consequently, higher partial loadings result in lower absorption fluxes, which will lead to larger process equipment and increased costs in real applications.
Aboudheir et al. [33] determined the absorption rate for partial loaded MEA solutions for three different degrees of CO_2 loading (0.0996, 0.3015, 0.4725 mol/mol) and also observed a strong decrease with increasing CO_2 loading degree.

To determine the concentration normalized reaction rate constant k_2, the apparent reaction rate constant is normalized for the actual concentration of free amines [AmA] in the solution at any concentration assuming a reaction stoichiometry of one molecule of CO_2 reacting with two molecules of potassium sarcosinate:

$$[AmA] = (1-2\alpha)\cdot[AmA]_0$$

When normalized for the free amine concentration available for the reaction with CO_2, the value of the reaction rate constant k_2 (○ in Figure 8) is independent of the CO_2 loading of the absorption liquid and directly related to the free amine concentration available for the reaction. It equals a value of 22915 ± 3050 $(L/mol \cdot s)^{1.66}$.

Conclusions

In this work gas absorption experiments in the pseudo-first-order regime were carried out to determine the reaction rate constant for the absorption of CO_2 in aqueous potassium sarcosinate solutions. Next to the influence of the sarcosine concentration (0.5 to 3.8 M) and the temperature (298 to 308 K), the reaction rate constant of partially CO_2 loaded sarcosine salt solutions was determined.

High reaction rate constants were obtained for the absorption of CO_2 in aqueous sarcosine salt solutions. The reaction order in CO_2 was found to be equal to one (in accordance with literature) and for the reaction order in potassium sarcosinate, an (apparent) reaction order of 1.66 was found. The activation energy was found to be approximately 26 kJ/mol.

The apparent reaction rate constant strongly decreases with increasing CO_2 loading of the absorption liquid. This decrease could be reasonably well described by taking into account the decrease in free amino acid concentration, assuming a reaction stoichiometry of one molecule of CO_2 reacting with two molecules of potassium sarcosinate. This observation is especially relevant for cyclic absorption processes such as gas-liquid membrane contactors, were incomplete solvent regeneration is likely to occur.

List of symbols

A	geometric gas-liquid contact area (m^2)
α	loading ($mol_{CO2}/mol_{sarcosine}$)
[AmA]	concentration amino acid salt solution (mol/L)
$[OH^-]$	concentration of OH^- (mol/L)
$c_{i,solution}$	concentration of ions in solution (mol/L)
$c_{CO2\text{-}liquid}$	CO_2 concentration in liquid phase (mol/L)
$D_{AmA\text{-}solution}$	diffusion coefficient of sarcosine in an aqueous sarcosine salt solution (m^2/s)
$D_{CO2\text{-}H2O}$	Diffusion coefficient of CO_2 in water (m^2/s)
$D_{CO2\text{-}solution}$	Diffusion coefficient of CO_2 in the solution (m^2/s)
$dp_{storage}/dt$	pressure decrease in time in the storage vessel
dN_{CO2}/dt	CO_2 molar flow (mol/s)
E	actual enhancement factor (-)
E_∞	infinite enhancement factor (-)
H_{CO2}	Henry coefficient (Pa m^3/mol)
h_g	gas specific parameter (Schumpe model) (L/mol)
$h_{g,0}$	gas specific parameter at 298K (Schumpe model) (L/mol)
h_i	ion specific parameter (Schumpe model) (L/mol)
h_T	temperature correction parameter (Schumpe model) (L/mol K)
Ha	Hatta number (-)
J_{CO2}	CO_2 flux (mol/m^2·s)
k_{app}	apparent reaction rate constant (1/s)
k_2	reaction rate constant ((L/mol s)^n)
k_L	physical mass transfer coefficient (m/s)
k_{OH}-	zwitterion mechanism deprotonation rate constant for OH^- (L/mol·s)
k_{ov}	overall reaction rate constant (1/s)
$m_{CO2\text{-}H2O}$	physical solubility of CO_2 in water (-)
$m_{CO2\text{-}solution}$	physical solubility of CO_2 in solution (-)
$m_{N2O\text{-}H2O}$	physical solubility of N_2O in water (-)

$m_{N2O\text{-}solution}$	physical solubility of N_2O in solution (-)
n	order of sarcosine in the reaction rate expression (-)
p_{CO2}	partial pressure of CO_2 (mbar)
p_{int}	initial pressure at the start of the experiment just after gas inlet (mbar)
p_{eq}	equilibrium pressure (mbar)
p_{vap}	vapor pressure of the solution (mbar)
R	gas constant = 8.3143 (J/mol K)
T	Temperature (K)
V_g	volume of the gas phase (m^3)
V_l	volume of the liquid phase (m^3)
μ_{H2O}	viscosity of water (Pa s)
$\mu_{solution}$	viscosity of solution (Pa s)
ν_{AmA}	stoichiometric coefficient for amino acid salt (-)

References

1. P.S. Kumar, J.A. Hogendoorn, P.H.M. Feron, G.F. Versteeg, New absorption liquids for the removal of CO_2 from dilute gas streams using membrane contactors, Chemical Engineering Science, 57 (2002) 1639

2. E.S. Hamborg, J.P.M. Niederer, G.F. Versteeg, Dissociation constants and thermodynamic properties of amino acids used in CO_2 absorption from (293 to 353) K, Journal of Chemical and Engineering Data, 52 (2007) 2491

3. J. Van Holst, S.R.A. Kersten, K.J.A. Hogendoorn, Physiochemical properties of several aqueous potassium amino acid salts, Journal of Chemical and Engineering Data, 53 (2008) 1286

4. A.F. Portugal, P.W.J. Derks, G.F. Versteeg, F.D. Magalhaes, A. Mendes, Characterization of potassium glycinate for carbon dioxide absorption purposes, Chemical Engineering Science, 62 (2007) 6534

5. P.H.M. Feron, A.E. Jansen, CO_2 separation with polyolefin membrane contactors and dedicated absorption liquids: Performances and prospects, Separation and Purification Technology, 27 (2002) 231

6. P.S. Kumar, J.A. Hogendoorn, G.F. Versteeg, P.H.M. Feron, Kinetics of the reaction of CO_2 with aqueous potassium salt of taurine and glycine, AIChE Journal, 49 (2003) 203

7. M.E. Majchrowicz, D.W.F. Brilman, M.J. Groeneveld, Precipitation regime for selected amino acid salts for CO_2 capture from flue gases, Energy Procedia, 1 (2009) 979

8. G.F. Versteeg, L.A.J. Van Dijck, W.P.M. Van Swaaij, On the kinetics between CO_2 and alkanolamines both in aqueous and non-aqueous solutions. An overview, Chemical Engineering Communications, 144 (1996) 133

9. A. Jamal, A. Meisen, C. Jim Lim, Kinetics of carbon dioxide absorption and desorption in aqueous alkanolamine solutions using a novel hemispherical contactor-II: Experimental results and parameter estimation, Chemical Engineering Science, 61 (2006) 6590

10. S.Y. Horng, M.H. Li, Kinetics of absorption of carbon dioxide into aqueous solutions of monoethanolamine + triethanolamine, Industrial and Engineering Chemistry Research, 41 (2002) 257

11. R.J. Littel, G.F. Versteeg, W.P.M. Van Swaaij, Kinetics of CO_2 with primary and secondary amines in aqueous solutions-II. Influence of temperature on zwitterion formation and deprotonation rates, Chemical Engineering Science, 47 (1992) 2037

12. K. Simons, K. Nijmeijer, M. Wessling, Gas-liquid membrane contactors for CO2 removal, Journal of Membrane Science, 340 (2009) 214

13. A.F. Portugal, F.D. Magalhaes, A. Mendes, Carbon dioxide absorption kinetics in potassium threonate, Chemical Engineering Science, 63 (2008) 3493

14. P.W.J. Derks, T. Kleingeld, C. van Aken, J.A. Hogendoorn, G.F. Versteeg, Kinetics of absorption of carbon dioxide in aqueous piperazine solutions, Chemical Engineering Science, 61 (2006) 6837

15. P.V. Danckwerts, The reaction of CO_2 with ethanolamines, Chemical Engineering Science, 34 (1979) 443

16. K. Nymeijer, T. Visser, W. Brilman, M. Wessling, Analysis of the Complexation Reaction between Ag+ and Ethylene, Ind. Eng. Chem. Res., 43 (2004) 2627-2635

17. E.S. Hamborg, W.P.M. Van Swaaij, G.F. Versteeg, Diffusivities in aqueous solutions of the potassium salt of amino acids, Journal of Chemical and Engineering Data, 53 (2008) 1141

18. M. Vucak, J. Peric, A. Zmikic, M.N. Pons, A study of carbon dioxide absorption into aqueous monoethanolamine solution containing calcium nitrate in the gas-liquid reactive precipitation of calcium carbonate, Chemical Engineering Journal, 87 (2002) 171-179

19. S.W. Park, B.S. Choi, K.J. Oh, J.W. Lee, Absorption of carbon dioxide into aqueous PAA solution containing diethanolamine, Journal of the Chinese Institute of Chemical Engineers, 38 (2007) 461

20. J. Haubrock, J.A. Hogendoorn, G.F. Versteeg, The applicability of activities in kinetic expressions: A more fundamental approach to represent the kinetics of the system CO_2-OH--salt in terms of activities, Chemical Engineering Science, 62 (2007) 5753

21. R. Pohorecki, W. Moniuk, Kinetics of reaction between carbon dioxide and hydroxyl ions in aqueous electrolyte solutions, Chemical Engineering Science, 43 (1988) 1677

22. P.M.M. Blauwhoff, G.F. Versteeg, W.P.M. Van Swaaij, A study on the reaction between CO_2 and alkanolamines in aqueous solutions, Chemical Engineering Science, 38 (1983) 1411

23. A. Schumpe, The estimation of gas solubilities in salt solutions, Chemical Engineering Science, 48 (1993) 153

24. J.v. Holst, G.F. Versteeg, D.W.F. Brilman, J.A. Hogendoorn, Kinetic study of CO_2 with various amino acid salts in aqueous solution, Chemical Engineering Science, 64 (2009) 59

25. S. Weisenberger, A. Schumpe, Estimation of gas solubilities in salt solutions at temperatures from 273 K to 363 K, AIChE Journal, 42 (1996) 298-300

26. D.W.F. Brilman, W.P.M. Van Swaaij, G.F. Versteeg, Diffusion coefficient and solubility of isobutene and trans-2-butene in aqueous sulfuric acid solutions, Journal of Chemical and Engineering Data, 46 (2001) 1130

27. A.F. Portugal, F.D. Magalhaes, A. Mendes, Carbon dioxide absorption kinetics in potassium threonate, Chemical Engineering Science, 63 (2008) 3493-3503

28. P.M.M. Blauwhoff, selective absorption of hydrogen sulphide from sour gases by alkanolamine solutions, Dissertation, University of Twente, The Netherlands, (1982)

29. S. Lee, H.J. Song, S. Maken, H.C. Shin, H.C. Song, J.W. Park, Physical solubility and diffusivity of N_2O and CO_2 in aqueous sodium glycinate solutions, Journal of Chemical and Engineering Data, 51 (2006) 504

30. B.P. Mandal, M. Kundu, S.S. Bandyopadhyay, Physical solubility and diffusivity of N_2O and CO_2 into aqueous solutions of (2-Amino-2-methyl-1-propanol + monoethanolamine) and (N-methyldiethanolamine + Monoethanolamine), Journal of Chemical and Engineering Data, 50 (2005) 352

31. P.S. Kumar, J.A. Hogendoorn, P.H.M. Feron, G.F. Versteeg, Equilibrium solubility of CO_2 in aqueous potassium taurate solutions: Part

1. Crystallization in carbon dioxide loaded aqueous salt solutions of amino acids, Industrial and Engineering Chemistry Research, 42 (2003) 2832

32. G.F. Versteeg, M.H. Oyevaar, The reaction between CO_2 and diethanolamine at 298 K, Chemical Engineering Science, 44 (1989) 1264

33. A. Aboudheir, P. Tontiwachwuthikul, A. Chakma, R. Idem, Kinetics of the reactive absorption of carbon dioxide in high CO_2-loaded, concentrated aqueous monoethanolamine solutions, Chemical Engineering Science, 58 (2003) 5195

CHAPTER 4

Highly selective amino acid salt solutions as absorption liquid for CO_2 capture in gas-liquid membrane contactors

Abstract

The strong anthropogenic increase in the emission of CO_2 and the related environmental impact force the developments towards sustainability and Carbon Capture and Storage (CCS). In the present work, we combine the high product yields and selectivities of CO_2 absorption processes with the advantages of membrane technology in a membrane contactor for the separation of CO_2 from CH_4 using amino acid salt solutions as competitive absorption liquid to alkanol amine solutions.

Amino acids, such as sarcosine, have the same functionality as alkanol amines (e.g. MEA), but in contrast to MEA they exhibit a better oxidative stability and resistance to degradation. In addition, they can be made non-volatile by adding a salt functionality, which significantly reduces the liquid loss due to evaporation at elevated temperatures in the desorber.

Membrane contactor experiments using CO_2/CH_4 feed mixtures to evaluate the overall process performance including a full absorption/desorption cycle show that even without a temperature difference between absorber and desorber, a CO_2/CH_4 selectivity of over 70 can be easily achieved with the sarcosine salt solution as absorption

liquid. This selectivity reaches values of 120 at a temperature difference between absorber and desorber of 35°C, compared to a value of only 60 for MEA under the same conditions. Although CO_2 permeance values are somewhat lower than the values obtained for MEA, the results clearly show the potential of amino acid salt solutions as competitive absorption liquids for the energy efficient removal of CO_2. In addition, due to the low absorption of CH_4 in sarcosine compared to MEA, the loss of CH_4 is reduced and significantly higher CH_4 product yields can be obtained.

Introduction

The strong anthropogenic increase in the emission of CO_2 and the related environmental consequences force the developments in the direction of sustainability and Carbon Capture and Storage (CCS). More than one-third of the CO_2 emissions come from the combustion of fossil fuels in power plants worldwide [1, 2]. The combustion of gaseous fuels (e.g. natural gas) accounted for 1521 million metric tons of carbon in 2006, which equals 18.5% of the total emissions from fossil fuels [3]. In addition, also the emission of CO_2 associated with the exploration and production of natural gas is more than significant [4]. The number of easy accessible, low CO_2 containing natural gas sources is limited, urging the exploration of natural gas sources with high(er) concentrations of CO_2. Next to its environmental impact, CO_2 reduces the heating value of the CH_4 gas streams in power plants and it causes corrosion in pipes and equipment [5].

The common methods to separate CO_2 from gas mixtures are pressure swing adsorption, cryogenic distillation and amine absorption [6, 7]. Amine absorption is the most frequently used method and high product yields and purities can be obtained. The disadvantage of this method is its high energy consumption, especially during desorption [8, 9], in combination with high liquid losses due to evaporation of the solvent in the stripper [10, 11]. In addition also the occurrence of flooding and entrainment of the absorption liquid limits the process and the liquid and gas streams cannot be controlled independently [12-15].

Membrane technology is an attractive, energy and cost effective alternative for conventional absorption processes [6, 16]. It is easy to scale-up and has a high area-to-volume ratio [2]. A limitation can be found in the permeability-selectivity tradeoff relation: more permeable membrane materials are generally less selective and vice versa [17]. Since 1980s gas separation with membranes has emerged into a commercially viable method [18]. Nowadays, several hundreds of small and large industrial membrane plants for the separation of gases exist. Most plants use cellulose-acetate membranes, which have CO_2/CH_4 selectivities of only 15 [19]. According to Baker [19], the competiveness of membranes for the

separation of CO_2/CH_4 would strongly increase if stable membranes with a selectivity of 40 during operation would become available. Due to plasticization in the presence of CO_2, membranes often loose their performance at elevated pressure. Swelling stresses on the polymer network and an increase in free volume and segmental mobility upon exposure to CO_2 cause a rise in permeability for all components [20], and especially the permeability of the low permeating component, consequently resulting in a decrease in selectivity [21-23]. The development of polymeric membranes and membrane processes with improved plasticization resistance that maintain selectivity and permeability, even at higher CO_2 partial feed pressures is crucial and an important field of research.

In the present work, we combine the high product yields and selectivities of absorption processes [14] with the advantages of membrane technology in a membrane contactor for the separation of CO_2 from CH_4 (Figure 1) using amino acid salt solutions as competitive absorption liquid to alkanol amine solutions.

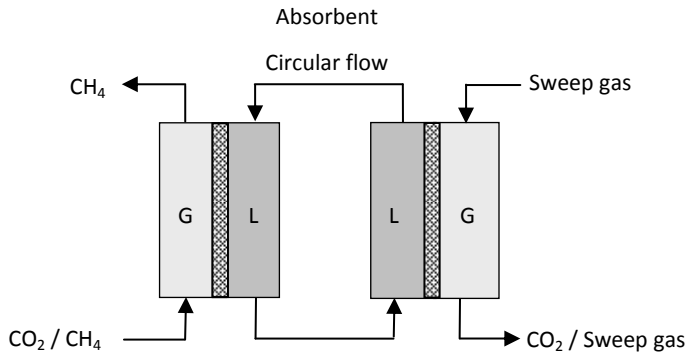

Figure 1: Schematic representation of a membrane contactor for the separation of CO_2 and CH_4.

The membrane in the contactor has no selectivity but only a contacting function and it separates the gas flow on one side and the absorption liquid on the other side of the membrane [24]. CO_2 diffuses from the gas side through the membrane and is selectively absorbed by the absorption

liquid. The CO_2-loaded liquid flows to a second membrane contactor, the desorber, where the CO_2 is expelled from the liquid. The membrane in most cases is porous with no selectivity [25] or non-porous with a certain selectivity [25-28].
Gas-liquid membrane contactors have a high operational flexibility as the gas and the liquid stream can be controlled independently [13, 27, 29, 30]. This make them a viable technology for gas-liquid contacting processes such as the separation of olefins and paraffins [27, 31, 32], blood oxygenation [33] and the separation of CO_2 from light gases [25].

The traditional solvents used for CO_2 absorption are aqueous alkanol amine solutions, like mono ethanol amine (MEA, Figure 2), due to their high CO_2 absorption capacity and relatively high CO_2 absorption rates [34].

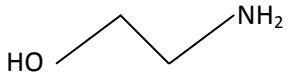

Figure 2: Chemical structure of mono ethanol amine (MEA).

Major disadvantages of this group of absorption liquids are their corrosiveness and sensitivity towards oxygen [35]. Degradation of the alkanol amine in the presence of oxygen may occur, resulting in very toxic degradation products and solvent loss [36].
A non-volatile alternative for alkanol amine solutions are amino acid salt solutions as absorption liquid for gas-liquid contacting processes. Amino acids have the same functionality as alkanol amines (e.g. MEA), but in contrast to MEA they are expected to have a higher oxidative stability [35, 37] and a better resistance to degradation [38]. In addition, they can be made non-volatile by adding a salt functionality, which significantly reduces the liquid loss and energy consumption associated to that [14, 35, 38].
Yan et al. [8] used an amino acid salt solution (potassium salt of glycinate) as absorption liquid for the removal of CO_2 from flue gas. A polypropylene (PP) hollow fiber membrane contactor was used as absorber and a stripper (no membrane) as desorber. The influence of the liquid flow rate (0.02-0.1

m/s), concentration of absorbent (0.5-3 M), liquid temperature (30-50°C), CO_2 volume fraction in feed gas (7.9-20.5 vol.%) and gas flow rate (0.211-0.528 m/s) on the CO_2 flux was determined and compared to the use of MEA and MDEA as absorption liquid. The performance of CO_2 absorption using the amino acid salt solutions was always superior to MEA and MDEA under the same operating conditions. Kumar et al. [37] studied the wetting characteristics of polyolefin membranes using an amino acid salt solution (potassium salt of taurine). In comparison to aqueous alkanol amine solutions, the amino acid salt solution does not wet the polyolefin microporous membranes. Furthermore Kumar et al. [37] carried out CO_2 absorption experiments with a single fiber membrane contactor as absorber. Both with increasing liquid flow rate and increasing partial pressure an increase in CO_2 flux could be observed.
Feron et al. [14] used CORAL solutions as absorption liquids, which are based on mixtures of salts and amino acids, in a membrane gas absorber with a porous polypropylene hollow fiber membrane as absorber and a stripper (no membrane) as desorber for CO_2 removal. They determined the mass transfer rates as a function of CO_2 partial pressure, liquid loading and liquid temperature and compared the results to literature data of membrane gas absorption systems using PTFE or PP hollow fiber membranes and MEA, AMP (2-Amino-2-methyl-1-propanol) or K_2CO_3 solutions as absorption liquid. They observed the highest mass transfer coefficient ($1.6 \cdot 10^{-3}$ m/s for a 2 M solution at 20-25°C) and high system stability for the system with the amino acid salt solutions.

One of the disadvantages of amino acid salts is that the salt can easily precipitate in the presence of CO_2, an effect that deserves special attention in membrane-assisted gas-liquid contacting processes for CO_2 removal. Majchrowicz et al. [39] showed the relationship between precipitation behavior, CO_2 partial pressure and salt concentrations. Of the four tested amino acid salt solutions (potassium salt of taurine, ß-alanine L-proline and sarcosine), sarcosine showed the largest operating window. At a CO_2 partial pressure of 0.1 bar precipitation starts at a sarcosine concentration of 4 M, while at a partial pressure of 1 bar a concentration of 3 M is the

limit. In our experiments the CO_2 partial pressure is 0.24 bar and the sarcosine concentration is 1.5 M and precipitation is not expected to occur. Next to this, the potassium salt of sarcosine is expected to have high CO_2 loading capacities due to the presence of a secondary amine group (Figure 3).

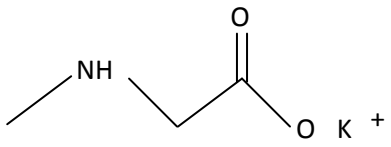

Figure 3: Chemical structure of the potassium salt of sarcosine.

The literature results show the potential of amino acid salt solutions as absorption liquid for gas-liquid membrane contactors. Unfortunately in literature very frequently only CO_2 mass fluxes and absorption rates are determined, which provide only limited information about the performance of the process in the real application, including both absorption and desorption.

In our previous work [40] we investigated the kinetics of the absorption of CO_2 in sarcosine salt solutions and observed very high reaction rate constants for the reaction between CO_2 and the amine (carbamate formation).

In the present work we explore the performance of such amino acid salt solutions (potassium salt of sarcosine) as competitive absorption medium to alkanol amine solutions (MEA) in a regenerative cyclic process using a gas-liquid membrane contactor for the selective separation of CO_2 from CH_4. In this work, process performance data for the cyclic process, consisting of both an absorber and a desorber membrane module, using feed mixtures are reported and compared to the corresponding data obtained when MEA is used as absorption liquid. Whereas in literature often only CO_2 mass fluxes and absorption rates are reported, which

provide only limited information about the performance of the process in the real application, the work presented here reports real process performance data (permeances and selectivities) for the full process comprising an absorption and a desorption stage under practical conditions using feed mixtures instead of a single components. Although the mini plant system used in this study is not optimized and potentially even much higher absolute performance data can be obtained with an optimized system, the system allows us identifying the relative potential of amino acid salt solutions compared to MEA for gas-liquid contacting processes for the removal of CO_2 from CH_4.

Experimental Part

Materials

Nitrogen and the gas mixture (CO_2/CH_4 20/80%) were obtained from Praxair, Belgium. Mono ethanol amine (purity > 99 %) was obtained from Merck, The Netherlands. Sarcosine was obtained from Fluka, Germany, the solid potassium hydroxide and hydrochloric acid solutions from Merck, The Netherlands. All chemicals were used without further purification.

Sarcosine salt solution preparation

The solid sarcosine was mixed with an equimolar amount of solid potassium hydroxide. The actual purity of the KOH was determined by acid titration. The reaction of sarcosine and potassium hydroxide is exothermic and has water as side product. The actual concentration of the aqueous sarcosine salt solution was determined by titration with standard 1 mol/L HCl solution.

Membrane modules

Multiple fiber membrane modules were used as absorber and desorber membrane contactor. Each module contained 10 hollow fiber membranes,

which have an effective length of 23.5 cm each, resulting in a membrane area of 200.5 cm^2 per module. The fibers were porous, microfiltration Accurel® S6/2 polypropylene (PP) hollow fibers purchased from Membrana GmbH (Germany). According to the supplier these fibers had an outer diameter of 2.7 mm, an inner diameter of 1.8 mm and an average pore size of 0.27 µm.

Membrane contactor experiments

To evaluate the performance of the absorption liquids, experiments with a membrane contactor were performed (Figure 4). Experimental details of the set up can be found elsewhere [25].

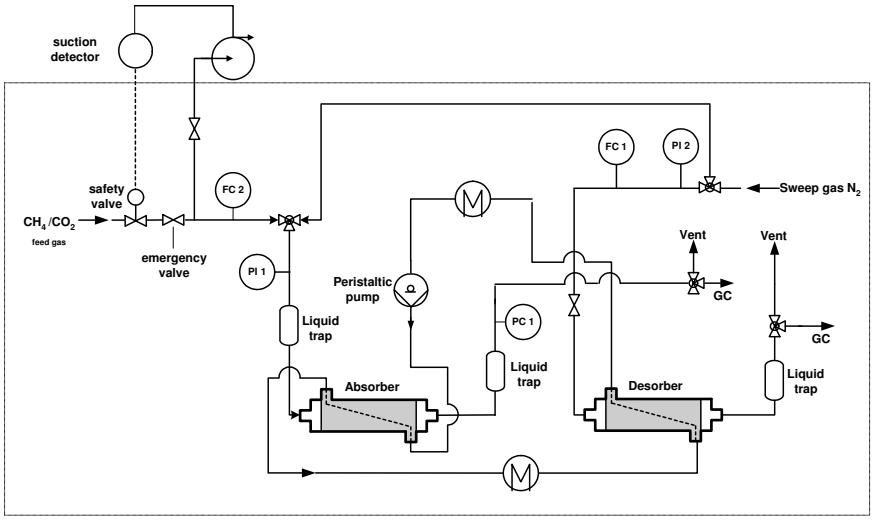

Figure 4: Schematic representation of the experimental membrane contactor setup used for CO_2/CH_4 separation.

The feed gas mixture (CO_2/CH_4 20/80 vol.%) was fed through the lumen side of the absorber membranes, and the feed gas pressure was set at a constant value of 1.2 bar by a backpressure controller in the retentate flow. The absorption liquid was circulated at the shell side of the membranes using a Masterflex peristaltic pump. The gas-loaded liquid was

circulated to the desorber (second membrane contactor) via a heat-exchanger to increase the temperature to the desorber temperature. In the desorber, nitrogen was used as a sweep gas to provide a driving force for desorption of the absorbed gas from the circulation liquid. The regenerated liquid leaving the desorber, was cooled to the absorption temperature before returning to the absorber module.

The gas flow rate was determined with a soap bubble meter and the composition of the gas mixture in the retentate and permeate were analyzed using a gas chromatograph (Shimadzu GC-14B). The gas permeance P (in GPU = $1 \cdot 10^{-6}$ $cm^3(STP)/cm^2 \cdot s \cdot cmHg$ = $3.348 \cdot 10^{-10}$ $mol/m^2 \cdot s \cdot Pa$) is calculated as the volume flow rate of the permeate stream V multiplied by the volume fraction of the specific gas in the permeate stream γ, divided by the partial pressure difference over the membranes ($\Delta p = p_{feed} - p_{permeate}$) and the membrane area A of one membrane module.

$$P = \frac{\gamma \cdot \mathrm{V}}{A \cdot \Delta p}$$

Calculation of the CO_2 permeance is based on the membrane area of one membrane module only, because either absorption or desorption limits the process and determines the final CO_2 flux of the process: under steady state conditions the gas flow that enters the liquid through the absorber membranes can only leave the liquid through the desorber membranes. Because absorber and desorber have the same membrane area, permeance values based on the total membrane area can be easily calculated as half the permeances shown.

The selectivity α (CO_2/CH_4) is calculated as:

$$\alpha = \frac{\mathrm{Y}_{CO_2} / \mathrm{Y}_{CH_4}}{\mathrm{X}_{CO_2} / \mathrm{X}_{CH_4}}$$

Where Y_i is the concentration of component i in the permeate stream that leaves the desorber and X_i is the concentration of component i in the feed.

Mono ethanol amine (MEA, 10 wt.% aqueous solution) and the sarcosine salt solution (sarcosine, 1.5 M aqueous solution of potassium salt of sarcosine) were used as absorption liquids in the membrane contactor. The effect of the temperature difference between absorption and desorption (ΔT = 0 – 35°C) was investigated, while keeping the absorber temperature constant at 29°C and the liquid flow rate constant at 160 ml/min. In addition the influence of the liquid flow rate was investigated. The flow rate of the circulated absorption liquid was varied between 19 and 160 ml/min while the temperature difference between absorber and desorber was kept constant at 35°C, with an absorber temperature of 29°C.

Results

Introduction

The gas-liquid membrane contactor process used in this study consists of an absorber and a desorber membrane module. In both the absorber and the desorber, the overall resistance to mass transfer is determined by three consecutive individual resistances in series: 1) the gas phase boundary layer resistance, 2) the resistance of the porous membrane and 3) the liquid phase boundary layer resistance. Compared to the liquid phase boundary layer resistance, the gas phase boundary layer resistance is relatively small and can be neglected. When porous membranes are used, as is the case in this work, the resistance of the membranes is also relatively small compared to the liquid phase boundary layer resistance, as long as the porous membrane is not wetted by the absorption liquid. When the absorption liquid penetrates into the pores of the porous membrane, the mass transfer resistance for diffusion through the (in that case liquid-filled) pores can become considerable. Wetting of the porous support was not observed in our experiments.

In the liquid phase boundary layer, next to physical absorption of both gases (CO_2 and CH_4) also chemical absorption occurs due to the chemical, reversible reaction between CO_2 and the active component (sarcosinate or MEA) in the absorption liquid. The intrinsic kinetics of the chemical reaction between CO_2 and the amino acid salt solution sarcosine have been investigated in our previous paper [40]. The hydrodynamically determined liquid phase mass transfer resistance can be influenced by the liquid flow rate of the absorption liquid, whereas the temperature affects both the chemical and physical absorption/desorption processes. The process performance on variation of these parameters will be discussed below.

Effect of temperature on process performance

Due to strong influence of the temperature on the gas absorption capacity and ab- and desorption reaction kinetics [40], the effect of the temperature difference between absorber and desorber on the overall process performance for the new amino acid salt solution and the traditionally used alkanol amine solution MEA has been investigated. The resulting CO_2 permeance values are presented in Figure 5.

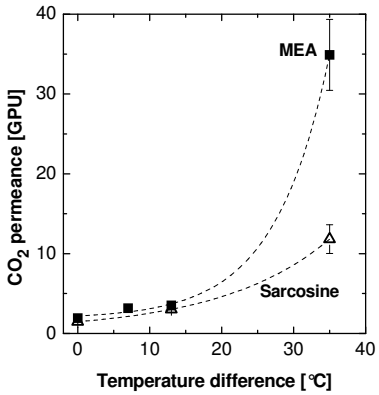

Figure 5: CO_2 permeance as a function of the temperature difference between absorption and desorption (T_{abs} = 29°C; Liquid flow rate = 160 ml/min; Feed gas mixture: CO_2/CH_4 (20/80 vol.%); Feed pressure = 1.2 bar).

The CO_2 permeance for both liquids increases with increasing temperature difference. The increase at lower temperature difference is less pronounced, but for higher desorber temperatures, a strong increase in CO_2 permeance is observed especially for MEA. As the results presented in Figure 5 were obtained at constant absorber temperature (29°C) and variable desorber temperature, these results show that desorption is the limiting step in the process.

At low temperature differences, the CO_2 permeances for both absorption liquids are relatively similar, while at larger temperature differences the CO_2 permeance values using MEA as absorption liquid start to deviate and are significantly higher than the values found for the low volatile amino acid salt solution. CO_2 Loading tests performed separately at 29°C (absorber temperature) show relatively similar values (in the range of 0.76 mol CO_2/mol amine) for the maximum CO_2 loading capacity of both absorption liquids. Consequently, differences in maximum CO_2 loading between the two liquids do not explain the differences in performance between the two absorption liquids. It is hypothesized that the observed differences in permeance are caused by a more effective CO_2 desorption at elevated temperatures in the case of MEA compared to the sarcosine salt solution. Kinetic studies [40] show higher activation energy for MEA than for the sarcosine salt solution, and consequently a stronger effect of the temperature on the sorption/desorption kinetics of CO_2 in MEA is expected, which supports our hypothesis.

Hamborg et al. [38] investigated dissociation constants and thermodynamic properties of amino acids and discussed the correlation between the standard enthalpy change of the dissociation reaction ($\Delta_r H°_m$ in kJ/mol) and the favorability to shift the dissociation reaction at absorber and desorber temperature conditions. They suggested that a high value of $\Delta_r H°_m$ would lead to a favorable shift of the dissociation reaction at absorber and desorber temperature conditions and might reduce the required temperature difference between absorption and desorption. For MEA they reported a literature value for $\Delta_r H°_m$ of 50.5 kJ/mol, which was

higher than the value of 39.7 kJ/mol for sarcosine as found by the authors. This observation is in agreement with the results observed in this work, where at a temperature difference of 35°C, higher CO_2 permeances for MEA are found. To obtain equal CO_2 permeance values for sarcosine, higher temperature differences are required.

Figure 6 shows the permeance for CH_4 as a function of the temperature difference between absorption and desorption.

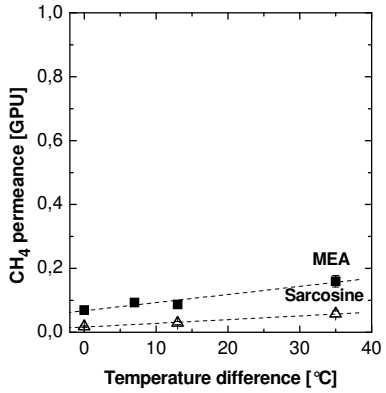

Figure 6: CH_4 permeance as a function of the temperature difference between absorption and desorption (T_{abs} = 29°C; Liquid flow rate = 160 ml/min; Feed gas mixture: CO_2/CH_4 (20/80 vol.%); Feed pressure = 1.2 bar).

The CH_4 permeance increases with increasing desorber temperature (increasing temperature difference between absorber and desorber). Over the temperature difference range investigated, the CH_4 permeance for sarcosine is lower than the CH_4 permeance using MEA. This difference in CH_4 permeance for the two aqueous solutions can be explained by the salting out effect [41]. The solubility coefficient of gases in salt solutions is lower when the solution has a higher salt concentration. Measurement of the conductivity of both aqueous solutions showed a conductivity of 84 mS/cm for the sarcosine salt solution, whereas the MEA solution has a conductivity of only 1.2 mS/cm. Consequently, the physical solubility of the gases in the amino acid salt solution is considerably lower than in MEA,

which was also observed in CH_4 solubility tests performed separately and supports the lower values found for the CH_4 permeance for the sarcosine solutions. Due to the low absorption of CH_4 in sarcosine compared to MEA, the loss of CH_4 is reduced and significantly higher CH_4 product yields can be obtained.

As CH_4 is only physically absorbed, the results show that with higher temperature difference, the physical solubility of CH_4 decreases, resulting in higher CH_4 permeances. The same effect is expected to occur for the *physical* solubility of CO_2 in both absorption liquids. Separate physical solubility tests of N_2O, which is commonly used to estimate the physical solubility of CO_2 in absorption liquids, revealed that the physical gas solubility in the amino acid salt solutions indeed decreases with increasing temperature [40]. Consequently desorption of physically dissolved CO_2 is increased at higher temperatures.
In the case of physical absorption/desorption only, an increase in the desorption temperature with 35°C results in a ~2 (MEA) to ~3 (sarcosine) times relative increase in the permeance value of the physically absorbed CH_4. When this is compared to the effect of the temperature on the (both physically and chemically absorbed) CO_2, a much stronger and opposite relative increase is observed: an ~8 times increase for sarcosine and an ~18 times increase for MEA. When assuming equal behavior for the physical absorption of CO_2 and CH_4, the chemical absorption of CO_2 is the major mechanism governing the CO_2 absorption/desorption, especially in the case of MEA, but also the physical absorption still plays a significant contribution in the current experimental configuration, especially for sarcosine. So despite the higher reaction rate constant found for the absorption of CO_2 in sarcosine when compared to MEA [40], the chemical absorption/desorption process in the current experimental configuration is more effective when MEA is used. Most probably this is related to the kinetics of the *desorption* reaction, which are apparently less favorable in the case of sarcosine than for MEA.

The influence of the temperature difference between absorber and desorber on the CO_2/CH_4 selectivity is presented in Figure 7. The absorber temperature was kept constant at a value of 29°C and the desorber temperature was varied.

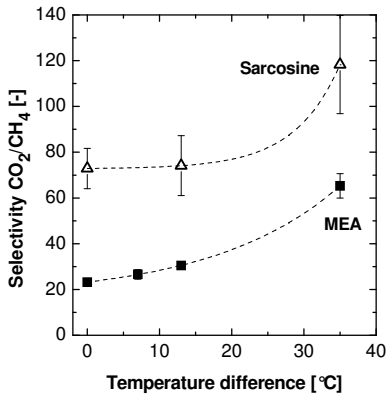

Figure 7: CO_2/CH_4 selectivity as a function of temperature difference between absorption and desorption (T_{abs} = 29°C; Liquid flow rate = 160 ml/min; Feed gas mixture: CO_2/CH_4 (20/80 vol.%); Feed pressure = 1.2 bar).

Although the CO_2 permeance for sarcosine was somewhat lower than that for MEA, Figure 7 shows that much higher CO_2/CH_4 selectivities can be obtained with sarcosine over the whole temperature range investigated. The reason for this higher selectivity, also at elevated desorber temperatures where MEA results in significantly higher CO_2 permeances than sarcosine, is the relatively low CH_4 permeance in the case of sarcosine due to the salting out effect. The CO_2/CH_4 selectivity for both liquids increases with increasing temperature difference due to the more effective CO_2 desorption at elevated desorber temperature and the less pronounced effect of the temperature on the desorption of CH_4.

Even without a temperature difference, CO_2/CH_4 selectivities of over 70 can be achieved with sarcosine salt solutions, while at higher temperature differences values of at least 100-120 can be easily reached, compared to values of maximum 60 when MEA is used as absorption liquid. Next to the

strong reduction in energy consumption due to the non-volatile character of the liquid and its improved oxygen stability, the results show the competitive character of sarcosine as absorption liquid for CO_2/CH_4 separation over the traditional absorption liquid MEA.

Effect of liquid flow rate on process performance

Next to the temperature difference between absorption and desorption, the liquid flow rate of the absorption liquid has a profound influence on the process performance of a membrane contactor. Figure 8 shows this effect of the liquid flow rate on the CO_2 and CH_4 permeance for the two different absorption liquids.

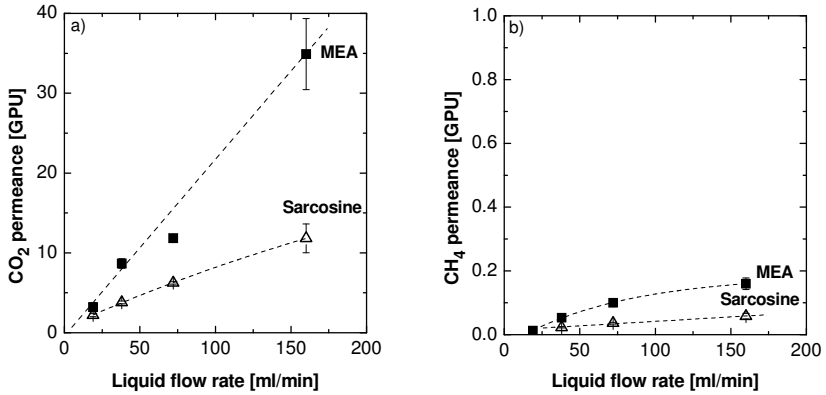

Figure 8: a) CO_2 permeance and b) CH_4 permeance as a function of absorbent liquid flow rate (Δ T = 35°C; T_{abs} = 29°C; Feed gas mixture: CO_2/CH_4 (20/80 vol.%); Feed pressure = 1.2 bar).

Figure 8 shows that for both absorption liquids the CO_2 and the CH_4 permeance increases with increasing liquid flow rate. Yan et al. [8] found similar effects for the CO_2 permeance for an aqueous glycinate solution (potassium salt of glycinate) and for aqueous alkanol amine-solutions.

Upon increasing the flow rate of the absorption liquid, potentially three different effects may occur:

1) An increase in flow rate decreases the boundary layer thickness and consequently decreases the resistance to mass transfer. This affects both CO_2 and CH_4.
2) An increase in liquid flow rate increases the supply of gas-loaded solution in the desorber (the limiting step in the process) and may consequently lead to an increase in productivity. This affects both the CO_2 and CH_4 permeance. Although these first two effects both influence both the CO_2 and CH_4 permeance, the absolute contribution of each of the effects on both gases can be different because CO_2 is chemically and physically absorbed whereas CH_4 is only physically absorbed.
3) Due to the increased liquid flow rate, the time available for desorption of gas in the desorber membrane module (the limiting step) decreases. When the time scales for the desorption reaction to occur and the occurrence of physical desorption are longer than the time scale in which a liquid volume element is in contact with the membrane area, this will result in a decrease in productivity. This can affect both CO_2 and CH_4 productivity, but is expected to have a stronger effect on the CO_2 permeance, as in the case of CO_2 next to purely physical desorption, chemical desorption preceding the physical desorption needs to occur.

To identify which effect is dominant, Figure 9 shows the relative (normalized) increase in both CO_2 and CH_4 permeance for both absorption liquids as a function of the flow rate. Normalization is done based on the values found for a flow rate of 19 ml/min.

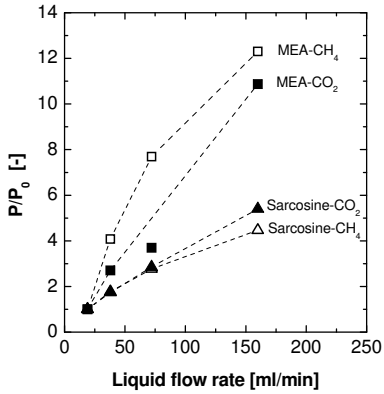

Figure 9: Normalized CO_2 and CH_4 permeance as a function of the absorption liquid flow rate ($\Delta T = 35°C$; $T_{abs} = 29°C$; Feed gas mixture: CO_2/CH_4 (20/80 vol.%); Feed pressure = 1.2 bar). Normalization is done based on the values found for a flow rate of 19 ml/min.

In the case of MEA, the relative increase in CH_4 permeance with increasing flow rate is stronger than the corresponding relative increase in CO_2 permeance. Assuming equal behavior for the physically absorbed CH_4 and CO_2, this would imply that the CO_2 permeance due to chemical desorption is less sensitive to changes in the liquid flow rate and an increase in flow rate has a stronger positive effect on the physical desorption than on the chemical desorption. In the case of a comparable impact of the liquid flow rate on both physical and chemical desorption, the values for CO_2 and CH_4 would coincide. This suggests that the reduction in boundary layer effects (effect 1) and the increase in the supply of gas-loaded solution (effect 2) are dominant, but that the reduction in time for the chemical desorption to occur (effect 3) does play a role as well.

In the case of sarcosine, desorption (limiting step) is less sensitive to changes in the liquid flow rate. Both the values for CO_2 and CH_4 coincide. This suggests that both physical and chemical desorption are affected to the same extent by an increase in flow rate. However, at this stage we are unable to distinguish between the contribution of each of the three above-mentioned (competing) effects.

Figure 10 shows the influence of the liquid flow rate on the CO_2/CH_4 selectivity for the two different absorption liquids.

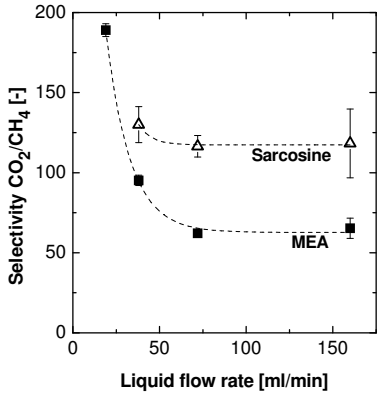

Figure 10: CO_2/CH_4 selectivity as a function of the absorbent liquid flow rate (Δ T = 35°C; T_{abs} = 29°C; Feed gas mixture: CO_2/CH_4 (20/80 vol.%); Feed pressure = 1.2 bar).

The selectivity decreases with increasing liquid flow rate for both absorption liquids and especially for MEA, due to a higher relative increase in CH_4 permeance than in CO_2 permeance. Selectivities obtained with sarcosine are significantly higher than the values found for MEA, due to the lower CH_4 solubility for sarcosine salt solutions (salting-out effect). This high CO_2 over CH_4 selectivity shows the potential of this solvent for competitive CO_2 removal in gas-liquid membrane contactors.

Shelekhim et al. [41] showed both in model calculations and experimentally that at low liquid flow rates the absorption liquid determines the selectivity whereas at higher liquid flow rates the membrane selectivity becomes dominant. This would imply that at higher liquid flow rates, the selectivity of the system would reach the intrinsic selectivity of the membrane (a value of ~1 in the case of the porous membrane used in our study). For both solutions over the investigated liquid flow rate the selectivity does not reach this intrinsic membrane selectivity, which suggests that for the investigated liquid flow rate the absorption liquid still significantly contributes to the process selectivity. It

is expected that further increase of the liquid flow rate would finally lead to a process selectivity equal to the membrane selectivity [41].

Next to a potentially strong reduction in energy consumption due to the non-volatile character of the liquid and its improved oxygen and degradation stability, the results show the strong competitive character of sarcosine as absorption liquid over the traditional absorption liquid MEA. Very high CO_2/CH_4 selectivities due to very low CH_4 permeances can be obtained with sarcosine as absorption liquid. Even without a temperature difference between absorber and desorber a selectivity of 70 can be easily reached. At a temperature difference of 35°C between absorber and desorber, selectivity values of at least 100-120 can be reached, compared to values of maximally 60 when MEA is used as absorption liquid. This work shows the potential of amino acid salt solutions and more specifically sarcosine salt solutions as absorption liquid in gas-liquid contacting processes for the energy-efficient removal of CO_2, as already at much lower desorber temperatures high selectivities can be obtained. In addition, due to the low absorption of CH_4 in sarcosine compared to MEA, the loss of CH_4 is reduced and significantly higher CH_4 product yields can be obtained.

Conclusions

In this work we investigated the potential of an amino acid salt solutions, more specifically the potassium salt of sarcosine, as new absorption liquid for the selective absorption of CO_2 from CH_4 in a gas-liquid membrane contactor. Amino acids, such as sarcosine, have the same functionality as alkanol amines (e.g. MEA), but in contrast to MEA they are expected to exhibit a high oxidative and degradation stability. In addition, they can be made non-volatile by adding a salt functionality, which significantly reduces the liquid loss due to evaporation of the solvent in the desorber.
The CO_2 permeance for both liquids increases with increasing temperature difference. For higher desorber temperatures, a strong increase in CO_2

permeance is observed especially for MEA. These results show that desorption is the limiting step in the process. CO_2 permeance values found for sarcosine as absorption liquid are somewhat lower than the values obtained with MEA

The CH_4 permeance increases with increasing desorber temperature. Over the temperature difference range investigated, the CH_4 permeance for sarcosine is lower than the CH_4 permeance using MEA due to the salting out effect. For both absorption liquids the CO_2 and the CH_4 permeance increases with increasing liquid flow rate. Due to the low absorption of CH_4 in sarcosine compared to MEA, the loss of CH_4 is reduced and significantly higher CH_4 product yields can be obtained.

Even without a temperature difference, CO_2/CH_4 selectivities of over 70 can be achieved with sarcosine salt solutions, while at higher temperature differences values of at least 100-120 can be easily reached, compared to values of maximally 60 when MEA is used as absorption liquid.

Next to the strong reduction in energy consumption due to the non-volatile character of the liquid and its improved oxygen and degradation stability, the results show the strong competitive character of amino acid salt solutions and more specifically sarcosine salt solutions as absorption liquid in gas-liquid contacting processes for the energy-efficient removal of CO_2.

References

1. H.-Y. Zhang, R. Wang, D.T. Liang, J.H. Tay, Modeling and experimental study of CO_2 absorption in a hollow fiber membrane contactor, Journal of Membrane Science, 279 (2006) 301

2. IEA, CO_2 emissions from fuel combustion, 1971-2007, OECD/IEA, (2009)

3. T.A. Boden, G. Marland, and R.J. Andres., Global, Regional and National Fossil-Fuel CO_2 Emissions, Carbon Dioxide Information Analysis Center, Oak Ridge National Laborator, U.S. Department of Energy, Oak Ridge, Tenn., U.S.A. doi 10.3334/CDIAC/00001,

4. IPCC Special Report on Carbon Dioxide Capture and Storage, Cambridge University Press: Cambridge (England), (2005)

5. S. Ma'mun, V.Y. Dindore, H.F. Svendsen, Kinetics of the reaction of carbon dioxide with aqueous solutions of 2-((2-aminoethyl)amino)ethanol, Industrial and Engineering Chemistry Research, 46 (2007) 385

6. S. Freni, S. Cavallaro, S. Donato, V. Chiodo, A. Vita, Experimental evaluation on the CO_2 separation process supported by polymeric membranes, Materials Letters, 58 (2004) 1865

7. A.F. Ismail, N. Yaacob, Performance of treated and untreated asymmetric polysulfone hollow fiber membrane in series and cascade module configurations for CO2/CH4 gas separation system, Journal of Membrane Science, 275 (2006) 151

8. S.-p. Yan, M.-X. Fang, W.-F. Zhang, S.-Y. Wang, Z.-K. Xu, Z.-Y. Luo, K.-F. Cen, Experimental study on the separation of CO_2 from flue gas using hollow fiber membrane contactors without wetting, Fuel Processing Technology, 88 (2007) 501

9. C. Alie, L. Backham, E. Croiset, P.L. Douglas, Simulation of CO_2 capture using MEA scrubbing: A flowsheet decomposition method, Energy Conversion and Management, 46 (2005) 475

10. J. Zhang, S. Zhang, K. Dong, Y. Zhang, Y. Shen, X. Lv, Supported Absorption of CO_2 by Tetrabutylphosphonium Amino Acid Ionic Liquids, Chemistry - A European Journal, 12 (2006) 4021-4026

11. P.H.M. Feron, A.E. Jansen, Capture of carbon dioxide using membrane gas absorption and reuse in the horticultural industry, Energy Conversion and Management, 36 (1995) 411

12. J.-G. Lu, Y.-F. Zheng, M.-D. Cheng, L.-J. Wang, Effects of activators on mass-transfer enhancement in a hollow fiber contactor using activated alkanolamine solutions, Journal of Membrane Science, 289 (2007) 138

13. D. deMontigny, P. Tontiwachwuthikul, A. Chakma, Using polypropylene and polytetrafluoroethylene membranes in a membrane contactor for CO_2 absorption, Journal of Membrane Science, 277 (2006) 99

14. P.H.M. Feron, A.E. Jansen, CO_2 separation with polyolefin membrane contactors and dedicated absorption liquids: Performances and prospects, Separation and Purification Technology, 27 (2002) 231

15. S. Atchariyawut, R. Jiraratananon, R. Wang, Separation of CO_2 from CH_4 by using gas-liquid membrane contacting process, Journal of Membrane Science, 304 (2007) 163

16. X. Hu, J. Tang, A. Blasig, Y. Shen, M. Radosz, CO_2 permeability, diffusivity and solubility in polyethylene glycol-grafted polyionic membranes and their CO2 selectivity relative to methane and nitrogen, Journal of Membrane Science, 281 (2006) 130

17. B.D. Freeman, Basis of permeability/selectivity tradeoff relations in polymeric gas separation membranes, Macromolecules, 32 (1999) 375

18. S. Sridhar, B. Smitha, T.M. Aminabhavi, Separation of carbon dioxide from natural gas mixtures through polymeric membranes - A review, Separation and Purification Reviews, 36 (2007) 113

19. R.W. Baker, Future Directions of Membrane Gas Separation Technology, Ind. Eng. Chem. Res., 41 (2002) 1393-1411

20. T. Visser, M. Wessling, When do sorption-induced relaxations in glassy polymers set in? Macromolecules, 40 (2007) 4992

21. A. Bos, I.G.M. Puent, M. Wessling, H. Strathmann, CO_2-induced plasticization phenomena in glassy polymers, Journal of Membrane Science, 155 (1999) 67

22. J.D. Wind, S.M. Sirard, D.R. Paul, P.F. Green, K.P. Johnston, W.J. Koros, Relaxation Dynamics of CO_2 Diffusion, Sorption, and Polymer

Swelling for Plasticized Polyimide Membranes, Macromolecules, 36 (2003) 6442-6448

23. T. Visser, G.H. Koops, M. Wessling, On the subtle balance between competitive sorption and plasticization effects in asymmetric hollow fiber gas separation membranes, Journal of Membrane Science, 252 (2005) 265

24. Y. Lee, R.D. Noble, B.-Y. Yeom, Y.-I. Park, K.-H. Lee, Analysis of CO_2 removal by hollow fiber membrane contactors, Journal of Membrane Science, 194 (2001) 57

25. K. Simons, K. Nijmeijer, M. Wessling, Gas-liquid membrane contactors for CO_2 removal, Journal of Membrane Science, 340 (2009) 214

26. D.C. Nymeijer, B. Folkers, I. Breebaart, M.H.V. Mulder, M. Wessling, Selection of Top Layer Materials for Gas-Liquid Membrane Contactors, Journal of Applied Polymer Science, 92 (2004) 323

27. K. Nymeijer, T. Visser, R. Assen, M. Wessling, Super selective membranes in gas-liquid membrane contactors for olefin/paraffin separation, Journal of Membrane Science, 232 (2004) 107

28. K. Nymeijer, T. Visser, R. Assen, M. Wessling, Olefin-Selective Membranes in Gas-Liquid Membrane Contactors for Olefin/Paraffin Separation, Industrial and Engineering Chemistry Research, 43 (2004) 720

29. V.Y. Dindore, D.W.F. Brilman, P.H.M. Feron, G.F. Versteeg, CO_2 absorption at elevated pressures using a hollow fiber membrane contactor, Journal of Membrane Science, 235 (2004) 99

30. A. Gabelman, S.T. Hwang, Hollow fiber membrane contactors, Journal of Membrane Science, 159 (1999) 61

31. M. Teramoto, S. Shimizu, H. Matsuyama, N. Matsumiya, Ethylene/ethane separation and concentration by hollow fiber facilitated transport membrane module with permeation of silver nitrate solution, Separation and Purification Technology, 44 (2005) 19

32. D.C. Nymeijer, T. Visser, R. Assen, M. Wessling, Composite hollow fiber gas-liquid membrane contactors for olefin/paraffin separation, Separation and Purification Technology, 37 (2004) 209

33. S. Karoor, K.K. Sirkar, Gas absorption studies in microporous hollow fiber membrane modules, Ind. Eng. Chem. Res., 32 (1993) 674-684

34. S. Ma'mun, R. Nilsen, H.F. Svendsen, O. Juliussen, Solubility of carbon dioxide in 30 mass % monoethanolamine and 50 mass % methyldiethanolamine solutions, Journal of Chemical and Engineering Data, 50 (2005) 630

35. J. Van Holst, S.R.A. Kersten, K.J.A. Hogendoorn, Physiochemical properties of several aqueous potassium amino acid salts, Journal of Chemical and Engineering Data, 53 (2008) 1286

36. P.S. Kumar, J.A. Hogendoorn, P.H.M. Feron, G.F. Versteeg, Equilibrium solubility of CO2 in aqueous potassium taurate solutions: Part 1. Crystallization in carbon dioxide loaded aqueous salt solutions of amino acids, Industrial and Engineering Chemistry Research, 42 (2003) 2832

37. P.S. Kumar, J.A. Hogendoorn, P.H.M. Feron, G.F. Versteeg, New absorption liquids for the removal of CO2 from dilute gas streams using membrane contactors, Chemical Engineering Science, 57 (2002) 1639

38. E.S. Hamborg, J.P.M. Niederer, G.F. Versteeg, Dissociation constants and thermodynamic properties of amino acids used in CO2 absorption from (293 to 353) K, Journal of Chemical and Engineering Data, 52 (2007) 2491

39. M.E. Majchrowicz, D.W.F. Brilman, M.J. Groeneveld, Precipitation regime for selected amino acid salts for CO_2 capture from flue gases, Energy Procedia, 1 (2009) 979

40. K. Simons, D.W.F. Brilman, H. Mengers, K. Nijmeijer, M. Wessling, Kinetics of CO_2 absorption in aqueous sarcosine salt solutions - Influence of concentration, temperature and CO_2 loading, submitted for publication to Industrial and Engineering Chemistry Research, (2010)

41. A.B. Shelekhim, I.N. Beckman, Gas separation processes in membrane absorber, Journal of Membrane Science, 73 (1992) 73

CHAPTER 5

How do polymerized room-temperature ionic liquid membranes plasticize during high pressure CO_2 permeation?

Abstract

Room-temperature ionic liquids (RTILs) are a class of organic solvents that have been explored as novel media for CO_2 separations. Polymerized RTILs (poly(RTILs)) can be synthesized from RTIL monomers to form dense, solid gas selective membranes. It is of interest to understand the permeation properties under single gas and mixed gas conditions at elevated pressure of CO_2. The ionic nature of the polymers may result in tight arrangements between the oppositely charged ionic domains in the poly(RTIL) eventually preventing the membrane from excessive swelling and deterioration of its performance at increased pressure and/or temperature. In this work we characterize the permeation behaviour of three different poly(RTILs) at single and mixed gas pressures up to 40 bar and over a temperature range from T=10 to 40°C . We find that CO_2 is an equally strong plasticizer in single gas as well as mixed gas experiments: the permeability of CO_2 increases by more than 60% over a pressure range of 40 bar. Methane does not plasticize the poly(RTIL) by itself in single gas experiments, however the presence CO_2 accelerates its transport by more than 250%. The plasticization effect of CO_2 is fully reversible on the time-scale of the diffusional processes. Even though the poly(RTILs) are glassy in nature, the

plasticization behaviour is distinctly different from regular glassy polymers such as polyimides, polysulfones or polycarbonates due to the reversibility of swelling extent. Tailoring the length of the side chain of poly(RTIL) indicates that short side chains suppress plasticization and acceleration of the methane permeability up to a pressure of 10 bars CO_2: longer side chains however do not. This suggests the interpretation that a molecular energy balance of ionic attraction and swelling induced relaxation exists: however, the swelling induced relaxations overrule the ionic interaction.

Introduction

CO_2 is one of the major contributors to the greenhouse effect: the power and industrial sectors combined account for about 60% of annual global CO_2 emissions [1]. To minimize the impact of CO_2 on the environment, carbon capture and sequestration (CCS) is essential. The traditional method of separating CO_2 from other gases is aqueous amine scrubbing. Although high product yields and purities can be obtained, the disadvantage of this technology is its high energy consumption - especially during desorption - in combination with a high liquid loss due to evaporation, entrainment and flooding of the solvent [2-5]. Room Temperature Ionic Liquids RTILs are salts that are molten at ambient temperature and have a non-measurable vapor pressure. Furthermore they are thermally stable and able to solvate a large variety of organic and inorganic species [6-8]. RTILs have been explored as possible alternative media for CO_2 capture applications [9]. RTILs have been studied in combination with porous membranes as supported ionic liquid membranes (sILMs), where the liquid is captured in the pores of the support membrane. Due to the relatively weak capillary forces, these membranes are not very stable in high-pressure applications. The high trans-membrane pressure difference results in liquid loss and deteriorates the sILM [10]. Furthermore the introduction of the RTIL into the pores of the membranes introduces a significant increase in resistance to mass transfer and limits the gas flux through the membrane due to the relatively large thicknesses of these membranes. Reducing the thickness of the immobilized liquid layer is an issue of ongoing research [11].

A way to use the advantages of RTILs without being limited by the disadvantages of sILMs is to polymerize the RTIL and to prepare dense films or even composite membranes of the poly(RTIL) [12]. The RTIL can be synthesized as a monomer and subsequently be polymerized to obtain gas selective membranes.

Bara et al. [10] showed the potential of imidazolium-based poly(RTILs) as promising membrane materials for CO_2 removal. With single gas permeation experiments, ideal CO_2/CH_4 selectivities of 30 and CO_2

permeabilities of over 30 Barrers could be achieved with a feed pressure of 2 bar at 20°C. CO_2 solubility values up to 4.4 cm^3 (STP)/cm^3 and diffusivities of $7.7 \cdot 10^8$ cm^2/s were reported. Very little is known about the permeation behaviour of these poly(RTILs) at elevated pressures for mixed gasses. It is an open question whether and how a highly sorbing gas like CO_2 affects its own transport (auto-plasticization) or the transport of a slower diffusing component such as methane (mutual plasticization).

At low feed pressures, glassy polymers show a decreasing permeability with increasing feed pressure as frequently described by the Dual-Mode Sorption Model. At low pressures, Langmuir type sorption dominates the solubility over regular Henry type solution of the permeating gas. This causes the permeability to decrease until only Henry sorption is dominant and the permeability levels off to a constant value. At even high feed pressures, glassy polymers often suffer from plasticization by a highly sorbing gas [13-15]. Due to the presence of the plasticizing gas such as CO_2, relaxational phenomena and swelling stresses on the polymer network cause an increase in free volume and segmental mobility of the polymer matrix, which often induces an increase in permeability for both gases in the feed mixture. Typical for plasticization is a relatively larger increase in permeability of the low permeating component, which results in a decrease in selectivity [16, 17]. Besides being dependent on the properties of the specific polymer, plasticization phenomena are especially dependent on the CO_2 partial pressure and the temperature [14]. Due to simultaneous presence of competitive sorption and plasticization [18], a minimum evolves at elevated feed pressures for highly sorbing gasses: the feed pressure at which the permeability starts to increase is called the plasticization pressure [16]. Methods to increase the resistance against plasticization and swelling of glassy polymer membranes include physical and chemical crosslinking [19-21], thermal treatments [16, 21, 22] and polymer blending [23].

Very little is known with respect to transport properties of poly(RTIL) at elevated CO_2 feed pressure. The inherent properties of poly(RTILs) may

offer a versatile route to reduce swelling and plasticization phenomena in such polymer membranes. Tight arrangements between the oppositely charged ionic domains present in the poly(RTIL) may have the potential to prevent the membrane from excessive swelling and deterioration of its performance at increased pressure and/or temperature. Wang et al. [24, 25] systematically investigated the gas transport properties of various poly(aryl ether ketone)s and observed an increased gas selectivity at the expense of the permeability in polymers with stronger ionic interactions. However, high-pressure CO_2 permeation measurements were not performed and the effect of the presence of stronger ionic interpolymer chain interactions on the plasticization resistance of the polymer membranes was not investigated. In their previous work, Bara et al. [10] showed a decrease in diffusion rate and gas permeability at shorter alkyl side chain length of the poly(RTIL), which supports the assumption of tighter ionic domains at shorter alkyl side chain lengths, as longer alkyl side chains in the poly(RTIL) directly reduce the density of ionic groups and consequently ionic interactions in the membrane [26].

In this work we study this potential property of ionic association of poly(RTILs) as a tool to increase the resistance against plasticization and to restrict strong swelling of the polymer membrane to maintain its permeation properties in the presence of a strong plasticizing agent such as CO_2 at higher pressures. An imidazolium-based poly(RTIL) is used as base material and the length of the alkyl chain serves as a tool to strengthen or weaken the ionic interactions within the poly(RTIL). High pressure mixed CO_2/CH_4 gas separation measurements at different temperatures are performed to evaluate the potential of this concept.

Experimental Part

Materials

The styrene-based 1-[(4-ethenyl phenyl) methyl]-3-alkyl-imidazolium bis-(trifluoromethane)sulfonamide RTIL monomers with three different lengths of the alkyl substituent R (R = methyl, n-butyl or n-hexyl) were synthesized as described by Bara et al. [10]. Figure 1 shows the molecular structure of the RTIL monomers.

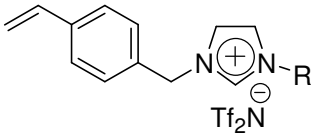

R = Me, *n*-Bu, *n*-Hx

Figure 1: Structure of the RTIL monomers.

Supor 200 PES (polyethersulfone) flat sheet membranes were used as support for the poly(RTIL) and obtained from Pall, USA.

Pure CH_4, CO_2 and the CO_2/CH_4 50/50vol.% gas mixture used for gas permeation measurements were obtained from Praxair, Belgium.

Membrane formation

The RTIL monomer was mixed with 5 mol% cross-linking agent (divinylbenzene) and 1 wt.% photo-initiator (2-hydroxy-2-methylpropiophenone). The mixture of monomer, cross-linking agent and photo-initiator was spread over the supported surface, clamped between Rain-X coated quartz plates and photo-polymerized with a 365 nm UV lamp, with an intensity of 8.5 mW/cm^2 for 30 minutes. Afterwards the plates were removed and the film was carefully removed from the surface. Circular samples with a surface area of 11.95 cm^2 were cut from the films and used for mixed gas permeation experiments. Membrane thickness was

measured with a micrometer and reconfirmed through scanning electron microscopy. SEM photos showed complete filling of the porosity.

Gas permeation measurements

The separation performance of the poly(RTIL) membranes was investigated with a temperature-controlled high pressure gas permeation setup using a constant volume-variable pressure method as described elsewhere [27]. A constant feed pressure was applied and during the measurement, the permeate side was kept under vacuum. The gas permeability through the membrane was calculated from the steady state pressure increase in time in a calibrated volume at the permeate side. The permeability values are expressed in Barrer, where 1 Barrer = 10^{-10} cm^3 (STP)·cm/(cm^2·s·cmHg). In the case of mixed gas permeation experiments the feed and permeate composition were analyzed with a Varian gas chromatograph (Varian).

The permeability and separation performance of the membranes using mixed gasses (CO_2/CH_4 (50/50vol%)) was determined at different feed pressures (10, 20, 30, 40 bar) and different temperatures (10°C, 20°C and 40°C) and all experiments were performed in duplicate.

After every mixed gas experiment, a pure CH_4 permeation experiment was performed, at the same temperature as the previous mixed gas experiment and at a feed pressure of 7 bar, to identify possible (ir)reversible network changes.

Results

Effect of pressure

Single and mixed gas permeation

Figure 2a shows the mixed gas CO_2 permeability for the three poly(RTILs) as a function of the total feed pressure at 20ºC. C_1 refers to the poly(RTIL) with a short methyl group as alkyl substituent, while C_4 refers to the poly(RTIL) with n-butyl as alkyl substituent and C_6 to the one with the longer n-hexyl-substituent. Figure 2b shows the normalized CO_2 permeability (P_{CO2}/P_0) for the three polymers. The normalized permeability is the ratio of the absolute permeability at a certain pressure (P_{CO2}) and the absolute permeability at 10 bar (P_0) and is plotted as a function of CO_2 fugacity. For comparison single gas normalized CO_2 permeability for n-butyl and n-hexyl substituent poly(RTILs) are as well plotted in Figure 2b. Lines in the Figures are only added to guide the eye.

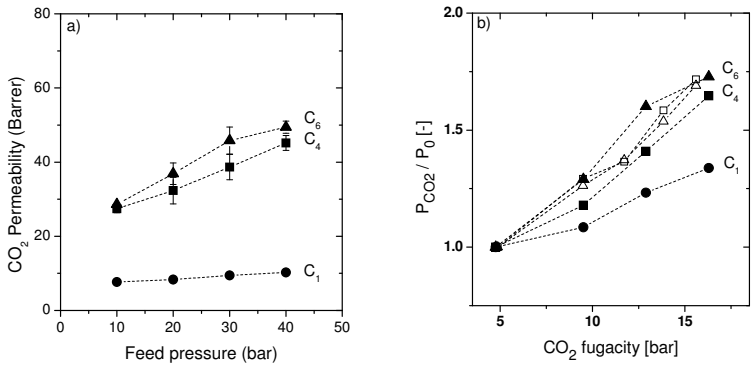

Figure 2: a) CO_2 permeability as a function of the feed pressure and b) normalized CO_2 permeability of the methyl (C_1), n-butyl (C_4) and n-hexyl (C_6) poly(RTIL) membranes as a function of CO_2 fugacity for the mixed gas experiments (closed symbols) and single gas experiments (open sympols). All experiments performed at 20°C. Feed mixed gas: CO_2/CH_4 (50/50 vol.%).

For all films an increase in CO_2 permeability with increasing feed pressure is observed. Over the tested pressure range the n-hexyl-substituent membranes have the highest CO_2 permeability, while the methyl-substituent membranes, with the shortest side chain and the strongest ionic interactions within the material, have the lowest permeability. The n-butyl and n-hexyl-substituted poly(RTILs) show similar behavior and have comparable permeabilities.
Cadena et al. [28] concluded that for imidazolium-based RTILs, the anion dominates the interactions (solubility) with the CO_2, whereas the cation plays a secondary role and the addition of alkyl groups only has a relatively small influence on the CO_2 solubility. For low pressures, Bara et al. [10] found an increase in diffusivity for all gases with increasing side chain length of the styrene based poly(RTIL) membranes used in this work, while the effect of the chain length on the CO_2 solubility was very small. This observed increase in diffusivity could explain the increase in permeability with increasing side chain length.

Also the normalized CO_2 permeability increases for the three poly(RTILs) investigated, but the polymer membranes with the longer side chain lengths (C_4 and C_6) obviously show a stronger increase in permeability with increasing pressure than the methyl (C_1) substituted polymer membrane. The single gas permeation experiments for the polymer membranes with the longer side chains (C_4 and C_6) show a similar increase in permeability as the mixed gas results. The presence of CH_4 in the gas mixture does not influence the gas permeation of CO_2, which suggests the absence of competitive sorption. Competitive sorption by a second gas causes a reduction in the permeation of the first component. This suggests that the transport in poly(RTILs) is distinctly different from transport in regular glassy polymers, were competitive sorption does play a role. Although corresponding pure gas values for the methyl substituted polymer are not shown, it is reasonable to assume that the same behavior would be observed for this polymer. The less distinct increase in the CO_2 permeability for the C_1-poly(RTIL) supports the hypothesis that the methyl-

substituted polymer membrane has tighter ionic interactions and is hence less sensitive to volume dilation induced plasticization phenomena.

Figure 3 shows a) the CH_4 permeability and b) the normalized CH_4 permeability as determined from mixed gas permeation experiments. For comparison, also the single gas CH_4 permeability is presented. As in the case of CO_2, the normalized values are normalized based on the mixed gas CH_4 permeability at 10 bar.

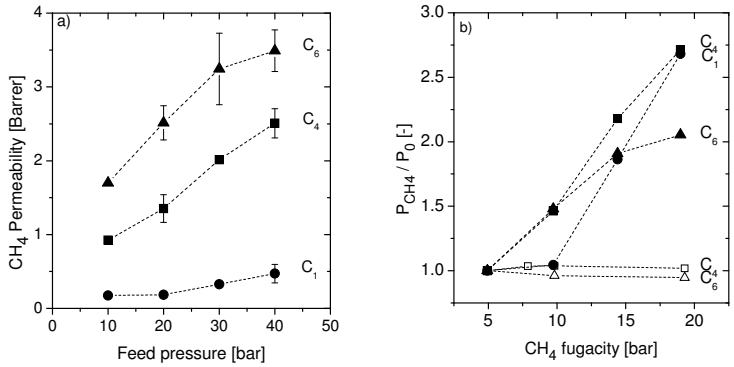

Figure 3: a) CH_4 permeability as a function of the feed pressure and b) normalized CH_4 permeability of the methyl (C_1), n-butyl (C_4) and n-hexyl (C_6) poly(RTIL) membranes as a function of CH_4 fugacity for the mixed gas experiments (closed symbols) and single gas experiments (open sympols). All experiments performed at 20°C. Feed mixed gas: CO_2/CH_4 (50/50 vol.%).

For the mixed gas permeation experiments, the CH_4 permeability increases with increasing feed pressure. The highest absolute values are again obtained for the n-hexyl-substituted poly(RTIL). Although the CO_2 solubility in the poly(RTILs) with the same anion but with variations in the alkyl group length of the cation is very similar [28], Bara et al. [10] did find an influence of the side chain length on the CH_4 solubility. With increasing length of the side chain from the methyl-substituent to the n-butyl and n-hexyl-substituent, the solubility more than doubled, most probably caused

by the preferred dissolution of the non-polar CH_4 in the less polar domains of the poly(RTIL). Aki et al. [29] found in their study on the polarity of RTILs, that the longer side chain imidazolium-based RTILs are less polar than the ones with a shorter alkyl side chain and it can be expected that this is applicable to poly(RTILs) as well.

Until feed pressures of 20 bar, the relative increase in CH_4 permeability from a mixed feed for the methyl substituted polymer seems to be limited, especially when compared to the two other polymers, showing the concept of using ionic interactions as a tool to prevent excessive swelling of the membrane. At higher mixed feed pressures, a distinct increase in relative CH_4 permeability for all three polymer membranes is visible. At these high feed pressures, the ionic interactions in the polymer are apparently overcome by the dilating, plasticizing effect of the absorbed CO2, resulting in a strong increase in CH_4 permeability with increasing feed pressure.

This is confirmed when the results of the mixed gas and the pure gas permeation for CH_4 are compared. In contrast to the CO_2 permeability, the CH_4 permeability shows a strong difference between the pure and the mixed values. With increasing fugacity, the pure gas CH_4 permeabilities remain constant and are independent of the fugacity, while the mixed gas results clearly show a strong increase with increasing CH_4 and consequently increasing CO_2 fugacity. Although corresponding pure gas values for the methyl-substituted polymer are not presented, it is reasonable to assume the same behavior for this polymer. These results show that the increase in CH4 permeability in the mixed gas experiments is directly related to the presence of CO_2. The strong plasticizing effect of CO_2 and the corresponding excessive swelling of the polymer, especially at higher pressures, overrules the ionic bonds in the n-butyl and the n-hexyl substituted polymer and at higher pressures it also overcomes the tighter ionic bonds in the methyl substituted polymer.

We assume that the concept of tighter ionic bonds has a stronger effect on CO_2 permeability, since CO_2 interacts with the ionic charges, whereas CH_4 interacts predominantly with the alkyl tails due increased hydrophobicity.

As a consequence of the above observations, the mixed gas CO_2/CH_4 selectivity of the three polymers investigated decreases with increasing feed pressure. Figure 4 shows this CO_2/CH_4 selectivity and also the normalized CO_2/CH_4 selectivity values. Normalization is again based on the values obtained at 10 bar.

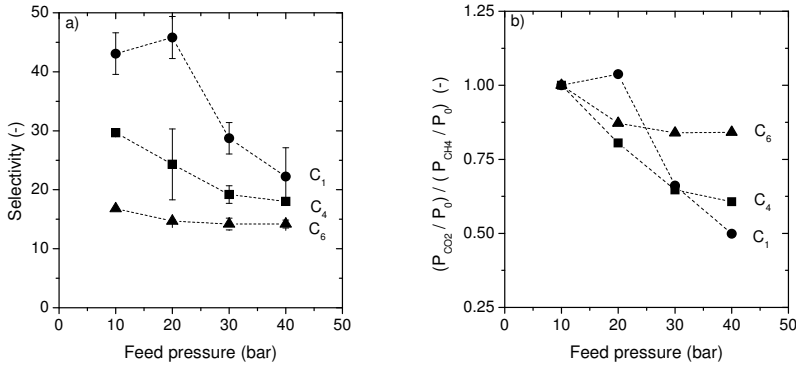

Figure 4: a) CO_2/CH_4 selectivity and b) normalized CO_2/CH_4 selectivity of the methyl (C_1), n-butyl (C_4) and n-hexyl (C_6) poly(RTIL) membranes as a function of the feed pressure. All experiments performed at 20°C. Feed: CO_2/CH_4 (50/50 vol.%).

The selectivity of the membranes strongly depends on the length of the side chain. The methyl-substituted poly(RTIL) gives the highest values for the selectivity whereas the values found for the n-hexyl-substituted materials have the lowest value. The methyl-substituted polymer films show a relatively stable selectivity up to 20 bar. The tighter ionic bonds in this material restrict excessive swelling up to feed pressures of 20 bar, thus preventing a loss in selectivity. Above 20 bar a strong decrease in selectivity with increasing feed pressure is nevertheless observed which is mainly the result of the stronger increase in CH_4 permeability at feed pressures above 20 bar, relative to the increase in CO_2 permeability at higher pressures. As mentioned already, the strong plasticizing effect of CO_2 and the corresponding excessive swelling of the polymer, especially at higher pressures, overrule the ionic bonds in the n-butyl and the n-hexyl

substituted polymer and at higher pressures it also overcomes the tighter ionic bonds in the methyl substituted polymer.

This is also reflected in the normalized selectivity where a strong decrease in relative selectivity at higher mixed feed pressures is observed. Apparently the ionic interactions are not tight enough yet to prevent excessive swelling and at higher pressures the tight ionic bonds in the material are overruled by the higher pressure. For the longer side chain polymers, where ionic bonds are less tight and lower in density, a permanent, less pronounced selectivity decrease can be observed. For pure gas selectivities (not shown here) a gradual increase in normalized selectivity with increasing fugacity is observed, as expected from the permeability data, which confirms the plasticizing effect of CO_2. Although further optimization is required, these experimental results show the potential of the concept and support our hypothesis that stronger ionic interactions offer a versatile route to improve the plasticization resistance of polymer membranes.

CH_4 permeability decay in time

Permeation of strongly plasticizing penetrant molecules (e.g. CO_2) through the polymer film may cause changes in the packing of the polymer chains in the polymer matrix due to swelling. This can induce significant polymer network dilation resulting in increased permeability values for the other components in the feed mixture. Upon removal of the feed pressure desorption of the penetrant molecules takes place. In highly flexible, rubbery polymers, the polymer chains eventually relax back to their original state (reversible effect) on the time scale of the permeation experiment. For glassy polymers, the polymer chains have very little mobility due to its frozen in glassy nature and do not relax back into their original state: this is generally observed as a hysteresis loop in pressurization/de-pressurization permeation experiments and stands for the irreversible nature of the sorption induced conditioning of glassy polymers [30].

A method to study the effect of the presence of penetrants on the polymer structure and packing of the polymer chains in the polymer matrix is to perform pure gas permeation measurements directly after mixed gas permeation measurements and to normalize the obtained values for the initial pure component permeability before the mixed gas permeation experiments. A normalized CH_4 permeability of 1 suggests the absence of irreversible changes in the polymer chain packing, whereas values higher than 1 suggest the occurrence of volume dilation. A value smaller than 1 suggests compaction. If also at longer time scale the CH_4 permeability after mixed gas permeation experiments does not reach its initial value, the changes in the polymer network are considered irreversible. Figure 5 shows the normalized CH_4 permeability decay in time for the three polymers investigated.

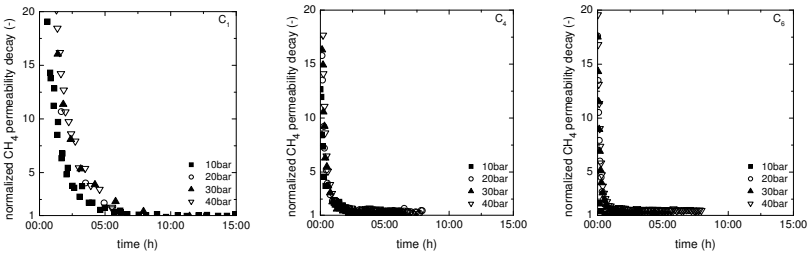

Figure 5: Normalized CH_4 permeability decay in time for the methyl, n-butyl and n-hexyl poly(RTIL) membranes after mixed feed gas permeation experiments at different pressures. All pure gas experiments are performed at 7 bar and 20°C.

All poly(RTIL) membranes show a strong decay of the normalized CH_4 permeability immediately after the start of the pure gas permeation experiments, finally reaching the original values again. The results suggest the absence of irreversible changes in the polymer network when exposed to CO_2. All changes are reversible. Longer times to reach the original values are required for the methyl substituted polymer and when mixed gas experiments at higher pressures prior to pure CH_4 permeation measurements are performed. This reflects the slower transport rate of the gases in the methyl-substituted polymer due to the tighter ionic

interactions in that case. As expected the required times decrease in the order methyl, n-butyl and n-hexyl substituted poly(RTIL).

Effect of temperature

Mixed gas permeation

Besides pressure, also temperature determines the transport rates through the poly(RTIL) membranes. Figure 6 shows the CO_2 permeability and the normalized CO_2 permeability of the membranes as obtained from mixed gas permeation experiments for different pressures at 40°C. Normalization is based on the values found at a feed pressure of 10 bar.

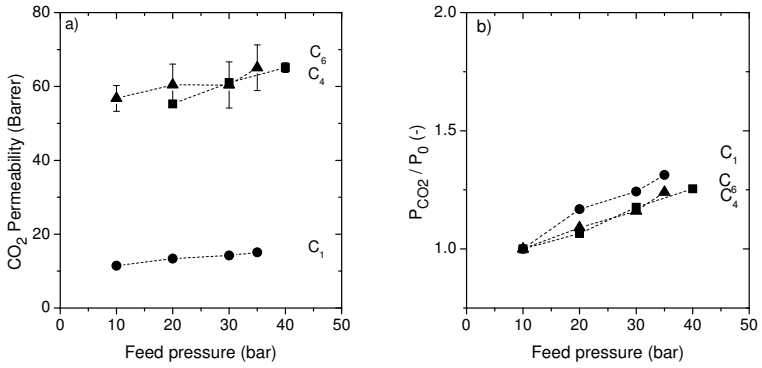

Figure 6: a) CO_2 permeability and b) normalized CO_2 permeability of the methyl, n-butyl and n-hexyl poly(RTIL) membranes as a function of the feed pressure. All experiments performed at 40°C. Feed: CO_2 (50 vol.%) / CH_4 (50 vol.%).

For all films, a slight increase in CO_2 permeability with increasing feed pressure is observed. Highest permeability values are found for the n-butyl and n-hexyl-substituted polymers, while the methyl-substituted poly(RTIL) has significantly lower permeabilities. The same was observed at lower temperatures and attributed to a decreased diffusivity and tighter ionic interactions in the methyl substituted poly(RTIL). The relative increase in permeability (normalized permeability) is almost equal for all three

polymers and no significant differences can be observed at 40°C. This is in contrast to the values found at 20°C, where the relative increase in CO_2 permeability for the methyl substituted poly(RTIL) is obviously lower than the relative increase in permeability for the two other polymers. The increase in temperature increases the segmental mobility of the polymer chains, which overrules the tighter ionic interactions, thus reducing the resistance toward plasticization at higher temperatures.

Figure 7 shows the CO_2/CH_4 selectivity and the normalized CH_4 permeability (normalization based on the values obtained at 10 bar) at 40° C.

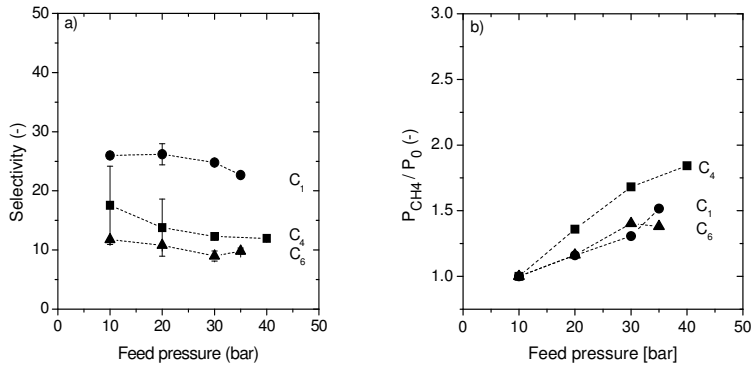

Figure 7: a) CO_2/CH_4 selectivity and b) CH_4 permeability of the methyl, n-butyl and n-hexyl poly(RTIL) membranes as a function of the feed pressure. All experiments performed at 40°C. Feed: CO_2 (50 vol.%) / CH_4 (50 vol.%).

At 40°C, selectivity values are almost constant over the pressure range investigated, but lower values than the values measured at 20°C are obtained. The methyl-substituted poly(RTIL) has a higher selectivity than the other two polymers. The normalized CH_4 permeability as a function of the feed pressure is almost equal for all three poly(RTILs), although the relative increase is somewhat larger for the n-butyl-substituted polymer than for the others. Apparently the effect of the tighter ionic domains is at least partially compensated by the temperature, which increases the mobility and molecular motion of the polymer chains, thus increasing the

flexibility of the polymer chain. Apparently this to some extent overcomes the attraction of the ionic domains in the poly(RTIL) and somewhat reduces the plasticization resistance of the methyl substituted polymer compared to the performance at 20°C.

Pure gas permeation measurements after the mixed gas permeation experiments support the previous hypothesis and show a very fast decrease in CH_4 permeability towards its original value for all poly(RTILs). This shows the absence of irreversible changes in the polymer network, also at higher temperatures.

In addition, also measurements at a temperature of 10°C and a feed pressure of 30 bar were performed. Figure 8 presents the influence of the temperature on the CO_2 and CH_4 permeability at a feed pressure of 30 bar for the three types of poly(RTILs) investigated.

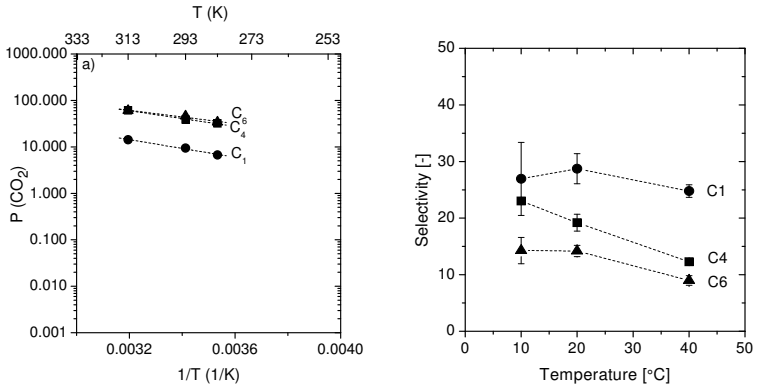

Figure 8: a) Arrhenius plot showing the temperature dependency of the CO_2 permeability and b) the corresponding CO_2/CH_4 selectivities of the methyl, n-butyl and n-hexyl poly(RTIL) membranes at a feed pressure of 30 bar. Feed: CO_2 (50 vol.%) / CH_4 (50 vol.%).

With increasing temperature, the CO_2 (and CH_4) permeability through the three tested membranes increases. This is due to the increased diffusion at higher temperatures, which more than compensates the decrease in solubility with increasing temperature [31]. The CO_2 (and CH_4) permeabilities for the methyl-substituted polymer membranes are over

the whole temperature range lower than the values found for the poly(RTILs) with the longer side chains, most probably due to the decreased diffusivity with shorter chain length and increased ionic interaction [10].

Compared to the other two polymer membranes, the selectivity of the methyl-substituent membrane stays almost constant over the tested temperature range. This supports our hypothesis that the stronger ionic interactions in the methyl substituted poly(RTIL) obviously increase the resistance towards plasticization of the polymer when exposed to highly plasticizing components such as high pressure CO_2.

Conclusions

In this work we investigate the transport and plasticization behaviour of poly(RTILs) at elevated CO_2 pressures. An imidazolium based poly(RTIL) was used as base material and the length of the alkyl chain served as a tool to strengthen and tailor the ionic interactions within the poly(RTIL). High pressure mixed CO_2/CH_4 gas permeation experiments at different temperatures were performed.

As opposed to regular glassy polymers, poly(RTILs) do not show a minimum in permeation rates for CO_2: the permeability increases continuously with increasing feed pressure. Non-plasticizing methane shows a pressure independent permeability. In gas mixtures, the permeability of CO_2 is not suppressed by the presence of methane as is normally observed for glassy polymers due to competitive sorption, but CO_2 does accelerate the transport rate of methane. Only for the C_1-poly(RTIL), at low feed pressures, plasticization in the form of accelerated methane permeability is not present. We interpret this to be related to the strong ionic interactions counter-balancing the volume dilation induced by the sorbed CO_2. The methyl substituted C_1-poly(RTIL) shows an increased gas selectivity at the expense of the permeability compared to the polymers with the longer side chains.

References

1. C.-S. Tan, J.-E. Chen, Absorption of carbon dioxide with piperazine and its mixtures in a rotating packed bed, Separation and Purification Technology, 49 (2006) 174

2. P.H.M. Feron, A.E. Jansen, CO_2 separation with polyolefin membrane contactors and dedicated absorption liquids: Performances and prospects, Separation and Purification Technology, 27 (2002) 231

3. D. deMontigny, P. Tontiwachwuthikul, A. Chakma, Using polypropylene and polytetrafluoroethylene membranes in a membrane contactor for CO_2 absorption, Journal of Membrane Science, 277 (2006) 99

4. S. Atchariyawut, R. Jiraratananon, R. Wang, Separation of CO_2 from CH4 by using gas-liquid membrane contacting process, Journal of Membrane Science, 304 (2007) 163

5. J.-G. Lu, Y.-F. Zheng, M.-D. Cheng, L.-J. Wang, Effects of activators on mass-transfer enhancement in a hollow fiber contactor using activated alkanolamine solutions, Journal of Membrane Science, 289 (2007) 138

6. P. Scovazzo, J. Kieft, D.A. Finan, C. Koval, D. DuBois, R. Noble, Gas separations using non-hexafluorophosphate $[PF_6]$- anion supported ionic liquid membranes, Journal of Membrane Science, 238 (2004) 57

7. R. Fortunato, L.C. Branco, C.A.M. Afonso, J. Benavente, J.G. Crespo, Electrical impedance spectroscopy characterisation of supported ionic liquid membranes, Journal of Membrane Science, 270 (2006) 42

8. D. Camper, C. Becker, C. Koval, R. Noble, Low Pressure Hydrocarbon Solubility in Room Temperature Ionic Liquids Containing Imidazolium Rings Interpreted Using Regular Solution Theory, Ind. Eng. Chem. Res., 44 (2005) 1928-1933

9. J. Tang, W. Sun, H. Tang, M. Radosz, Y. Shen, Enhanced CO2 Absorption of Poly(ionic liquid)s, Macromolecules, 38 (2005) 2037-2039

10. J.E. Bara, S. Lessmann, C.J. Gabriel, E.S. Hatakeyama, R.D. Noble, D.L. Gin, Synthesis and performance of polymerizable room-temperature ionic liquids as gas separation membranes, Industrial and Engineering Chemistry Research, 46 (2007) 5397

11. F.F. Krull, M. Hechinger, W. Kloeckner, M. Verhuelsdonk, F. Buchbender, H. Giese, T. Melin, Ionic liquid imbibition of ceramic nanofiltration membranes, Colloids and Surfaces A: Physicochemical and Engineering Aspects, 345 (2009) 182

12. B.D. Bhide, A. Voskericyan, S.A. Stern, Hybrid processes for the removal of acid gases from natural gas, Journal of Membrane Science, 140 (1998) 27

13. R.D. Raharjo, B.D. Freeman, E.S. Sanders, Pure and mixed gas CH_4 and n-C_4H_{10} sorption and dilation in poly(1-trimethylsilyl-1-propyne), Polymer, 48 (2007) 6097

14. M. Wessling, M. Lidon Lopez, H. Strathmann, Accelerated plasticization of thin-film composite membranes used in gas separation, Separation and Purification Technology, 24 (2001) 223

15. T. Visser, N. Masetto, M. Wessling, Materials dependence of mixed gas plasticization behavior in asymmetric membranes, Journal of Membrane Science, 306 (2007) 16

16. A. Bos, I.G.M. Puent, M. Wessling, H. Strathmann, CO_2-induced plasticization phenomena in glassy polymers, Journal of Membrane Science, 155 (1999) 67

17. J.D. Wind, D.R. Paul, W.J. Koros, Natural gas permeation in polyimide membranes, Journal of Membrane Science, 228 (2004) 227

18. T. Visser, G.H. Koops, M. Wessling, On the subtle balance between competitive sorption and plasticization effects in asymmetric hollow fiber gas separation membranes, Journal of Membrane Science, 252 (2005) 265

19. C. Staudt-Bickel, W. J. Koros, Improvement of CO_2/CH_4 separation characteristics of polyimides by chemical crosslinking, Journal of Membrane Science, 155 (1999) 145

20. P.S. Tin, T.S. Chung, Y. Liu, R. Wang, S.L. Liu, K.P. Pramoda, Effects of cross-linking modification on gas separation performance of Matrimid membranes, Journal of Membrane Science, 225 (2003) 77

21. A. Bos, I.G.M. Puent, M. Wessling, H. Strathmann, Plasticization-resistant glassy polyimide membranes for CO_2/CO_4 separations, Separation and Purification Technology, 14 (1998) 27

22. J.J. Krol, M. Boerrigter, G.H. Koops, Polyimide hollow fiber gas separation membranes: preparation and the suppression of plasticization in propane/propylene environments, Journal of Membrane Science, 184 (2001) 275

23. A. Bos, I. Puent, H. Strathmann, M. Wessling, Suppression of gas separation membrane plasticization by homogeneous polymer blending, AIChE Journal, 47 (2001) 1088

24. Z. Wang, T. Chen, J. Xu, Novel poly(aryl ether ketone)s containing various pendant groups. II. Gas-transport properties, Journal of Applied Polymer Science, 64 (1997) 1725

25. Z. Wang, T. Chen, J. Xu, Gas and water vapor transport through a series of novel poly(aryl ether sulfone) membranes, Macromolecules, 34 (2001) 9015

26. J.E. Bara, D.L. Gin, R.D. Noble, Effect of Anion on Gas Separation Performance of Polymer-Room-Temperature Ionic Liquid Composite Membranes, Industrial & Engineering Chemistry Research, 47 (2008) 9919-9924

27. G.C. Kapantaidakis, G.H. Koops, High flux polyethersulfone-polyimide blend hollow fiber membranes for gas separation, Journal of Membrane Science, 204 (2002) 153

28. C. Cadena, J.L. Anthony, J.K. Shah, T.I. Morrow, J.F. Brennecke, E.J. Maginn, Why Is CO_2 So Soluble in Imidazolium-Based Ionic Liquids? Journal of the American Chemical Society, 126 (2004) 5300-5308

29. S.N.V.K. Aki, J.F. Brennecke, A. Samanta, How polar are room-temperature ionic liquids? Chemical Communications, (2001) 413

30. S.M. Jordan, W.J. Koros, Characterization of CO_2-induced conditioning of substituted polycarbonates using various 'exchange' penetrants, Journal of Membrane Science, 51 (1990) 233

31. D.Q. Vu, W.J. Koros, S.J. Miller, High pressure CO_2/CH_4 separation using carbon molecular sieve hollow fiber membranes, Industrial and Engineering Chemistry Research, 41 (2002) 367

CHAPTER 6

Plasticization behavior of thin and thick polymer films of ODPA-based Polyetherimides for CO_2 separation

Abstract

Plasticization phenomena can significantly reduce the performance of polymeric membranes in high-pressure applications. Polyetherimides (PEIs) are a promising group of membrane materials that combine relatively high CO_2/CH_4 selectivities with high chemical and thermal stability. In this work sorption, swelling, and mixed gas separation performance of 3,3',4,4'-oxydiphthalic dianhydride (ODPA)-based PEI polymers, with 1, 2 or 3 para-aryloxy substitutions in the diamine moeiety, is investigated under conditions where commercial membranes suffer from plasticization. Particular focus is on the influence of the amount of para-aryloxy substitutions and the film thickness. Results are compared with those of commercially available polymeric membrane materials.

The glassy polymers display increasing CO_2 sorption with increasing T_g. The larger extent of sorption results from a larger non-equilibrium excess free volume. Swelling of the polymers is induced by sorption of CO_2 molecules in the non-equilibrium free volume as well as from molecules dissolved in the matrix. Dilation of the polymer is similar for each molecule sorbed. Correspondingly, the partial molar volume of CO_2 is similar for molecules

present in both regions. The smallest molar volume is found for the material with the highest T_g. All such properties are compared to the properties of a sulphonated PEEK, a segmented block-co-polymer PEBAX and the polyimide Matrimid.

The extent of swelling of the ODPA PEI films is very low, which is beneficial for CO_2 removal at elevated pressures. Mixed gas separation experiments showed high CO_2/CH_4 selectivities for the ODPA PEI films at elevated pressure, confirming the potential of this material for the effective separation of CO_2 from CH_4.

Introduction

The separation of CO_2 from CH_4 is an important industrial application. Common examples are Enhanced Oil Recovery (EOR), natural gas sweetening and CO_2 recovery from landfill gas [1]. Next to its environmental impact, CO_2 reduces the heating value of the CH_4 gas streams in power plants and it causes corrosion in pipes and equipment [2]. Currently, CO_2 is removed from gas mixtures mainly by absorption technology (such as amine or hot potassium scrubbing) and pressure swing adsorption [3], but also membrane technology using polymer membranes is frequently applied for this high pressure separation [4], due to its reduced energy requirements, abdication of amine solutions, flexible design and compactness [5].

Polymeric membranes can be based on glassy and rubbery polymers. The state in which the polymer appears determines its mechanical, chemical, thermal and permeation properties. The temperature at which transition from the glassy to the rubbery state occurs is referred to as the glass transition temperature (T_g). Rubbery polymers typically have higher permeabilities than glassy polymers, because of the increased segmental mobility of the polymer chains in the rubbery state, whereas in the glassy state the mobility of the polymeric chains is restricted [6]. Due to the rigid structure of glassy polymers, they usually exhibit higher selectivities [7]. According to Baker [4] the competitive position of membranes for the separation of CO_2 and CH_4 would strengthen, if stable membranes with a selectivity of 40 during operation would become available.

Generally, at low feed pressures the permeability of glassy polymers decreases with increasing feed pressure, as frequently described by the dual-mode sorption model [8, 9]. Even though the postulation of two sorption populations is simplistic, the model has proven to give some insight into the physical phenomena governing the sorption of gasses into the non-equilibrium polymeric glass. At these lower pressures, the solubility of the gas in the polymer is dominated by Langmuir type sorption

and regular Henry type solution of the permeating gas is less important. This causes the permeability to decrease with feed pressure until Henry sorption becomes the dominant mechanism and the permeability levels off to a constant value. Most of the industrial processes to separate CO_2 from CH_4 are however high pressure applications (up to 100 bar feed pressure) [4]. Especially these higher pressures of highly sorbing gases (e.g., CO_2) can induce severe plasticization phenomena in glassy polymer membranes [10-12]. Due to the presence of the plasticizing gas, relaxational phenomena and swelling stresses on the polymer network may occur, resulting in an increase in free volume and segmental mobility of the polymer network. This causes a rise in permeability for all components [13], but as the permeability of the low permeable component is usually more affected, plasticization results in a decrease in selectivity [14-16]. A plot of the permeability versus the CO_2 partial pressure shows a minimum at elevated feed pressures for highly sorbing gasses. [17]. The feed pressure at which the permeability starts to increase is called the plasticization pressure [14]. Next to the properties of the specific polymer, plasticization phenomena are especially depend on the CO_2 concentration in the polymer network, which is directly related to the CO_2 partial pressure and the temperature [11]. Methods to increase the resistance against plasticization and swelling of glassy polymer membranes include physical and chemical crosslinking [18-20], thermal treatments [14, 20, 21] and polymer blending [22].

Most gas separation membranes are based on cellulose acetate or polyimide [4], but both materials types suffer from the occurrence of severe plasticization. Staudt-Bickel et al. [18] showed high CO_2/CH_4 selectivities for fluorinated 6FDA-based polyimide membranes, but the uncrosslinked material shows a rapid decrease in selectivity at higher feed pressures. Crosslinking or blending of the polymer avoids this rapid decrease. Visser et al. [12] evaluated a blend of the polyimide Matrimid® and the co-polyimide P84 and showed a strong improvement in performance in comparison to commonly used cellulose-acetate. Mixed gas permeation experiments showed significantly higher CO_2/CH_4 selectivities, although the selectivity still slightly decreases with increasing

pressure due to the occurrence plasticization. Next to polyimides, poly etherimides are an attractive class of polymers as they posses relatively high CO_2/CH_4 selectivities, high chemical and thermal stability and the potential to prepare asymmetric fibers as high flux membranes [23].

A way to increase the CO_2 flux through the membrane is the preparation of the material into ultrathin layers. Changes in film thickness however can generate changes in membrane performances [11]. CO_2 sorption and plasticization phenomena in thin films can be distinctively different from sorption in bulk materials [11, 24]. Kim et al. [25] showed for glassy 6FDA-based polyimide films that the aging rate is greatly accelerated for thin films compared to thick bulk films and that a correlation of aging rate to free volume is expected. Plasticization in thin films usually occurs at lower feed pressures when compared to bulk materials [11, 26].

In this work a specific group of poly(etherimide)s, i.e. 3,3',4,4'-oxydiphthalic dianhydride (ODPA)-based PEI's, as membrane material for CO_2 separation is evaluated. High CO_2 affinity is expected due to two imide groups in the main chain of the polymer. The number of para arylether moieties in the polymer chain is used as a tool to tailor the segmental mobility and the non-equilibrium excess free volume of the polymer, expressed in the glass transition temperature of the polymer. CO_2 sorption and swelling behavior in thin and bulk polymer films is evaluated and the CO_2 partial molar volume in the polymer films is calculated. The results are related to the gas permeation performance of the films. As a reference, the transport behavior of three other polymeric membrane materials is evaluated: the glassy polymer SPEEK, the glassy polymer Matrimid®, which is known for the occurrence of strong plasticization in the presence of CO_2 [12] and the rubbery polymer PEBAX®.

Theory

Sorption

Ideal polymers are considered to be in a hypothetical thermodynamic equilibrium liquid state. For such systems solubility is independent of concentration and the concentration of gas in the polymer can be described by Henry's law [10, 27] (see Figure 1):

$$C = k_D \cdot p \qquad (1)$$

In Equation (1) C (cm^3 gas (STP) / cm^3 polymer) is the concentration of the sorbed component in the polymer, k_D (cm^3 gas (STP) / (cm^3 polymer · bar)) is the Henry's law constant, and p (bar) is the partial pressure of the gaseous component in the environment surrounding the polymer sample in equilibrium with the concentration of the component in the sample. This linear relationship between pressure and concentration is generally observed for sorption of gases in rubbery polymers [27], i.e., at temperatures above the glass transition temperature (T_g) of a polymer.
At temperatures below their glass transition temperature, polymers contain non-equilibrium excess free volume associated with the glassy state. For glassy polymers, sorption can usually be described by the dual mode sorption model. In this model the glassy polymer is considered to consist of a homogeneous dense polymer matrix in which microcavities are embedded [28, 29]. The dense polymer matrix is considered to be in the ideal hypothetical equilibrium liquid state, and Henry's law can be used to describe sorption of gases in this matrix. The microcavities correspond to the non-equilibrium excess free volume and are considered to be fixed, independent sorption sites. Sorption in the microcavities can be described as Langmuir sorption [27].

Following the dual mode sorption model, the total concentration of a gas in a polymer below its glass transition temperature in equilibrium with the surrounding pressure consequently follows from [27, 30]:

$$C = k_D p + \frac{C'_H bp}{1 + bp} \quad (2)$$

In Equation (2) the constant C'_H (cm^3 gas (STP) / cm^3 polymer) is the Langmuir capacity and describes the sorption capacity of the non-equilibrium excess free volume related to the glassy state of the polymer. The parameter b (1/bar), the Langmuir affinity, is an equilibrium constant that includes the affinity of the penetrant molecules for Langmuir sorption sites in the polymer. Figure 1 shows a schematic representation of the dual mode sorption model (C) composed of Langmuir sorption (C'_H) and sorption according to Henry's law (C_D).

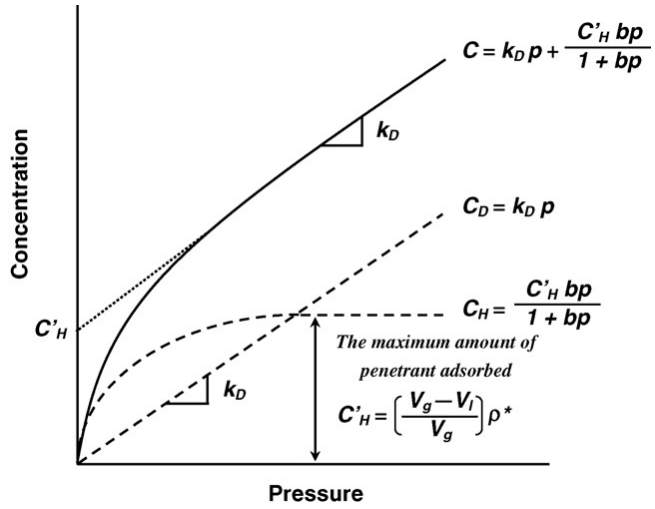

Figure 1: Schematic representation of the dual-mode sorption model, composed of Langmuir sorption (C_H) and sorption according to Henry's law (C_D) [27].

Ellipsometry

Spectroscopic ellipsometry is a non-destructive optical technique in which a sample is illuminated with a polarized light beam after which the polarization state of the reflecting light beam is analyzed by a detector. Subsequent fitting of the experimental data with an optical model allows quantification of the thickness and refractive index of thin films. For more details the reader is referred to, for instance, Tompkins [31].

For a single thin, polymer film on a glass substrate, this optical model contains the wavelength dependent refractive index (referred to as dispersion) of the substrate, the dispersion of the thin film, and the thickness of the film as fitting parameters. Both the glass substrate and thin film are dielectric materials and their dispersion can be described by the Cauchy relation [26, 32]:

$$n = a + \frac{b}{\lambda^2} + \frac{c}{\lambda^4} \qquad (3)$$

In Equation (3) n (-) is the refractive index, λ (nm) is the wavelength of the light, and a, b and c are constants.

The change in refractive index of the film upon sorption of a gaseous component (here CO_2) can be directly related to the concentration of this component in the film. The mass based concentration of the sorbed gas in the polymer (C_{CO2} in g/cm^3) required to construct the sorption isotherm, can be calculated using the Clausius-Mosotti Equation as described by Sirard et al. [33]:

$$\frac{\langle n_f \rangle^2 - 1}{\langle n_f \rangle^2 + 2} = q_{CO_2} C_{CO_2} + q_{polymer} C_{polymer} \qquad (4)$$

In Equation (4) $\langle n_f \rangle$ (-) is the effective refractive index of the swollen film, as determined with the Cauchy relation (Equation 3) from the experimental results, C_{CO2} and $C_{polymer}$ (g/cm^3) are the mass based concentration of the sorbed gas or the polymer respectively, and q_{CO2} and $q_{polymer}$ (cm^3/g) are characteristic constants for the gas or the polymer respectively that can be determined from pure component data, as described by Sirard et al. [33]:

$$\frac{\langle n_j \rangle^2 - 1}{\langle n_j \rangle^2 + 2} = q_j \rho_j \qquad (5)$$

Where $\langle n_j \rangle$ (-) is the refractive index of the pure component (gas or polymer) and ρ_j is the density of the pure component. The densities of the gas and the polymer and the refractive index of pure CO_2 can be obtained from literature [33], whereas the refractive index of the pure polymer can be experimentally determined from an ellipsometry experiment at zero pressure (vacuum).

The mass based concentration of the swollen polymer ($C_{polymer}$) is calculated from:

$$C_{polymer} = \rho_{polymer} \frac{h_0}{h} \qquad (6)$$

In Equation (6) $\rho_{polymer}$ (g/cm^3) is the density of the non-swollen polymer film, h_0 is the initial thickness of the non-swollen polymer film (cm) and h is the thickness of the swollen film (cm), which is determined from the fitting parameters of the experimental ellipsometry data. The volume based CO_2 concentration in the polymer in cm^3 (STP)/cm^3 polymer required for the sorption isotherm can subsequently be recalculated from the mass based concentration ($C_{polymer}$ in g/cm^3) using the molar volume at standard conditions and the molecular weight of the gas.

Experimental part

Materials

ODPA PEI

Figure 2 shows the general structure of the 3,3',4,4'-oxydiphthalic dianhydride (ODPA)-based polyetherimide (PEI) series.

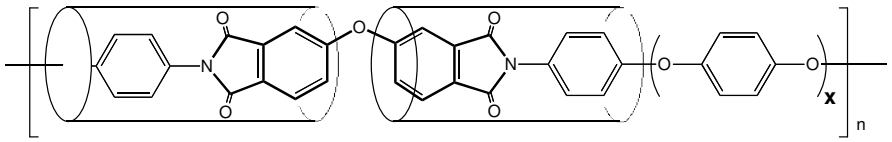

ODPA-P$_x$ where **x** = 1,2 or 3

Figure 2: Structure of the ODPA-based poly(ether imide)s with an increasing para-arylether content (X = 1, 2 or 3).

Poly(ether imide)s with different numbers of para-arylether substitutions (X = 1, 2 or 3) were used and subsequently denoted as ODPA-P1, -P2 and -P3. The monomer syntheses were performed at Delft University of Technology, The Netherlands according to the procedure described elsewhere [34]. 1-Methyl-2-pyrrolidinone (NMP) was used as the solvent for film preparation, and was obtained from Acros (The Netherlands). 3,3',4,4'-Oxydiphthalic dianhydride (ODPA) was purchased from Sigma-Aldrich and used as received.

SPEEK

S-PEEK (Figure 3) with a sulfonation degree of 70% (y = 0.7; x = 0.3), was obtained from the sulfonation of PEEK, as described by Komkova et al. [35]. SPEEK was recently identified as membrane material for the dehydration of (flue) gas streams with extremely high water vapor permeabilities combined with very high water vapor over N_2 and CO_2 selectivities [36, 37].

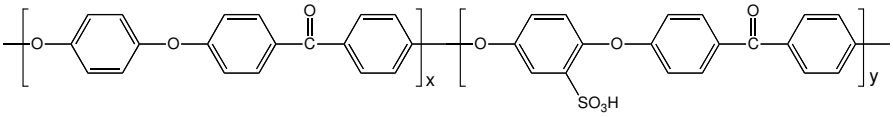

Figure 3: Chemical structure of SPEEK.

PEEK was purchased from Victrex (United Kingdom) and sulfuric acid (95-98 wt %) was obtained from Merck, Germany. Methanol was used as solvent for film preparation and was obtained from Merck, Germany.

Matrimid® 5218

Matrimid® 5218 (Figure 4) is a commercially available polyimide (3,3',4,4'-benzophenonetetracarboxylic dianhydrid and diamino-phenylindane), frequently studied and used for membranes for gas separation [12, 20, 38].

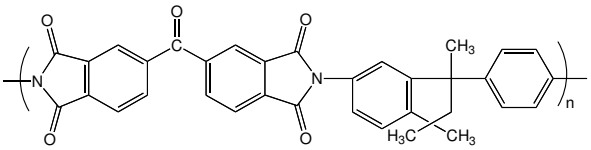

Figure 4: Chemical structure of Matrimid® 5218.

Matrimid® was obtained from Huntsman and THF (Tetrahydrofuran) and NMP (1-methyl-2-pyrrolidinone) were used as solvent and obtained from Merck, Germany and from Acros, the Netherlands, respectively.

PEBAX ® 2533

Poly(amide-6-b-ethylene oxide) (PEBAX® 2533) is a hydrophilic, commercially available block copolymer consisting of a soft polyether (PTMEO (poly(tetramethyleneoxide)) block and a hard polyamide (PA 12 (nylon-12)) block. Permeation of gases preferentially occurs through the soft polyether blocks whereas the hard polyamide blocks provide the mechanical stability. Poly ether based block copolymers offer an attractive material for high permeance CO_2 separation membranes [39]. The Figure 5 shows the chemical structure of PEBAX®.

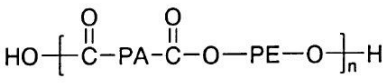

Figure 5: Chemical structure of PEBAX®.

The polymer used for this work was PEBAX® 2533, which contains 20 wt. % hard segment. PEBAX® 2533 is a rubbery polymer. The PE constituents' glass transition temperature is -77°C. 1-butanol and 1-propanol were used as solvent for film preparation and obtained from Merck, Germany.

Preparation of free standing films

ODPA PEI flat films were prepared by reacting ODPA with an equimolar amount of the appropriate diamine, i.e. P1, P2 or P3, in 1-methyl-2-pyrrolidinone (NMP) at room temperature (25 wt.% solids) and casting the resulting polyamic acid solution with a 0.25 mm casting knife on a glass plate. The solvent was evaporated in a nitrogen box for 24 hours. After that the films were heat treated (imidization) in an oven under nitrogen atmosphere according to the temperature program 100°C, 200°C and 300°C, each temperature for 1 hour. After that the films were placed in a water bath, released from the glass plate and subsequently dried in an oven at 30°C for 24 h. Finally, the free standing films were placed in an oven at 260°C for 1 hour. To avoid crystallization the films were immediately cooled down in air when removed from the oven. Freestanding films with a thickness of 17 to 27 µm were obtained.

Thin film preparation

Supported thin films were prepared as described below. Films were supported by a glass plate.

ODPA PEI (P1, P2 and P3)

Solutions containing 25 wt.% of the appropriate polyamic acid in NMP were prepared. An excess amount of solution was dropped on the glass substrate and a spin coater (WS-400B-6NPP/LITE) rotating at 3000 rpm for 1 minute was used to prepare a thin polymer layer. The solvent was evaporated in a nitrogen box for 24 hours. After that the films were heat treated (imidization) in an oven under nitrogen atmosphere according to the temperature program 100°C, 200°C and 300°C, each temperature for 1 hour. To avoid crystallization the films were immediately cooled down in air when removed from the oven. Films with a thickness in the range of 0.5-3.8 µm were obtained.

SPEEK

A 3 wt.% SPEEK in methanol solution was prepared. The solution was dropped directly on a glass plate and dried under nitrogen atmosphere at room temperature for 3 days. Films with a thickness of approximately 1 µm were obtained.

Matrimid® 5218

A mixture of 30 wt. % THF and 70 wt. % NMP was used as solvent for the preparation of thin supported Matrimid® films. Matrimid® (3 wt. %) was mixed with the solvent and the solution was spread on a glass plate. The film was placed in a nitrogen atmosphere for 3 days and afterwards in a vacuum oven at 150°C for approx. 1 week to allow evaporation of the solvent. Films with a thickness of approximately 2 µm were obtained.

PEBAX® 2533

A mixture of 25 wt.% 1-butanol and 75 wt.% 1-propanol was used as solvent for the preparation of thin PEBAX® films. PEBAX® (3 wt. %) was dissolved in the solvent mixture and the solution was spread on a glass plate. To evaporate the solvent, the film was placed in a nitrogen atmosphere for 3 days. Films with a thickness of approximately 2.5 µm were obtained.

Gas sorption

Single gas sorption of CO_2 and CH_4 in freestanding thick, bulk polymer films was investigated using a gravimetric sorption balance (Rubotherm) as described elsewhere [17]. The measured weight (w_t in g) was corrected for buoyancy according to the Archimedes principle by subtracting the weight at zero sorption at a certain pressure from the initial weight of the sample

(w_0 in g). The mass increase of the polymer sample upon sorption (m_t in g) was calculated according to Equation 7 [17]:

$$m_t = w_t - \left(w_0 - V_t \rho_{gas}\right) \quad (7)$$

Where V_t is the sample volume in m^3 and ρ_{gas} is the density of the surrounding gas in g/m^3 (which is determined using the van der Waals Equation). The density of the polymer sample was determined with a Micromeritics AccuPyc 1330 pycnometer at room temperature. The concentration of gas in the polymer (in cm^3 (STP)/cm^3 polymer) was subsequently calculated from this corrected mass increase, the volume of the polymer sample, the molar volume at standard conditions and the molecular weight of the gas.

Before each experiment, the sample with an approximate weight of 0.06 g, was degassed in the sample chamber for at least 12 hours. The gas sorption, monitored as the weight increase of the sample in time was then determined for different pressures (2, 4, 5, 10, 20, 30 and 35 or 40 bar) at a constant temperature of 35 °C. For CO_2, after the pressure-increase run, the pressure was reduced stepwise again to study possible non equilibrium hysteresis. All experiments were performed until equilibrium was reached and the mass remained constant in time.

Ellipsometry

An Alpha-SE™ Spectroscopic Ellipsometer (SE) system was used to study the sorption behavior of the thin polymeric films. Samples were placed in a home-built test-cell with two windows perpendicular to the ellipsometric beam and the measurements were performed with an angle of incidence of 70° in the wavelength range from 370 to 900 nm.

The measurement procedure for all polymers was equal. For each sample, helium, N_2 and CO_2 were applied, consecutively. Before each measurement, the sample was degassed under vacuum for at least one hour. The temperature was kept constant at a value of 35°C. The pressure

was increased step wise from 1 to 51 bars (pressures: 1, 2, 4, 6, 11, 21, 31, 41, 51 bar). In order to study possible non-equilibrium hysteresis for CO_2, the pressure increase run was followed by a pressure decrease run.

For helium and N_2 the refractive index of the gaseous ambient was assumed to be unity and independent of the applied pressure and temperature. The pressure dependent refractive index of the CO_2 atmosphere was taken from literature [40].

The CO_2 sorption in the thin polymer films was determined as described in the theoretical section. The swelling of the thin polymeric films was determined from the change in film thickness:

$$Swelling = \frac{(h - h_0)}{h_0} \cdot 100\% \quad (8)$$

Where h (cm) is the thickness of the swollen film and h_0 (cm) is the initial thickness of the polymer film.

Gas permeation

The CO_2/CH_4 gas separation performance of the ODPA PEI membranes was investigated with a temperature-controlled high pressure gas permeation setup using a constant volume-variable pressure method as described elsewhere [41]. A constant feed pressure was applied and the permeate side was kept under vacuum. The gas permeability through the membrane was calculated from the steady state pressure increase in time in a calibrated volume at the permeate side. The permeability values are expressed in Barrer, where 1 Barrer = 10^{-10} cm^3 (STP)·cm/(cm^2·s·cmHg) (= $7.5 \cdot 10^{-18}$ m^3 (STP)·m/(m^2·s·Pa)). In the case of mixed gas permeation experiments the feed and permeate compositions were analyzed with a Varian gas chromatograph. The selectivity α (CO_2/CH_4) is calculated as:

$$\alpha = \frac{Y_{CO_2} / Y_{CH_4}}{X_{CO_2} / X_{CH_4}} \quad (9)$$

Where Y_i is the concentration of component i in the permeate stream and X_i is the concentration of component i in the feed.

The permeability and separation performance of the membranes using mixed gasses (CO_2/CH_4 (50/50vol.%)) was determined at different feed pressures (10, 20, 30, 35 bar) at 35°C and all experiments were performed in duplo.

Results and discussion

Glass transition temperature

The glass transition temperature, T_g, of a polymer is an important property of the polymer and related to the rigidity and excess free volume of that polymer [42]. For structurally related polymers, like a series of poly ether imides, lower molecular motion and higher rigidity can be expected for polymers with higher T_g [28]. Table 1 shows the T_g values of bulk films of the materials investigated.

Table 1: Glass transition temperature values of bulk films of ODPA-P1, -P2 and -P3 [34], SPEEK [43], Matrimid® [44] and of the soft segment of PEBAX® [39].

Material	T_g (°C)
ODPA P1	243
ODPA P2	214
ODPA P3	206
SPEEK	208
Matrimid	338
PEBAX	-77

The glass transition temperature values show that all investigated ODPA PEI materials are in their glassy state at the experimental temperature used. The T_g decreases with increasing amount of para-arylether substitutions (going from ODPA-P1 to ODPA-P3). This suggests a higher flexibility for the arylether group compared to the remainder of the main-chain and an increase in chain mobility for the polymer with the higher number of para-arylether units in the main chain.

Gas sorption in thick films

Figure 6 shows the CO_2 and CH_4 concentration in thick ODPA-P1, -P2 and -P3 polymer films as a function of the pure gas pressure.

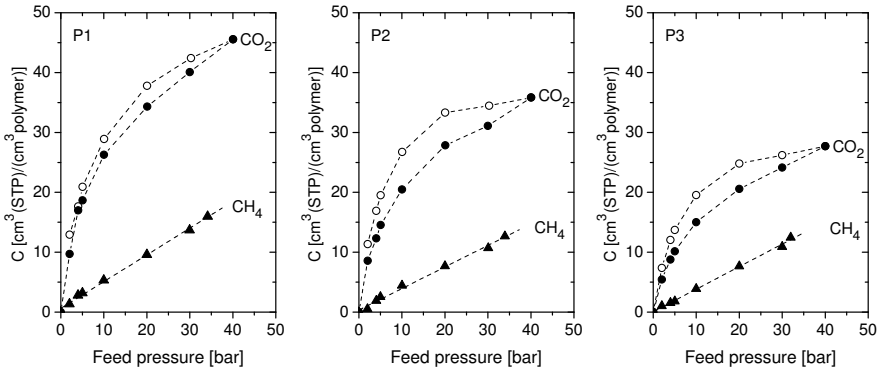

Figure 6: CO_2 sorption (●) and desorption (○) and CH_4 (▲) sorption as a function of the gas pressure for thick ODPA-P1, -P2 and -P3 films at 35°C.

For all three polymers the sorption of CH_4 linearly increases with pressure and this can be described by Henry's law. The linear relation between concentration and pressure suggests that sorption of CH_4 predominantly occurs in the homogeneous dense matrix of the ODPA PEI materials. Table 2 shows the Henry's law constant for CH_4 sorption in the thick ODPA PEI films.

Table 2: CH_4 Henry's law sorption parameter k_D in thick ODPA PEI (-P1, -P2 and -P3) films at 35 °C.

	k_D cm^3 (STP)/cm^3·bar
P1	0.44
P2	0.36
P3	0.37

The value of the Henry's law constant (k_D) for CH_4 of the thick ODPA PEI polymer films stays relatively constant with increasing amount of para-arylether groups. This suggests a similar affinity of CH_4 for the arylether moieties as compared to the imide groups.

Sorption of CO_2 shows different behavior. Figure 6 shows that at all feed pressures and for all three polymers the concentration of CO_2 in the polymer films is higher than the CH_4 concentration. In contrast to CH_4, sorption of CO_2 in the ODPA PEI polymer films does not follow Henry's law. Sorption of CO_2 can be described by the dual mode sorption model, indicating that CO_2 molecules do not only dissolve in the dense polymer matrix, but can also be present in the non-equilibrium excess free volume. For all three materials hysteresis is observed as the CO_2 sorption (closed symbols) and desorption (open symbols) isotherms do not coincide. Desorption values are higher for all polymers. Berens et al. [45] and Wessling et al. [11] interpret this hysteresis as the induction of new free volume sites and subsequent filling of this additional free volume during sorption, whereas during desorption, the collapse of the free volume occurs on longer time scales than the desorption of CO_2. Consequently a higher amount of free volume is available during desorption, resulting in higher CO_2 concentrations.

Table 3 lists the data for the different parameters of the dual mode sorption model for CO_2 as obtained from the experimental results.

Table 3: CO_2 dual mode sorption parameters in thick ODPA PEI (-P1, -P2 and -P3) films at 35°C.

	C'_H [cm^3 (STP)/cm^3]	k_D [cm^3 (STP)/cm^3·bar]	b [1/bar]
P1	32	0.43	0.23
P2	25	0.35	0.22
P3	18	0.29	0.19

The number of para-arylether moieties in the polymer influences both the contribution of the dissolution of the gas in the polymer matrix (sorption according to Henry's law) as well as the dissolution of the gas associated with the excess free volume in the polymer (Langmuir sorption). When compared to the values obtained for the Henry's law constants for CH_4, similar values for CO_2 were obtained. In the case of CO_2, the Henry's law constant (k_D) slightly decreases with increasing number of para-arylether moieties (going from ODPA P1 to P3). Correspondingly, also a slight decrease is observed in the Langmuir affinity parameter *b* with increasing number of para-arylether groups. The decreasing values of the Henry and Langmuir coefficients suggest a lower affinity of CO_2 for the arylether groups as compared to the imide groups. A pronounced decrease of C'_H with increasing number of para-arylether groups is observed. This is in accordance with the differences in glass transition temperature of the three polymers. The addition of para-arylether to the polymer chain results in enhanced macromolecular dynamics, and hence less pronounced non-equilibrium characteristics. With an increasing number of para-arylether moieties, the glass transition temperature and consequently the excess of non-equilibrium free volume decrease. Consequently, the parameter C'_H, which is related to the non-equilibrium excess free volume decreases as well with decreasing T_g.

Gas sorption behavior in thin films

Figure 7 shows the CO_2 concentration in the thin ODPA PEI films as determined by ellipsometry using thin (0.5-3.8 μm) supported films.

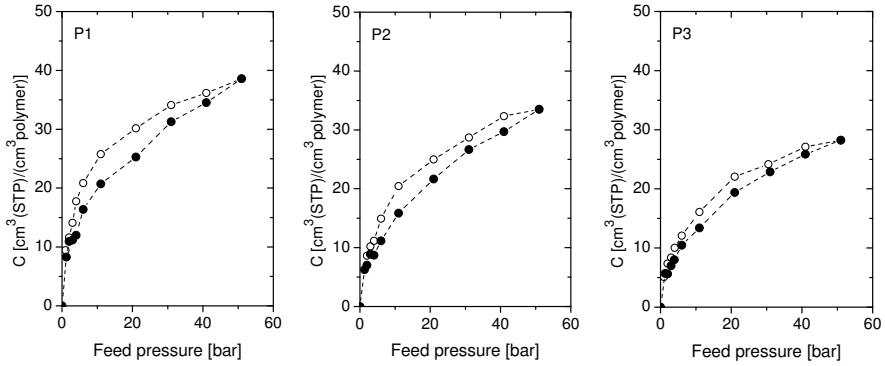

Figure 7: CO_2 sorption (●) and desorption (○) as a function of the CO_2 pressure for thin ODPA-P1, -P2 and -P3 films at 35°C.

The sorption isotherms obtained for the thin films are in general in very good agreement with the isotherms obtained for the thick films. In agreement with the observations for the thick polymer films, CO_2 sorption in all three materials follows the dual mode sorption model. As was the case for the thick films, hysteresis is also observed for the thin films. As hysteresis is a time-related effect and due to the difference in time scales of desorption of the gas and the collapse of the free volume, hysteresis in especially the ODPA-P2 and -P3 thin films is less pronounced than for the freestanding thick films.

The experimental results allow extracting the Henry's law and Langmuir sorption parameters and the results are summarized in Table 4. The same trends as obtained for the thick films are observed for the thin films (a decrease in all sorption parameters with increasing number of para-arylether moieties).

Table 4: CO_2 sorption parameters in thin ODPA PEI (-P1, -P2 and -P3) films at 35 °C.

	C'_H [cm^3 (STP)/cm^3]	k_D [cm^3 (STP)/cm^3·bar]	b [1/bar]
P1	21	0.40	0.25
P2	17	0.35	0.23
P3	15	0.30	0.22

Figure 8 compares the sorption parameters of the thin and the bulk ODPA PEI films as a function of the amount of para-arylether rings in the polymer.

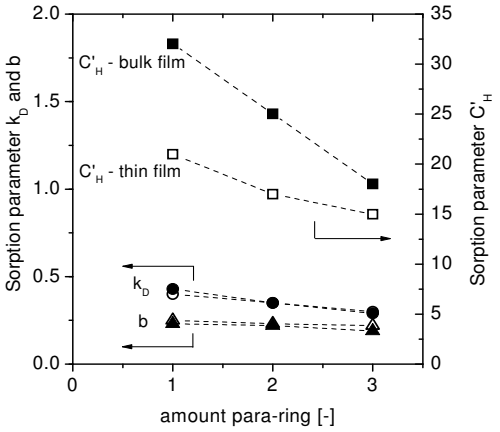

Figure 8: Gas sorption parameters in thin (open symbols) and thick, bulk (closed symbols) ODPA PEI (-P1, -P2 and -P3) films at 35 °C. k_D (● and ○) expressed in (cm^3 (STP)/(cm^3 polymer·bar)), C'_H (■ and □) expressed in (cm^3 (STP)/cm^3 polymer) and b (▲ and Δ) expressed in (1/bar).

Figure 8 clearly shows that the values obtained for the Henry's law constant (k_D) and the Langmuir affinity parameter b for both the thick and the thin films coincide. This indicates that the overall affinity of CO_2 for the polymer materials is determined predominantly by the inherent chemical characteristics of the material, rather than by the consolidation of the polymer from solution during film synthesis. In contrast, the values

obtained for the Langmuir capacity (C'_H) show distinctively lower values for the thin films compared to the thick films and the amount of non-equilibrium excess free volume of the thin films is low compared to that of the bulk materials. Others found the same result. Wind et al. [26] observed a reduced value for C'_H for very thin polyimide films (around 0.1μm), which they attributed to differences in aging of films of different thicknesses. The enhanced rate of aging of thin films can be associated with the thickness dependence of the rate of diffusion of free volume towards the outer surface of the polymer film. For thinner films the rate of diffusion of this free volume is faster [46]. Other possible reasons for the lower values of C'_H found for the thin supported ODPA PEI films can include restrictions imposed by the glass substrate on the polymer conformation close to the glass-polymer interface, and faster evaporation of the solvent from thinner films during film synthesis.

The results obtained for the sorption of CO_2 in thin ODPA PEI films were compared to the sorption behavior of CO_2 in two other glassy polymers (SPEEK and Matrimid®) and the rubbery polymer PEBAX®. Especially Matrimid® [12] and PEBAX® [39] are well known materials for CO_2 separation, whereas SPEEK has been considered for gas dehydration purposes [36, 37]. The sorption isotherms for thin films of these materials are presented in Figure 9.

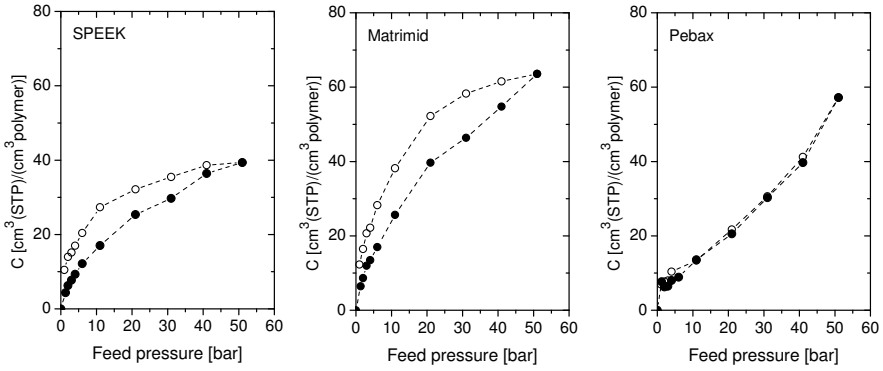

Figure 9: CO_2 sorption (●) and desorption (○) as a function of the CO_2 pressure for thin SPEEK, Matrimid® and PEBAX® films at 35°C (note the difference in Y-axis scale when compared to the values obtained for the ODPA PEI polymers).

Figure 9 shows that the two glassy polymers Matrimid® and SPEEK both follow the dual mode sorption model as well and that for both glassy materials hysteresis is also observed (as is the case for the ODPA PEI polymers). Especially Matrimid®, which has a very high glass transition temperature when compared to the other polymers (Table 1) and is known for its low plasticization resistance [12], shows strong hysteresis.

PEBAX® shows the behavior typically observed for rubbery polymers, and only sorption according to Henry's law occurs. As non-equilibrium excess free volume is absent in rubbery polymers, hysteresis phenomena are not observed.

Swelling

Sorption induced changes in polymer film thickness of ODPA PEI, Matrimid®, SPEEK and PEBAX® fims is studied with spectroscopic ellipsometry. The change in thickness upon sorption with respect to the initial film thickness in the absence of the pressurized gas is referred to as swelling.

Swelling of ODPA PEI (-P1, -P2 and -P3) films

Figure 10 shows the relative swelling of the thin ODPA PEI (-P1, -P2 and -P3) films as a function of the CO_2 or N_2 pressure. Safety reasons prohibited experiments with pressurized CH_4 in our ellipsometry set-up.

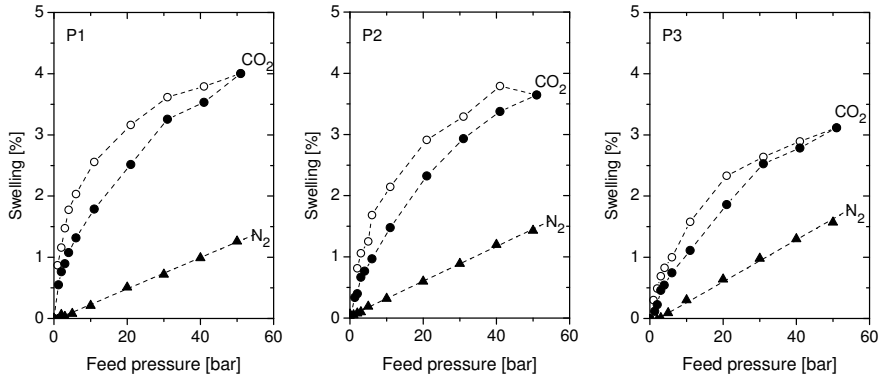

Figure 10: Swelling of the thin ODPA PEI films for CO_2 (● pressurized and ○ depressurized) and N2 (▲) as a function of the pressure at 35°C.

Figure 10 shows that swelling induced by N_2 increases linearly with pressure and is comparable for the three ODPA PEI materials. Similar to CH_4, N_2 molecules are not expected to have specific interactions with the ether and imide groups, and dissolve only in the polymer matrix (sorption according to Henry's law). The linear relation between pressure and swelling indicates that the extent of dilation of the polymer matrix is equal for each additional dissolved N_2 molecule. No pronounced effect of the number of para-arylether groups on the overall dilation is observed, as extent of swelling is comparable for the three materials. An explanation for the absence of an overall effect of ODPA group substitution on dilation is that the anticipated reduction in dilation for the more rigid polymers may be compensated by a larger extent of sorption for these materials. This will be discussed in more detail for CO_2 sorption induced swelling.

For CO_2 a non-linear dependence of swelling on pressure is observed, and the shapes of the graphs are similar as compared to the CO_2 sorption isotherms. The non-linear behavior implies that dilation of the polymer

results from CO_2 molecules present in the polymer matrix (Henry sorption) as well as in the non-equilibrium excess free volume (Langmuir sorption). A similar observation has been reported by Wessling for the polyimide 6FDA-3PDA, 4PDA and 3/4PDA [28]. The extent of swelling for polymers studied here decreases in the order: ODPA-P1 > ODPA-P2 > ODPA-P3. This order is opposite as compared to the order of polymer rigidity, or T_g. The larger dilation of the more rigid materials results from the increase in excess free volume of these materials, and a corresponding larger concentration of penetrant molecules in the polymer. Concurring with the enhanced T_g, for ODPA-P1 and ODPA-P2, hysteresis effects are more pronounced as compared to ODPA-P3. Hysteresis implies that the dynamics of relaxation of the macromolecular structure upon desorption are insufficient to allow the materials to return to their initial state.

Swelling of SPEEK, Matrimid®, and PEBAX® films

For comparison, the swelling behavior of the three other polymers (Matrimid® and SPEEK, which are both glassy polymers and PEBAX®, which is a rubbery polymer) was studied as well (Figure 11).

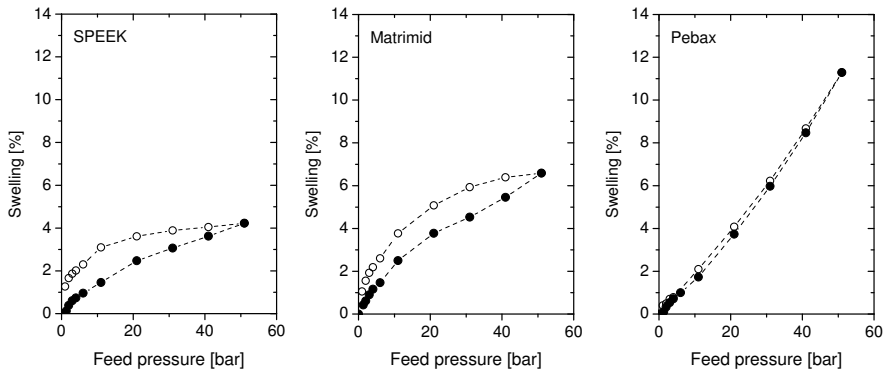

Figure 11: Swelling for CO_2 (● pressurized and ○ depressurized) as a function of pressure for thin SPEEK, Matrimid® and PEBAX® films at 35°C (note the difference in Y-axis scale when compared to the values obtained for the ODPA PEI polymers).

Figure 11 shows CO_2 induced swelling of SPEEK, Matrimid®, and PEBAX® films. SPEEK and Matrimid® are glassy polymers. Their CO_2 induced swelling behavior is analogue to that of the ODPA PEI films: dilation increases less than linear with pressure and hysteresis is observed upon desorption. The extent of swelling of SPEEK is in the same range as that of the ODPA PEI films. Matrimid® shows a larger degree of sorption induced swelling, due to the large excess free volume of this high T_g material (338°C) and the corresponding high concentration of sorbed CO_2. As compared to the ODPA PEI films, hysteresis is more distinct for SPEEK. For Matrimid hysteresis is even more pronounced. In contrast to the glassy polymers, PEBAX® shows a more than linear dependence of swelling on pressure with no significant hysteresis. The absence of hysteresis and the increasing slope of swelling versus pressure are due to the rubbery character of PEBAX®.

We attribute the enhanced swelling of the more rigid materials to the larger non-equilibrium excess free volume in these materials, and the corresponding higher concentration of sorbed CO_2 molecules in that volume. In the next section focus will be on comparing the extent of dilation induced by molecules sorbed in either the non-equilibrium or equilibrium regions of the polymers.

CO_2 partial molar volume

Sorption of CO_2 into the polymer causes an increase in thin film thickness. This change in film thickness can be used to calculate the partial molar volume of sorbed CO_2 molecules in the polymer film. For a thin film that shows sorption induced dilation in a single direction only, the partial molar volume of CO_2 in the polymer can be calculated from [26, 28]:

$$\upsilon_{CO_2} = 22400 \cdot \frac{\partial \frac{\Delta h}{h_0}}{\partial C} \qquad (10)$$

Where Δh is the change in film thickness due to gas sorption (cm), h_0 is the initial thickness of the polymer film (cm) and C is the CO_2 concentration in the polymer film ($cm^3(STP)/cm^3$). The slope of a plot of the concentration versus the swelling ($\Delta(h/h_0)$) (Figure 12) represents the partial molar volume of CO_2 in the corresponding polymer material.

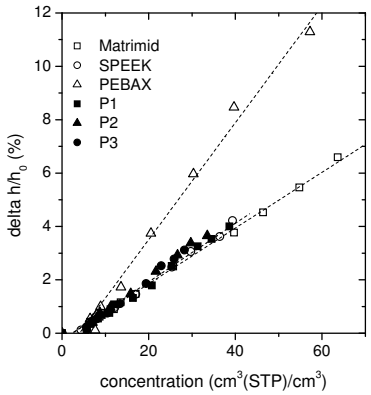

Figure 12: Swelling ($\Delta(h/h_0)$) of the thin ODPA-P1, -P2 and -P3 films and thin Matrimid®, SPEEK and PEBAX® films as a function of the CO_2 concentration at 35°C. The slope of the plots represent the partial molar volume of CO_2 in the corresponding polymer material.

For all films studied, the data in Figure 12 fit well to a linear relation with a small offset in the low pressure range. The offset could arise from molecules present in the material that do not induce swelling (pinholes etc.) but is more likely an artifact of our technique. The linear relation between swelling and concentration implies that the molar volume of CO_2 in the polymer is independent of concentration. For the glassy polymers in the low concentration range, changes in concentration arise predominantly from molecules entering the non-equilibrium excess free volume. At higher concentration this free volume has become more or less saturated and changes in concentration arise predominantly from molecules dissolving in the polymer matrix. The independence of molar volume on concentration suggests that CO_2 molecules in the non-equilibrium and equilibrium regions of the polymer have a similar partial molar volume. Wessling observed similar effects [28] and Wijmans puts

the role of partial molar volume into a perspective for the solution diffusion model [47].

The values obtained for the partial molar volume of CO_2 in the different polymer matrices (slopes of Figure 12) are summarized in Table 5.

Table 5: Partial molar volume of CO_2 in the polymer matrix and the glass transition temperature at 35 °C of the different polymers investigated.

	CO_2 partial molar volume (cm^3/mol)	T_g (°C)
ODPA-P1	24.6	243
ODPA-P2	26.7	214
ODPA-P3	27.1	206
Matrimid	23.4	338
SPEEK	24.6	208
Pebax	49.1	-77

Although the differences in partial molar volume of CO_2 in especially the glassy polymers are small and there is no linear correlation, a higher glass transition temperature results in a lower partial molar volume of CO_2 in the polymer. Comparing the ODPA PEI films, a slightly lower value of the molar volume is found for the most rigid material, i.e., P1. This is in agreement with the observations of Wessling [28]., who demonstrated that the partial molar volume increases when the T_g of the polymer decreases. ODPA P1 exhibits over the full pressure range investigated higher sorption and swelling values than the ODPA PEI polymer with three para-arylether moieties (ODPA P3). This is related to the higher affinity of P1 for CO_2. In addition, the partial molar volume of CO_2 in ODPA P1 is smaller than the value found for ODPA P3. This suggests a lower increase in swelling of the polymer per mol CO_2 for ODPA P1 when compared to ODPA P3 due to its more rigid structure, visualized by its higher T_g.

Of all materials Matrimid® has the largest T_g, and indeed shows the smallest partial molar volume. The inverse relation between partial molar volume and T_g results from the fact that less stiff polymer matrices can dilate more easily than stiff matrices [28]. In comparison to the glassy polymers, the rubbery PEBAX® has a very flexible matrix. In PEBAX® the partial molar volume of CO_2 is indeed much larger and comparable to the molar volume found for liquid CO_2.

Gas permeation

Figure 13 shows the CO_2 and CH_4 permeability through the three thick ODPA PEI polymer films as a function of the gas partial pressure at 35°C.

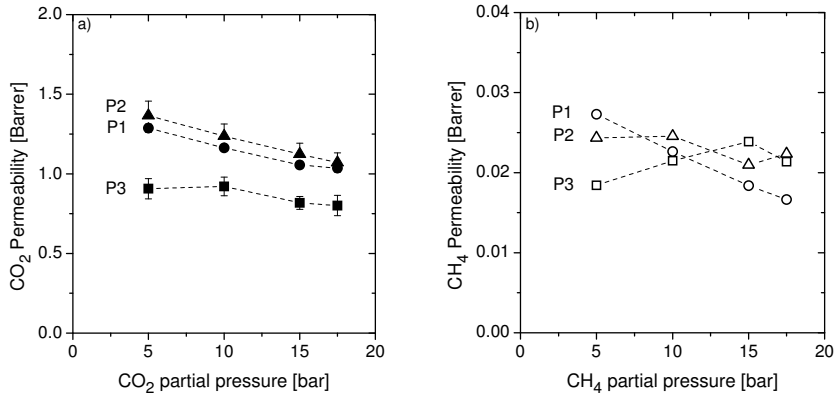

Figure 13: CO_2 (a) and CH_4 (b) permeability as a function of gas partial pressure for thick ODPA P1, P2 and P3 films at 35°C. Feed mixed gas: CO_2/CH_4 (50/50 vol.%).

The three materials all show a decrease in CO_2 permeability with increasing feed pressure. When the pressure is increased, the absolute amount of CO_2 molecules absorbed in the polymer still increases, but the relative increase in this amount with pressure decreases as increasingly less Langmuir sorption sites for CO_2 sorption are available.

Permeation of gases through dense polymeric membranes is generally described by the solution-diffusion model (P=D·S) [48] and both the solubility and the diffusivity determine the overall permeability of a gas. An increase in T_g generally gives rise to two counteracting phenomena: a

reduction in mobility of the CO_2 molecules (diffusivity) and an increase in the extent of their sorption (solubility). There are no general rules which of these two phenomena dominates and attempts to find a general correlation between T_g and permeability have failed [49]. For the ODPA PEI materials investigated, the enhanced sorption with increasing T_g seems to overcompensate the reduced mobility of CO_2 molecules, as compared to ODPA-P1 and ODPA-P2, polymer ODPA-P3 has the lowest T_g (206°C) and shows the lowest permeability. Considering the significant differences in T_g (P1: 243°C and P2: 214°C) and sorption for ODPA-P1 and ODPA-P2, the small difference in permeability between these two polymers implies a significant reduction in CO_2 mobility for ODPA-P1.

In the case of CH_4 sorption occurs predominantly in the polymer matrix, and saturation effects are not anticipated at higher pressures. For P1 the permeability of CH_4 shows a decrease with pressure. This is not likely due to competition for the Langmuir sorption sites by CH_4 and CO_2 [17], as CH_4 is not absorbed in the Langmuir sorption sides, but the mutual presence of both species in the equilibrium regions seems to reduce the transport of CH_4. For P2 the decrease in permeability with pressure is far less pronounced. For P3 an increase in permeability versus pressure is observed. Figure 14 shows the CO_2/CH_4 selectivity as a function of CO_2 partial pressure.

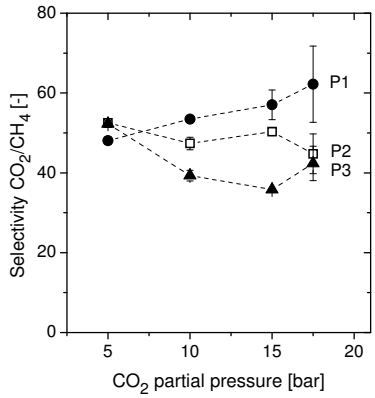

Figure 14: CO_2/CH_4 selectivity as a function of CO_2 partial pressure for thick ODPA P1, P2 and P3 films at 35°C. Feed gas mixture: CO_2/CH_4 (50/50 vol.%).

The different ODPA materials display a similar selectivity (around 50) at a CO_2 partial pressure of 5 bar. With increasing pressure, differences in selectivity are observed. ODPA-P3 shows a slight reduction in selectivity, the selectivity of ODPA-P2 remains relatively constant up to 15 bars and shows a subsequent decrease and the selectivity of ODPA-P1 increases with increasing CO_2 partial pressure. The decrease in selectivity can indicate weak plasticization behavior of the polymer. Plasticization effects appear more evident for polymer ODPA-P3 than for the other two polymers. This can be related to the relatively low T_g and large molar volume of CO_2 in the case of ODPA-P3. The large partial molar volume of CO_2 in this polymer corresponds to a larger dilation per sorbed CO_2 molecule, and hence more pronounced plasticization is anticipated.

Despite the reduction in selectivity for ODPA-P2 and -P3, these materials still have a selectivity of approximately 40 at a CO_2 partial pressure of 17.5 bar (total feed pressure of 35 bar). This selectivity is much higher than the selectivity of the commercially available polymer Matrimid®. Bos et al. observed a CO_2/CH_4 selectivity for Matrimid® (55/45 mol% feed mixture at 35°C) of approximately 30 at 35 bar [22]. For the rubbery polymer PEBAX®, even much lower ideal selectivities (16.2) by Sridhar et al. [50] are observed, although permeability is significantly higher (5.5 Barrer at 20 kg/cm^2). The high selectivities of the ODPA PEI films at high CO_2 partial pressure show the potential of this material for the effective separation of CO_2 from light gases.

Conclusions

Many CO_2/CH_4 gas separations involve high pressure CO_2 applications, for which membranes are an attractive separation technology. Plasticization phenomena can significantly reduce the performance of polymeric membranes. In this work sorption, swelling, and mixed gas separation performance of ODPA PEI polymers, with 1, 2 or 3 para-arylether substitutions, is investigated under conditions where commercial membranes suffer from plasticization. Particular focus is on the influence of the amount of para-arylether substitutions and the film thickness. Results are compared with those of three commercially available polymeric membrane materials, the glassy polymers SPEEK and Matrimid®, and the rubbery polymer PEBAX®.

The glassy polymers displayed increasing CO_2 sorption with increasing T_g. The larger extent of sorption results from a larger non-equilibrium excess free volume. Swelling of the polymers is induced by sorption of CO_2 molecules in the non-equilibrium free volume as well as from molecules dissolved in the matrix. Dilation of the polymer is similar for each molecule sorbed, irrespective of the fact if the molecule enters the non-equilibrium or equilibrium region. Correspondingly, the partial molar volume of CO_2 is similar for molecules present in both regions. The smallest molar volume is found for the material with the highest T_g, Matrimid®. For the rubbery polymer Pebax® the partial molar volume of CO_2 resembles that of pure liquid CO_2.

Sorption of CO_2 in thin films only differs from that in bulk materials regarding the Langmuir capacity (C'_H), while the values obtained for the Henry's law constant (k_D) and the Langmuir affinity parameter b coincide. This indicates that the overall affinity of CO_2 for the polymer materials is determined predominantly by the inherent chemical characteristics of the material, rather than by the consolidation of the polymer from solution during film synthesis.

The extent of swelling of the ODPA PEI films is very low, which is beneficial for CO_2 removal at elevated pressures. Mixed gas separation experiments showed high CO_2/CH_4 selectivities for the ODPA PEI films at elevated

pressure, confirming the potential of this material for the effective separation of CO_2 from CH_4.

References

1. A. Bos, High pressure CO_2/CH_4 separation with glassy polymer membranes, PhD thesis, (1996)

2. S. Ma'mun, V.Y. Dindore, H.F. Svendsen, Kinetics of the Reaction of Carbon Dioxide with Aqueous Solutions of 2-((2-Aminoethyl)amino)ethanol, Ind. Eng. Chem. Res., 46 (2007) 385-394

3. H. Lin, B.D. Freeman, Materials selection guidelines for membranes that remove CO2 from gas mixtures, Journal of Molecular Structure, 739 (2005) 57

4. R.W. Baker, Future Directions of Membrane Gas Separation Technology, Ind. Eng. Chem. Res., 41 (2002) 1393-1411

5. C. Staudt-Bickel, W. J. Koros, Improvement of CO_2/CH_4 separation characteristics of polyimides by chemical crosslinking, Journal of Membrane Science, 155 (1999) 145-154

6. M.H.V. Mulder, Basic principles of membrane technology, Kluwer Academic Publishers, (1996)

7. L.M. Robeson, Polymer membranes for gas separation, Current Opinion in Solid State and Materials Science, 4 (1999) 549

8. M. Wessling, S. Schoeman, T. van der Boomgaard, C.A. Smolders, Plasticization of gas separation membranes, Gas Separation and Purification, 5 (1991) 222

9. V.I. Bondar, Y. Kamiya,Y.P. Yampol'skii, On pressure dependence of the parameters of the dual-mode sorption model, Journal of Polymer Science, Part B: Polymer Physics, 34 (1996) 369

10. R.D. Raharjo, B.D. Freeman, E.S. Sanders, Pure and mixed gas CH_4 and n-C_4H_{10} sorption and dilation in poly(1-trimethylsilyl-1-propyne), Polymer, 48 (2007) 6097

11. M. Wessling, M. Lidon Lopez, H. Strathmann, Accelerated plasticization of thin-film composite membranes used in gas separation, Separation and Purification Technology, 24 (2001) 223

12. T. Visser, N. Masetto, M. Wessling, Materials dependence of mixed gas plasticization behavior in asymmetric membranes, Journal of Membrane Science, 306 (2007) 16

13. T. Visser, M. Wessling, When do sorption-induced relaxations in glassy polymers set in? Macromolecules, 40 (2007) 4992

14. A. Bos, I.G.M. Puent, M. Wessling, H. Strathmann, CO_2-induced plasticization phenomena in glassy polymers, Journal of Membrane Science, 155 (1999) 67

15. J.D. Wind, D.R. Paul, W.J. Koros, Natural gas permeation in polyimide membranes, Journal of Membrane Science, 228 (2004) 227

16. J.D. Wind, S.M. Sirard, D.R. Paul, P.F. Green, K.P. Johnston, W.J. Koros, Relaxation Dynamics of CO_2 Diffusion, Sorption, and Polymer Swelling for Plasticized Polyimide Membranes, Macromolecules, 36 (2003) 6442-6448

17. T. Visser, G.H. Koops, M. Wessling, On the subtle balance between competitive sorption and plasticization effects in asymmetric hollow fiber gas separation membranes, Journal of Membrane Science, 252 (2005) 265

18. C. Staudt-Bickel, W. J. Koros, Improvement of CO_2/CH_4 separation characteristics of polyimides by chemical crosslinking, Journal of Membrane Science, 155 (1999) 145

19. P.S. Tin, T.S. Chung, Y. Liu, R. Wang, S.L. Liu, K.P. Pramoda, Effects of cross-linking modification on gas separation performance of Matrimid membranes, Journal of Membrane Science, 225 (2003) 77

20. A. Bos, I.G.M. Puent, M. Wessling, H. Strathmann, Plasticization-resistant glassy polyimide membranes for CO_2/CO_4 separations, Separation and Purification Technology, 14 (1998) 27

21. J.J. Krol, M. Boerrigter, G.H. Koops, Polyimide hollow fiber gas separation membranes: preparation and the suppression of plasticization in propane/propylene environments, Journal of Membrane Science, 184 (2001) 275

22. A. Bos, I. Puent, H. Strathmann, M. Wessling, Suppression of gas separation membrane plasticization by homogeneous polymer blending, AIChE Journal, 47 (2001) 1088

23. D. Wang, K. Li, W.K. Teo, Preparation and characterization of polyetherimide asymmetric hollow fiber membranes for gas separation, Journal of Membrane Science, 138 (1998) 193

24. B.W. Rowe, B.D. Freeman, D.R. Paul, Physical aging of ultrathin glassy polymer films tracked by gas permeability, Polymer, 50 (2009) 5565

25. J.H. Kim, W.J. Koros, D.R. Paul, Physical aging of thin 6FDA-based polyimide membranes containing carboxyl acid groups. Part I. Transport properties, Polymer, 47 (2006) 3094

26. J.D. Wind, S.M. Sirard, D.R. Paul, P.F. Green, K.P. Johnston, W.J. Koros, Carbon dioxide-induced plasticization of polyimide membranes: Pseudo-equilibrium relationships of diffusion, sorption, and swelling, Macromolecules, 36 (2003) 6433

27. S. Kanehashi, K. Nagai, Analysis of dual-mode model parameters for gas sorption in glassy polymers, Journal of Membrane Science, 253 (2005) 117

28. M. Wessling, Relaxation phenomena in dense gas separation membranes, PhD thesis, (1993)

29. A.F. Ismail, W. Lorna, Penetrant-induced plasticization phenomenon in glassy polymers for gas separation membrane, Separation and Purification Technology, 27 (2002) 173

30. T.T. Moore, W.J. Koros, Gas sorption in polymers, molecular sieves, and mixed matrix membranes, Journal of Applied Polymer Science, 104 (2007) 4053-4059

31. H.G. Tompkins, Film thickness measurements using ellipsometry when the lower interface is uncharacterized, Thin Solid Films, 181 (1989) 285

32. J.A. Woollam, CompleteEASE Software Manual, J.A. Woollam Co., Inc., (2007)

33. S.M. Sirard, P.F. Green, K.P. Johnston, Spectroscopic ellipsometry investigation of the swelling of poly(dimethylsiloxane) thin films with high pressure carbon dioxide, Journal of Physical Chemistry B, 105 (2001) 766

34. T.J. Dingemans, E. Mendes, J.J. Hinkley, E.S. Weiser, T.L. StClair, Poly(ether imide)s from diamines with para-, meta-, and ortho-arylene substitutions: Synthesis, characterization, and liquid crystalline properties, Macromolecules, 41 (2008) 2474

35. E.N. Komkova, M. Wessling, J. Krol, H. Strathmann, N.P. Berezina, Influence of the nature of polymer matrix and the degree of sulfonation on the properties of membranes, Polymer Science - Series A, 43 (2001) 300

36. H. Sijbesma, K. Nymeijer, R. van Marwijk, R. Heijboer, J. Potreck, M. Wessling, Flue gas dehydration using polymer membranes, Journal of Membrane Science, 313 (2008) 263

37. J. Potreck, F. Uyar, H. Sijbesma, K. Nijmeijer, D. Stamatialis, M. Wessling, Sorption induced relaxations during water diffusion in S-PEEK, Physical Chemistry Chemical Physics, 11 (2009) 298

38. Y. Huang, D.R. Paul, Effect of film thickness on the gas-permeation characteristics of glassy polymer membranes, Industrial and Engineering Chemistry Research, 46 (2007) 2342

39. V.I. Bondar, B.D. Freeman, I. Pinnau, Gas transport properties of poly(ether-b-amide) segmented block copolymers, Journal of Polymer Science, Part B: Polymer Physics, 38 (2000) 2051

40. J. Obriot, J. Ge, T.K. Bose, J.M. St-Arnaud, Determination of the density from simultaneous measurements of the refractive index and the dielectric constant of gaseous CH_4, SF_6, and CO_2, Fluid Phase Equilibria, 86 (1993) 314

41. G.C. Kapantaidakis, G.H. Koops, High flux polyethersulfone-polyimide blend hollow fiber membranes for gas separation, Journal of Membrane Science, 204 (2002) 153

42. Y. Hirayama, T. Yoshinaga, Y. Kusuki, K. Ninomiya, T. Sakakibara, T. Tamari, Relation of gas permeability with structure of aromatic polyimides I, Journal of Membrane Science, 111 (1996) 169

43. S.M.J. Zaidi, S.D. Mikhailenko, G.P. Robertson, M.D. Guiver, S. Kaliaguine, Proton conducting composite membranes from polyether ether ketone and heteropolyacids for fuel cell applications, Journal of Membrane Science, 173 (2000) 17

44. T.S. Chung, S.S. Chan, R. Wang, Z. Lu, C. He, Characterization of permeability and sorption in Matrimid/C60 mixed matrix membranes, Journal of Membrane Science, 211 (2003) 91

45. A.R. Berens, Effects of sample history, time, and temperature on the sorption of monomer vapor by PVC, Journal of Macromolecular Science, Part B: Physics, 14 (1977) 483 - 498

46. Y. Xiao, B.T. Low, S.S. Hosseini, T.S. Chung, D.R. Paul, The strategies of molecular architecture and modification of polyimide-based membranes for CO_2 removal from natural gas-A review, Progress in Polymer Science (Oxford), 34 (2009) 561

47. J.G. Wijmans, The role of permeant molar volume in the solution-diffusion model transport equations, Journal of Membrane Science, 237 (2004) 39

48. J.G. Wijmans, R.W. Baker, The solution-diffusion model: A review, Journal of Membrane Science, 107 (1995) 1

49. S. Matteucci, Y. Yampolskii, I. Pinnau, B.D. Freeman, Transport of gases and vapors in glassy and rubbery polymers, in Yampolskii, Pinnau, Freeman (Eds), Materials science of membranes, John Wiley&Sons, Ltd., (2006)

50. S. Sridhar, R. Suryamurali, B. Smitha, T.M. Aminabhavi, Development of crosslinked poly(ether-block-amide) membrane for CO_2/CH_4 separation, Colloids and Surfaces A: Physicochemical and Engineering Aspects, 297 (2007) 267

CHAPTER 7

Conclusions and Outlook

This thesis investigates the potential of membrane technology for the effective removal of CO_2 from CH_4. The work focuses on two distinctively different membrane processes to accomplish the separation, i.e. the use of a gas-liquid membrane contactor for the selective absorption of CO_2 (described in Chapter 2 to 4) and the use of thin, dense gas separation membranes to establish the separation (described in Chapter 5 and 6). Chapter 2 to 4 predominantly focuses on process technology and system design related aspects, whereas the focus of Chapter 5 and 6 is primarily on the development of new membrane materials for CO_2 separation. In this final chapter the main conclusions of the work are summarized and an outlook for further research based on this work is presented.

Conclusions

In **Chapter 2** porous PP and asymmetric PPO hollow fiber membranes were used in a gas-liquid membrane contactor for the separation of CO_2 and CH_4 and the influence of different process parameters on productivity and selectivity was evaluated. The proposed approach allowed identifying the operating window and potential of the process. In the case of the porous PP fibers, the main resistance against mass transfer was located in the liquid boundary layer, whereas in the case of the asymmetric PPO membranes the resistance of the membranes was the dominant factor and determined the performance. For the PP membranes, an increase in liquid

flow rate thus resulted in a direct increase in CO_2 productivity. Desorption was the limiting step in the process and ways to overcome this by e.g. increasing the temperature of desorption immediately resulted in improved performance data. Although the performance of the PP membranes outperformed the performance of the PPO membranes in terms of productivity and selectivity, the PP fibers were extremely sensitive to only small variations in the feed pressure, resulting in severe performance loss. The PPO membranes showed their superior character, due to tremendously reduced sensitivity of the system towards variations in feed pressure, which thus improves the performance and significantly increases the operating window and potential of the membrane contactor process.

To test the potential of aqueous potassium sarcosinate solutions as new absorption liquid, gas absorption experiments in the pseudo-first-order regime were carried out in **Chapter 3** to determine the reaction rate constant for the absorption of CO_2 in the solution. Next to the influence of the sarcosine concentration (0.5 to 3.8 M) and the temperature (298 to 308 K), the reaction rate constant of partially CO_2 loaded sarcosine salt solutions was determined. Compared to the commonly used absorption liquid MEA, high reaction rate constants (22915 ± 3050 $(L/mol \cdot s)^{1.66}$) were obtained for the absorption of CO_2 in aqueous sarcosine salt solutions. The apparent reaction rate constant strongly decreases with increasing CO_2 loading of the absorption liquid. This decrease could be reasonably well described by taking into consideration the decrease in free amino acid concentration, assuming a reaction stoichiometry of one molecule of CO_2 reacting with two molecules of potassium sarcosinate. This observation is especially relevant for cyclic absorption processes such as gas-liquid membrane contactors, were incomplete solvent regeneration is likely to occur.

In **Chapter 4** the high product yields and selectivities of CO_2 absorption processes were combined with the advantages of membrane technology in a membrane contactor for the separation of CO_2 from CH_4 using amino acid salt solutions as competitive absorption liquid to alkanol amine solutions. In contrast to this work, literature very frequently only reports

CO_2 mass fluxes and absorption rates, which provide only limited information about the performance of the process in the real application.
Membrane contactor experiments showed that even without a temperature difference between absorber and desorber, a CO_2/CH_4 selectivity of over 70 could be achieved easily with the sarcosine salt solution as absorption liquid. This selectivity reached values of 120 at a temperature difference between absorber and desorber of 35°C, compared to a value of only 60 for MEA under the same conditions. Although CO_2 permeance values were somewhat lower than the values obtained for MEA, the results clearly showed the potential of amino acid salt solutions as competitive absorption liquids for the energy efficient removal of CO_2.
In **Chapter 5** the transport and plasticization behavior of poly(RTIL) membranes at elevated CO_2 pressures was investigated. An imidazolium based poly(RTIL) was used as base material and the length of the alkyl chain served as a tool to strengthen or tailor the ionic interactions within the poly(RTIL). High pressure mixed CO_2/CH_4 gas permeation experiments at different temperatures were performed. As opposed to regular glassy polymers, poly(RTIL)s did not show a minimum in permeation rates for CO_2: the permeability increased continuously with increasing feed pressure. Non-plasticizing methane showed a pressure independent permeability. In gas mixtures, CO_2 accelerates the transport rate of methane. The poly(RTIL) membranes with the short, methyl substituted side chain and stronger ionic interactions showed an increased resistance towards plasticization when compared to the two other polymers. The methyl substituted polymer membrane had increased gas selectivity at the expense of the permeability compared to the polymers with the longer side chains.
In **Chapter 6** sorption, swelling, and mixed gas separation performance of ODPA PEI polymers, with 1, 2 or 3 para-arylene substitutions, was investigated under conditions where commercial membranes suffer from plasticization. Particular focus was on the influence of the amount of para-arylene substitutions and the film thickness. Results were compared with

those of three commercially available polymeric membrane materials, the glassy polymers SPEEK and Matrimid®, and the rubbery polymer PEBAX®.
The glassy polymers displayed increasing CO_2 sorption with increasing T_g. The larger extent of sorption results from a larger non-equilibrium excess free volume. Swelling of the polymers is induced by sorption of CO_2 molecules in the non-equilibrium free volume as well as from molecules dissolved in the matrix. Dilation of the polymer is similar for each molecule sorbed, irrespective of the fact if the molecule enters the non-equilibrium or equilibrium region. Correspondingly, the partial molar volume of CO_2 is similar for molecules present in both regions. The smallest molar volume was found for the material with the highest T_g, Matrimid®. For the rubbery polymer Pebax® the partial molar volume of CO_2 resembles that of pure liquid CO_2.
The extent of swelling of the ODPA PEI films is very low, which is beneficial for CO_2 removal at elevated pressures. Mixed gas separation experiments showed high CO_2/CH_4 selectivities for the ODPA PEI films at elevated pressure, confirming the potential of this material for the effective separation of CO_2 from CH_4.

The results of the membrane contactor and the gas separation membrane experiments show the potential of both technologies for the effective separation of CO_2 from CH_4. Although the membrane contactor is a more complex system, with two membrane modules combined with an absorption liquid, at low pressures it shows its superior behavior with high CO_2 permeances and very high CO_2/CH_4 selectivities. High CO_2 permeances combined with high selectivities are especially found when using porous fibers in the membrane contactor. But this also immediately shows the limitation of the process as at higher feed pressures non-selective absorption and a severe drop in selectivity occur. This can be prevented when membranes with a dense (selective) top layer on top of a porous support (either asymmetric or composite membranes) are used. This however at the expense of a decrease in productivity. Under these conditions, plasticization resistant gas separation membranes like e.g. some of the materials investigated in this work, for the efficient separation

of CO_2 and CH_4 are preferred. Polymeric membranes for gas separation can be divided in glassy and rubbery polymers. Rubbery polymers have typically much higher permeabilities than glassy polymers, as in the glassy state the segments cannot rotate freely and mobility of the polymeric chains is restricted [1]. The advantage of the rigid structure of polymers in the glassy state is that they generally have higher selectivities [2], but plasticization leading to a severe decrease in performance may often occur as well. According to Baker [3] the competitive position of gas separation membranes on the CO_2/CH_4 separation market would change, if stable membranes with a selectivity of 40 during operation would become available.

Outlook

Membrane contactor

The membrane contactor experiments showed high CO_2 permeances and high CO_2/CH_4 selectivities, but also a clear potential for further improvements in the separation performance as e.g. incomplete solvent regeneration was observed. By optimizing the absorber and the desorber membrane contactors, CO_2 fluxes can be further increased. As it could be observed in the experiments, an increased desorber temperature significantly increased the CO_2 permeances and indicate desorption as the limiting step in the process. Next to an increased desorber temperature, a more effective desorption due to an improved module design with improved hydrodynamics, resulting in a decreased boundary layer thickness and consequently reduced resistance to mass transfer, would result in higher CO_2 fluxes. Less loaded solution would leave the desorber and more CO_2 could be absorbed again by the absorption liquid in the absorber membrane contactor. This would also be especially beneficial from a kinetic point of view, as the kinetic experiments showed that the apparent reaction rate constant strongly decreases with increasing CO_2 loading, due to a decrease in free amino acid concentration, which is an

additional possible limitation that can be reduced with an enhanced desorption.

Next to an increased module length, without too high pressure drop along the fibers, and higher packing densities of the fibers in the modules, different membrane and module designs can improve the mass transfer. The use of different membrane designs, like the use of helical wound hollow fiber membranes (twisted fibers) or structured fiber membranes, could increase the mass transfer. In addition, the design of the module, like transverse flow membrane modules [4] or helical wound hollow fiber modules [5, 6], can result in improved hydrodynamics, reduced boundary layer thickness and consequently lower mass transfer resistance.

Luque et al. [5] tested helically wound hollow fiber modules for microfiltration and compared their performance to linear hollow fiber modules and showed flux and capacity improvements of up to 3.2-fold under constant transmembrane pressure operation for the helical modules over those with the linear fiber modules. Also Liu et al. [6] compared coiled hollow fiber modules with the conventional linear fiber modules and observed for the stripping of dissolved oxygen from water remarkably enhanced mass transfer in both tube and shell side of the module. All combined, these improvements in process, membrane and module design will significantly improve mass transfer and are an interesting step to further improve the performance of the process for the separation of CO_2 from gas streams.

Reaction kinetics

The kinetic study showed high reaction rate constants for the absorption of CO_2 in aqueous sarcosine salt solutions when compared to MEA and the high potential of this solution as absorption liquid for CO_2 absorption. Nevertheless, when used in the gas-liquid membrane contactor, higher CO_2 permeances for the process with MEA than for sarcosine were observed. The results from the kinetic and contactor study suggest that the absorption reaction is not the limiting step in the process. Loading tests performed separately at 29°C (absorber temperature) showed relatively

similar values (in the range of 0.76 mol CO_2/mol amine) for the maximum CO_2 loading capacity of both absorption liquids. Consequently differences in CO_2 loading between the two liquids did not explain the differences in performance between the two absorption liquids. It is hypothesized that the observed differences in permeances are caused by a more effective CO_2 desorption at elevated temperatures in the case of MEA compared to the sarcosine salt solution. The determination of the kinetics of desorption as a function of temperature is of high importance for an effective and energy efficient CO_2 separation in cyclic absorption processes.

CO_2 selective membranes

For effective CO_2 separation using thin, dense gas separation membranes to establish the separation, stable membranes that do not loose their performance at high CO_2 pressure are desirable. However, due to the trade off between permeability and selectivity, membranes with higher selectivities often show limitations in their permeances and vice versa. A way to overcome this is to decrease the effective thickness of the membrane and to prepare the membrane as composite hollow fiber membrane, with a thin dense top layer on top of a porous support. Figure 1 shows a SEM image of such a composite hollow fiber membrane, with the porous support and a dense selective top layer.

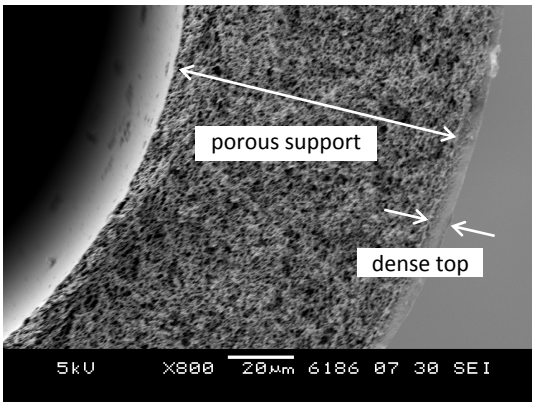

Figure 1: SEM image of a composite hollow fiber membrane; support: PPO fiber from Parker (The Netherlands); coating: ODPA PEI [Chapter 6].

The thin dense layer is the actual membrane and provides the separation, whereas the porous support provides the mechanical stability. Hollow fiber geometries are relatively easy to coat and they have high area-to-volume ratios, which is considerably important for compact module design.
In particular for the poly(RTIL) membranes investigated in Chapter 5 that are relatively thick (~240 μm), the preparation of composite hollow fiber membranes to reduce the membrane thickness is an important step to achieve sufficiently high gas fluxes. The idea is to coat the solution, containing the RTIL monomer, cross-linking agent and photo-initiator, on hollow fibers and photo-polymerize the coating afterwards in the UV-chamber (365 nm). To obtain a uniform and homogeneous coating layer on top of the hollow fiber surface, UV radiation over the full fiber area is required. In first tests where P84/Matrimid hollow fiber membranes [7] were used as support, fibers with very thin, but not completely defect free top layers are achieved (Figure 2). Further investigations to achieve thin defect free layers are necessary.

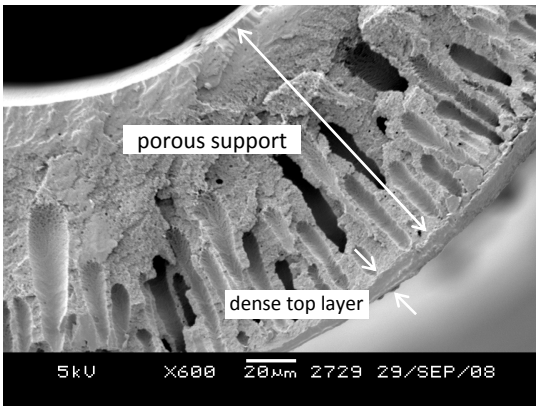

Figure 2: SEM image of a P84/Matrimid support fiber coated with poly(RTIL).

Next to more practical considerations regarding the preparation of the composite hollow fiber membranes, changes in film thickness may also result in changes in membrane performances [8]. Thin films of glassy polymers can show distinctively different aging, transport and plasticization behavior when compared to thick, bulk films [8, 9]. Kim et al.

[10] showed for glassy 6FDA-based polyimide films that the aging rate is greatly accelerated for thin films compared to thick bulk films and that a correlation of aging rate to free volume is expected. Also plasticization behavior can differ, depending on the film thickness and in thin films plasticization can occur at lower pressures when compared to bulk materials [8, 11]. After the preparation of composite hollow fiber membranes with thin selective top layers, the performance of these membranes has to be evaluated with respect to aging and plasticization resistance. This is especially relevant for glassy polymer membranes, i.e. the ODPA PEI membranes described in Chapter 6. Thick, bulk films of these materials showed strong resistance against plasticization and high CO_2/CH_4 selectivites even at elevated CO_2 partial pressures. Also thin layers of these materials seem to show only limited swelling when exposed to high pressure CO_2 in sorption experiments, but this requires further investigation.

References

1. M.H.V. Mulder, Basic principles of membrane technology, Kluwer Academic Publishers, (1996)

2. L.M. Robeson, Polymer membranes for gas separation, Current Opinion in Solid State and Materials Science, 4 (1999) 549

3. R.W. Baker, Future Directions of Membrane Gas Separation Technology, Ind. Eng. Chem. Res., 41 (2002) 1393-1411

4. F.N.M. Knops, H. Futselaar, I.G. Racz, The transversal flow microfiltration module. Theory, design, realization and experiments, Journal of Membrane Science, 73 (1992) 153

5. S. Luque, H. Mallubhotla, G. Gehlert, R. Kuriyel, S. Dzengeleski, S. Pearl, G. Belfort, A new coiled hollow-fiber module design for enhanced microfiltration performance in biotechnology, Biotechnology and Bioengineering, 65 (1999) 247

6. L. Liu, L. Li, Z. Ding, R. Ma, Z. Yang, Mass transfer enhancement in coiled hollow fiber membrane modules, Journal of Membrane Science, 264 (2005) 113

7. T. Visser, N. Masetto, M. Wessling, Materials dependence of mixed gas plasticization behavior in asymmetric membranes, Journal of Membrane Science, 306 (2007) 16

8. M. Wessling, M. Lidon Lopez, H. Strathmann, Accelerated plasticization of thin-film composite membranes used in gas separation, Separation and Purification Technology, 24 (2001) 223

9. B.W. Rowe, B.D. Freeman, D.R. Paul, Physical aging of ultrathin glassy polymer films tracked by gas permeability, Polymer, 50 (2009) 5565

10. J.H. Kim, W.J. Koros, D.R. Paul, Physical aging of thin 6FDA-based polyimide membranes containing carboxyl acid groups. Part I. Transport properties, Polymer, 47 (2006) 3094

11. J.D. Wind, S.M. Sirard, D.R. Paul, P.F. Green, K.P. Johnston, W.J. Koros, Carbon dioxide-induced plasticization of polyimide membranes: Pseudo-equilibrium relationships of diffusion, sorption, and swelling, Macromolecules, 36 (2003) 6433

Summary

CO_2 is one of the major contributors to the greenhouse effect: the power and industrial sectors combined account for about 60% of the global annual CO_2 emissions. To minimize the impact of CO_2 on the environment, carbon capture and sequestration (CCS) is essential. Next to its environmental impact, CO_2 reduces the heating value of natural gas (CH_4) in power plants and due, to its acidic character, the presence of CO_2 can lead to corrosion in equipment and pipelines. This makes the removal of CO_2 from natural gas of crucial importance.

The traditional method of separating CO_2 from other gases is aqueous amine scrubbing. High product yields and purities can be obtained with this method, but amine absorption suffers from several drawbacks like corrosiveness, instability in the presence of oxygen, high energy consumption, especially during desorption, and high liquid losses due to evaporation of the solvent in the stripper. In addition, also the occurrence of flooding and entrainment of the absorption liquid may occur and limits the process as the gas and the liquid streams cannot be controlled independently.

Next to absorption, membrane processes are frequently used for gas separation. Examples are e.g. the separation of oxygen and nitrogen from air to produce nitrogen enriched air, but also for the separation of CO_2 from CH_4. The energy requirements significantly benefit the use of membrane technology over other technologies. The main limitation of currently existing membranes is the occurrence of severe plasticization of the membrane in the presence of (high) pressure CO_2. Due to excessive swelling of the polymer membrane upon exposure to CO_2, the

performance (selectivity) decreases significantly. The development of polymeric membranes and membrane processes with improved plasticization resistance that maintain selectivity and permeability, even at higher CO_2 partial feed pressures is crucial and an important field of research.

This thesis investigates the potential of membrane technology for the effective removal of CO_2 from CH_4. The work focuses on two distinctively different membrane processes to accomplish the separation, i.e. 1) the use of a gas-liquid membrane contactor for the selective absorption of CO_2 from CH_4 and 2) the use of thin, dense gas separation membranes to establish the separation.

A membrane contactor combines the advantages of membrane technology with those of an absorption liquid. In a gas-liquid membrane contactor the membrane acts as an interface between the feed gas and the absorption liquid. The CO_2 from the CO_2/CH_4 gas mixture diffuses from the feed gas side through the membrane and is then absorbed in the selective absorption liquid. The loaded liquid circulates from the absorber to the desorber, which is a second membrane contactor, where desorption of CO_2 occurs. Gas-liquid membrane contactors offer a unique way to perform gas-liquid absorption processes in a controlled fashion while they have a high operational flexibility. The two major parts in a gas-liquid membrane contactor that determine the separation are the membrane and the absorption liquid.

Next to porous (PP) hollow fiber membranes, asymmetric (PPO) hollow fiber membranes with a dense, ultrathin skin at the outside of the membrane have been used in a membrane contactor and the influence of different process parameters on productivity and selectivity has been evaluated. The PP membranes outperform the PPO membranes in terms of productivity and selectivity, but the PPO membranes are much less sensitive towards variations in feed pressure, which increases the operating window and potential of the membrane contactor process.

Amino acid salt solutions are a promising class of absorption liquids for CO_2 absorption and a competitive alternative to the conventionally used

alkanol amines such as MEA. Amino acid salt solutions have similar reactivity and CO_2 absorption capacity as alkanol amines, but in addition they can be made non-volatile by adding a salt functionality, which significantly reduces the liquid losses. The kinetics of the absorption CO_2 in an amino acid salt solution (sarcosine) have been studied. Kinetic experiments are performed in the pseudo-first-order regime using a gas-liquid stirred cell contactor to determine the reaction rate constant of CO_2 absorption in aqueous sarcosine salt solutions. Next to the influence of the sarcosine concentration (0.5 to 3.8 M) and the temperature (298 to 308 K), the reaction rate constant of partially CO_2 loaded sarcosine salt solutions was determined. Reaction rate constants significantly higher than those found for MEA were obtained for the absorption of CO_2 in aqueous sarcosine salt solutions showing the potential of this new absorption liquid for efficient CO_2 separation.

The performance of this amino acid salt solution in a membrane contactor including both absorption and desorption for the separation of CO_2 and CH_4 is evaluated. Very high CO_2/CH_4 selectivities due to very low CH_4 permeances can be obtained with sarcosine as absorption liquid. In comparison to processes with MEA where higher selectivities can only be achieved at elevated desorber temperatures, high selectivities for sarcosine salt solutions can already be achieved without a temperature difference between absorber and desorber, which is a step forward towards energy-efficient CO_2 absorption.

Next to the applicability of a membrane contactor for the separation of CO_2 and CH_4 the use of gas separation membranes with improved plasticization resistance to establish the separation has been investigated. The ionic character of polymerized room temperature ionic liquids (poly(RTILs)) can be used as a tool to improve the plasticization resistance of these membranes. An imidazolium-based poly(RTIL) is used as base material and the length of the alkyl chain serves as a tool to strengthen or weaken the ionic interactions within the poly(RTIL). High pressure gas permeation experiments are done to observe the behavior of these materials under high pressure CO_2 atmosphere. As opposed to regular

glassy polymers, poly(RTIL)s do not show a minimum in permeation rates for CO_2: the permeability increases continuously with increasing feed pressure. In gas mixtures, CO_2 accelerates the transport rate of methane. The poly(RTIL) membranes with the short, methyl substituted side chain and stronger ionic interactions showed an increased resistance towards plasticization when compared to the two other polymers. The methyl substituted polymer membrane had increased gas selectivity at the expense of the permeability compared to the polymers with the longer side chains.

In Chapter 6 a promising high selective polymeric membrane (ODPA PEI) is tested and its sorption, swelling and permeation behavior at high pressure are analyzed. The mixed gas permeation experiments show high CO_2/CH_4 selectivities for the ODPA PEI films even at elevated pressure and therewith high potential of this material for the effective CO_2 removal.

Samenvatting

CO_2 is een van de belangrijkste veroorzakers van het broeikaseffect: De energiesector en de industrie zijn gezamenlijk verantwoordelijk voor ongeveer 60% van de totale jaarlijkse CO_2-uitstoot. Om de invloed van CO_2 op het milieu te minimaliseren is koolstofvastlegging en -opslag (Carbon Capture and Sequestration (CCS)) essentieel. Naast de gevolgen voor het milieu, vermindert CO_2 de verwarmingswaarde van aardgas (CH_4) in elektriciteitscentrales en vanwege het zure karakter kan de aanwezigheid van CO_2 leiden tot corrosie in apparatuur en leidingen. Dit maakt het verwijderen van CO_2 uit aardgas van cruciaal belang.

De traditionele methode om CO_2 te scheiden van andere gassen is aminescrubbing. Hoewel met deze methode een hoge opbrengst en zuiverheid van het product kan worden verkregen, kampt amine-absorptie met een aantal nadelen zoals corrosiviteit, instabiliteit in aanwezigheid van zuurstof, hoog energieverbruik vooral tijdens desorptie en een groot vloeistofverlies als gevolg van verdamping van het oplosmiddel in de stripper. Daarnaast kunnen de gas- en vloeistofstroom niet onafhankelijk van elkaar gecontroleerd worden. Dit beperkt het proces.

Behalve absorptie worden membraanprocessen vaak gebruikt voor gasscheiding. Voorbeelden hiervan zijn de scheiding van zuurstof en stikstof uit lucht voor de productie van stikstofverrijkte lucht, maar ook de scheiding van CO_2 en CH_4. De benodigde energie voor deze scheiding is aanzienlijk lager dan het energieverbruik bij andere technologieën. De belangrijkste beperking van de huidige membranen is het optreden van sterke zwelling (plastificering) van het membraan in aanwezigheid van CO_2 onder hoge druk. Door overmatige zwelling van het polymeermembraan

bij blootstelling aan CO_2, verminderen de prestaties van het membraan (selectiviteit) aanzienlijk. De ontwikkeling van polymeermembranen en membraanprocessen met een verbeterde weerstand tegen plastificering die selectiviteit en permeabiliteit behouden, zelfs bij hogere partiële CO_2 voedingdruk, is van cruciaal belang en een belangrijk gebied van onderzoek.
Dit proefschrift onderzoekt de mogelijkheden van membraantechnologie voor de effectieve verwijdering van CO_2 uit CH_4. Het werk richt zich op twee verschillende membraanprocessen om de scheiding te verwezenlijken, namelijk 1) het gebruik van een gas-vloeistof membraancontactor voor de selectieve absorptie van CO_2 uit CH_4 en 2) het gebruik van dunne, dichte gasscheidingsmembranen om de scheiding te verwezenlijken.

Een membraancontactor combineert de voordelen van membraantechnologie met die van een absorptie vloeistof. In een gas-vloeistof membraancontactor fungeert het membraan als grensvlak tussen het voedingsgas en de absorptievloeistof. De CO_2 uit het CO_2/CH_4 gasmengsel diffundeert vanuit het voedingsgas door het membraan en wordt vervolgens geabsorbeerd in de selectieve absorptievloeistof. De met CO_2 verzadigde vloeistof circuleert van de absorber naar de desorber, een tweede membraancontactor, waar desorptie van CO_2 plaatsvindt. Gas-vloeistof membraancontactoren bieden een unieke manier om gas-vloeistof absorptieprocessen op een gecontroleerde manier uit te voeren, terwijl ze een grote operationele flexibiliteit hebben. De twee belangrijkste onderdelen in een gas-vloeistof membraancontactor die bepalend zijn voor de scheiding zijn het membraan en de absorptievloeistof.
Naast poreuze (PP) holle vezel membranen zijn asymmetrische (PPO) holle vezel membranen met een dichte, ultra dunne toplaag aan de buitenkant van het membraan gebruikt in een membraancontactor en is de invloed van verschillende parameters op de productiviteit en de selectiviteit van het proces geëvalueerd. De PP membranen presteren beter dan de PPO membranen in termen van productiviteit en selectiviteit, daarentegen zijn PPO membranen veel minder gevoelig voor schommelingen in de

voedingsdruk, waardoor het operationele bereik en de potentie van het membraancontactorproces toeneemt.
Zoutoplossingen van aminozuren zijn een veelbelovende klasse van absorptievloeistoffen voor de absorptie van CO_2-opname en een concurrerend alternatief voor de conventioneel gebruikte alkanolamines zoals MEA. Deze aminozuren hebben een vergelijkbare reactiviteit en CO_2-absorptiecapaciteit als alkanolamines. Bovendien kunnen ze niet-vluchtig worden gemaakt door toevoeging van een zoutfunctionaliteit, waardoor de vloeistofverliezen aanzienlijk verminderen. De kinetiek van de CO_2 absorptie in een aminozuur zoutoplossing (Sarcosine) is bestudeerd. Kinetiek experimenten in het pseudo-eerste orde regime zijn uitgevoerd door gebruik te maken van een geroerde cel gas-vloeistof contactor en de reactiesnelheidconstante van de CO_2-absorptie in waterige zoutoplossingen (Sarcosine) te bepalen. Naast de invloed van de Sarcosine concentratie (0,5 tot 3,8 M) en de temperatuur (298 tot 308 K), is de reactiesnelheidconstante van gedeeltelijk met CO_2 verzadigde Sarcosine zoutoplossingen bepaald. De reactiesnelheidsconstanten voor de absorptie van CO_2 in waterige Sarcosine zoutoplossingen blijken aanzienlijk hoger te zijn dan die voor MEA en tonen het potentieel van deze nieuwe absorptievloeistof voor efficiënte CO_2-scheiding aan.
De prestaties van deze aminozuuroplossing (Sarcosine) in een membraancontactor voor zowel absorptie als desorptie voor de scheiding van CO_2 en CH_4 is geëvalueerd. een zeer hoge CO_2/CH_4 selectiviteit als gevolg van een zeer lage CH_4 productiviteit kan worden verkregen met Sarcosine als absorptievloeistof. In vergelijking met processen waar gebruik gemaakt wordt van MEA, waar een hogere selectiviteit alleen kan worden bereikt bij een verhoogde desorptie temperatuur, kan een hoge selectiviteit voor Sarcosine zoutoplossingen al worden bereikt zonder een temperatuur verschil tussen de absorber en desorber, wat een stap voorwaarts is in de richting van energie efficiënte CO_2-absorptie.

Naast de toepasbaarheid van een membraancontactor voor de scheiding van CO_2 en CH_4 is het gebruik van gasscheidingsmembranen met een verbeterde weerstand tegen plastificering en zwelling om de scheiding te

bewerkstelligen onderzocht. Het ionische karakter van gepolymeriseerde ionische vloeistoffen (poly(RTILs)) kan worden gebruikt als een instrument ter verbetering van de plastificeringsweerstand van deze membranen. Een imidazolium gebaseerd (RTIL) is gebruikt als uitgangspunt en de lengte van de alkylketen dient als een instrument om de ionische interacties binnen de poly(RTIL) te versterken of te verzwakken. Hoge druk gaspermeatie-experimenten zijn gedaan om het gedrag van deze materialen onder hoge druk CO_2-atmosfeer te observeren. In tegenstelling tot reguliere glasachtige polymeren, vertonen poly(RTIL)s geen minimum in de permeatie van CO_2: de permeabiliteit stijgt voortdurend met toenemende voedingsdruk. In gasmengsels versnelt CO_2 de permeatiesnelheid van methaan. De poly(RTIL) membranen met een korte, methyl gesubstitueerde zijketen en sterkere ionische interacties tonen een verhoogde weerstand tegen plastificering in vergelijking met de twee andere polymeren, gecombineerd met een verhoogde gasselectiviteit ten koste van de permeabiliteit ten opzichte van de polymeren met de langere zijketens.

In hoofdstuk 6 wordt een veelbelovend hoog selectief polymeer membraan (ODPA PEI) getest en zijn sorptie-, zwelling- en permeatiegedrag onder hoge druk geanalyseerd. De permeatie-experimenten met gasmengsels lieten een hoge CO_2/CH_4 selectiviteit voor de ODPA PEI films zien, zelfs bij verhoogde druk en zijn daarmee van groot potentieel belang voor de effectieve scheiding van CO_2.Vergelijking van het sorptiegedrag van dunne en dikke films van deze materialen laten zien dat de sorptie sterk beïnvloed wordt door de aanwezigheid van vrij volume in het polymeer.

Acknowledgements

Four years are over – the thesis is written and now its time to say Thank you to the people, who contributed to this work.

First of all I would like to thank my promotor Matthias and my assistant promotor Kitty, for giving me the opportunity to do this work and for all their support in the last four years.

Even though my project had no official cooperation, we built up several ones in the last years. I would like to thank Wim, Magdalena, Jason, Richard, Theo and Nieck for the great collaboration and all their support.

Several students contributed to this work and I would like to thank them for their input: Felix, Harro, Ceren, Belgin (part time) and Jordi.

I also would like to thank all the members of MTG group, and in particular Greet for all her help concerning paper work; Herman for his help in solving my problems with the gas permeation setup, Marcel for helping me with my computer problems (I still don't know my local.la password); Hans for his help with the ellipsometry setup and Antoine for his very friendly reactions always regarding my financial related questions.

John, how great it was for me to build new setups with you. I enjoyed a lot our working together and due to you I really improved my technical skills. Thanks for everything!

Erik thanks for all your help during the last four years. Your help, especially in the starting period, was very important for me.

During my time at the University of Twente I shared the office with several people, without whom it would have been a boring time.
In Langezijds I shared the room with Srivatsa, Saiful, Miriam, Magda, Clara and Szymon and in Meander with Ikenna, Wilbert, Mehrdad, Wendy, Giri, Enver and Wojciech – to all of you I would like to say thank you.

You do not only have roommates, you also have office neighbors and there I would like to mention in particular Al-hadidi and Zeynep. Thanks for being great neighbors, for feeding us with biscuits and I am really sorry for all the disturbances.

Karina, I will only mention you once in this acknowledgment (I know that you are counting), but therefore you are getting your own paragraph. I hope that is fine with you. Thanks for being a great colleague in the last four years – with special moments from enjoying the Waikiki Beach to surviving the RPK exam with Professor Lemstra.

In our group I met lots of people in the last four years, who made the working days nicer and with whom I also had nice activities outside the university. Thanks to all of them. In particular I would like to mention Jens, Maik, Hakan, Matias, Can, Laura, Joao, Jörg, Dana….
Furthermore I would like to thank my traveling colleagues Maik, Olga and Schwan. Crossing every day the border between Germany and the Netherlands is only nice in good company.
Thanks to the cool car people Olga, Anne Corine and Jeroen (and an additional thank to you for helping me with the Dutch summary) for accepting me -such an old person- in your group.

Doing a PhD is like a trip with a rollercoaster, with a lot of ups and downs. At my deepest point there were a group of people who helped me up again. In specific I would like to mention Maik, Hakan, Matias and Can. – Thanks guys, for all your support!

Maik, after sharing my deepest moment, I am very happy that we will now also share the final moment of my PhD-journey. Thanks for all your endless help!

Favorite roommate – Ikenna, thanks for sharing the last years with me, thanks for sharing the depression, the fun and the eating brain moments. It is a great pleasure for me to know you standing next to me, during my defense.
BTW: you are a very social person, even when you are sitting in the corner.

The world is not only the University; I also would like to thank all my friends from outside the UT, for their support during the last years.

Meiner alten und neuen Familie möchte ich auch ganz herzlich danken, für all ihre Hilfe und Unterstützung in den letzten Jahren. Im ganz besondern möchte ich meinen Eltern danken. Ohne Euch hätte das mit dem studieren und promovieren wohl nicht so geklappt, danke für all Eure Hilfe und dass Ihr so ein gutes Vorbild für mich seid.

Nun zum wichtigsten Menschen: Christoph, wie soll ich Dir danken? Ohne Deine Hilfe wäre das hier alles wohl nicht so gelaufen. Das Wissen das Du da bist, hat vieles möglich gemacht, auch das weiter machen in den schwierigsten Zeiten. Danke für deine unendliche Unterstützung und für all Deine Liebe. Ich liebe Dich!